UNIVERSITAT DE BARCELONA

Turnover of voltage-gated potassium channel Kv 1.3

Katarzyna Styrczewska

ADVERTIMENT. La consulta d'aquesta tesi queda condicionada a l'acceptació de les següents condicions d'ús: La difusió d'aquesta tesi per mitjà del servei TDX (**www.tdx.cat**) i a través del Dipòsit Digital de la UB (**diposit.ub.edu**) ha estat autoritzada pels titulars dels drets de propietat intel·lectual únicament per a usos privats emmarcats en activitats d'investigació i docència. No s'autoritza la seva reproducció amb finalitats de lucre ni la seva difusió i posada a disposició des d'un lloc aliè al servei TDX ni al Dipòsit Digital de la UB. No s'autoritza la presentació del seu contingut en una finestra o marc aliè a TDX o al Dipòsit Digital de la UB (framing). Aquesta reserva de drets afecta tant al resum de presentació de la tesi com als seus continguts. En la utilització o cita de parts de la tesi és obligat indicar el nom de la persona autora.

ADVERTENCIA. La consulta de esta tesis queda condicionada a la aceptación de las siguientes condiciones de uso: La difusión de esta tesis por medio del servicio TDR (**www.tdx.cat**) y a través del Repositorio Digital de la UB (**diposit.ub.edu**) ha sido autorizada por los titulares de los derechos de propiedad intelectual únicamente para usos privados enmarcados en actividades de investigación y docencia. No se autoriza su reproducción con finalidades de lucro ni su difusión y puesta a disposición desde un sitio ajeno al servicio TDR o al Repositorio Digital de la UB. No se autoriza la presentación de su contenido en una ventana o marco ajeno a TDR o al Repositorio Digital de la UB (framing). Esta reserva de derechos afecta tanto al resumen de presentación de la tesis como a sus contenidos. En la utilización o cita de partes de la tesis es obligado indicar el nombre de la persona autora.

WARNING. On having consulted this thesis you're accepting the following use conditions: Spreading this thesis by the TDX (**www.tdx.cat**) service and by the UB Digital Repository (**diposit.ub.edu**) has been authorized by the titular of the intellectual property rights only for private uses placed in investigation and teaching activities. Reproduction with lucrative aims is not authorized nor its spreading and availability from a site foreign to the TDX service or to the UB Digital Repository. Introducing its content in a window or frame foreign to the TDX service or to the UB Digital Repository is not authorized (framing). Those rights affect to the presentation summary of the thesis as well as to its contents. In the using or citation of parts of the thesis it's obliged to indicate the name of the author.

UNIVERSITAT DE BARCELONA

Turnover of the voltage-gated potassium channel Kv1.3

Katarzyna Styrczewska

This PhD Thesis has been performed under the direction of Dr. **Antonio Felipe Campo** in the Molecular Physiology laboratory in the Department of Biochemistry and Molecular Biomedicine, Institute of Biomedicince (IBUB), Faculty of Biology, University of Barcelona.

Antonio Felipe Campo
PhD thesis director

Katarzyna Styrczewska
PhD candidate

PhD Thesis
University of Barcelona, Faculty of Biology
Department of Biochemistry and Molecular Biomedicine
Doctoral programme in Biomedicine
Barcelona, 2017

W naturze nie ma linii prostej,
Ludzki to wymysł sztuczny.
Patrząc w skłębione żyworosty,
Chaosu, chaosu się uczmy.
Pogięty, kręty i strzępiasty
Jest każdy stwór w naturze,
A prostą linią łączą gwiazdy
Głupcy i tchórze.

Spostrzeżenie , J. Tuwim

Acknowledgement

Firstly, I would like to express my sincere gratitude to my advisor Prof. Antonio Felipe for the continuous support of my Ph.D study and related research, for his patience, motivation, and immense knowledge. His guidance helped me in all the time of research and writing of this thesis. Antonio, thank you for making me a part of MP family!

My sincere thanks also go to Dr Marta Camps who provided me an opportunity to join MP team.

I thank my lovely MP family! Ramon, Nuria, Laura, Mireia, Anna, Albert, Sara, Antonio, Clara, Jesusa, Dani and Irene, Maria and Sergi! You were always for me there, thanks all of you, I was having a loving home and family here. I hope you would be always present in my life.

Thank to all lovely people from department, you fulfill my daily trips through corridor with smile and kindness. Toni, thank you for dinosaur! Xico, Albert thanks for your support and for culture room singing sessions.

Chciałabym podziękować mojej rodzinie, rodzicom: Janinie i Wikotrowi, rodzeństwu: Klaudii, Karolinie Michałowi (autora wspaniałej okładki) i Kamilowi, za wasze wsparcie i waszą miłość. Za to, że zawsze wspieraliście moje szalone pomysły, bez was pewnie nigdy bym tak daleko (dosłownie i w przenośni) nie zaszła.

Table of contents

Table of contents

1. Introduction

1.1. Voltage-gated potassium channels

Potassium-selective channels are the largest and most diverse group of ion channels. Potassium channels are transmembrane proteins which allow the selective flow of potassium ions through the plasma membrane. These channels play crucial roles in different biological processes at the organismic level (generation and propagation of the nerve impulse and the cardiac action potential, promotion of insulin secretion), and also at the cellular level (cell volume control, induction of cell proliferation, apoptosis, migration and initiation of many signaling pathways). Potassium channels have been classified in three main groups, according to their predictive number of transmembrane domains (TMD).

1) Six TMD and divided in two subgroups:

- The voltage-dependent K^+ channels (Kv)

- Ca^{2+}-activated K^+ channels (KCa).

2) Four TMD and two pores (K2P).

3) Two TMD (inward-rectified K^+ channels Kir.)

The International Union of Pharmacology (IUPHAR) classified Kv channels into twelve families (Kv1-12), each of one can present different isoforms. The Kv subfamilies are named according to the homologous gene in *Drosophila melanogaster*. Taking into account the phylogenetic origin those channels are divided into two groups: the first one, comprised

by Kv1-9; and the second one, comprised by Kv10-12 (Fig. 1). This last group of channels also possesses a potential cyclic-nucleotide binding site in their C-terminus (Gutman et al. 2003).

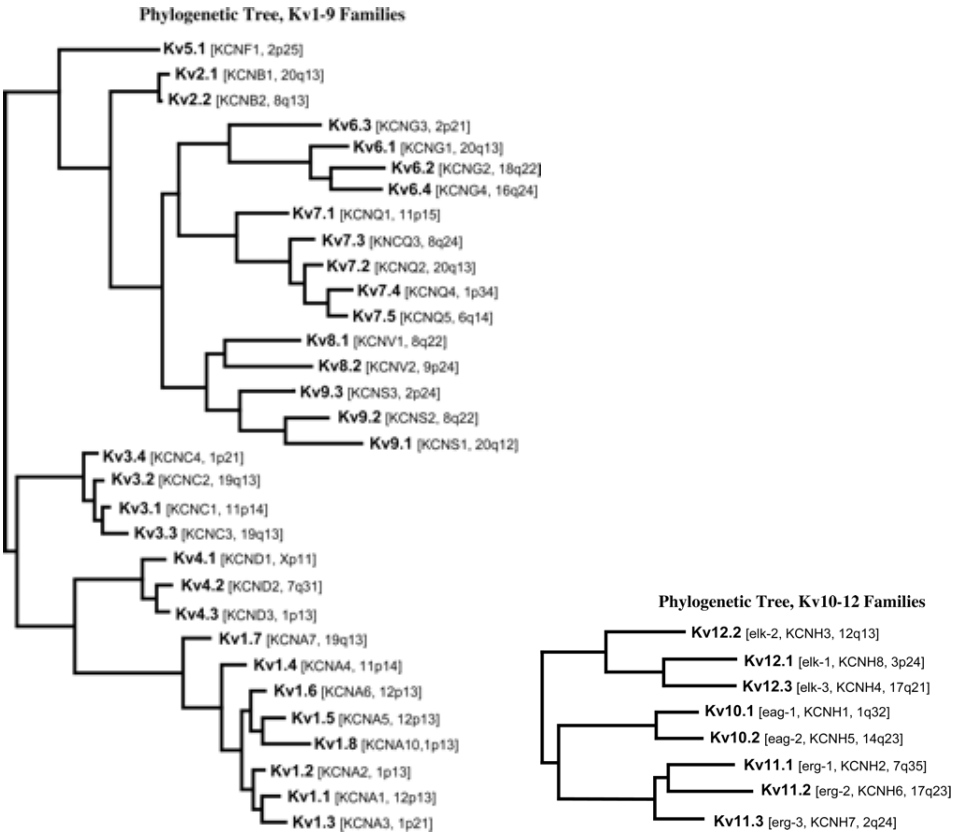

Figure 1. Phylogenetic tree of the Kv1-9 (top panel) and Kv10-11 (botton panel) families (Gutman et al., 2003).

Moreover, diversity of Kv channels can be increased due to the combination of different processes such as:

1) Alternative splicing of the mRNA. For instance, Kv3, 4, 6, 7, 9, 10 and 11 are code by exons and introns which may lead to different variants (Jenkinson 2006).
2) Homo- and hetero-tetramerization between subunits of different Kv members. The assembly can be formed between members from the same family, as for example Kv1.1- Kv1.4 (Shamotienko et al. 1997), Kv1.3-Kv1.5 (Vicente et al. 2006; Villalonga et al. 2007), or with silent subunits (Kv5, Kv6, Kv8 and Kv9). These silent subunits, do not homo-tetramerize, but can assemble to some members of Kv2 and Kv3 families in order to modulate their current (Hugnot et al. 1996; Post et al. 1996; Salinas et al.1997).
3) Post-translational modifications such as phosphorylation, glycosylation, ubiquitination, palmitoylation, oxidation, etc. (Nitabach et al. 2002; Zhang et al. 2007; Jindal et al. 2008; Noma et al. 2009)
4) Assembly of regulatory subunits which modulate the Kv characteristics (trafficking, current density and gating) such as AKAP proteins, Kvβ, KCNEs, etc (Pongs et al.1999; Pourrier et al. 2003).

1.1.1. Basic principles of Kv channels

Kv channels show a very conservative construction. Each channel gene among Kv family encodes one α-subunit (Kvα). To form a functional channel four α-subunits are required. Thus, Kv channels are formed by the tetramerization of 4 α subunits (MacKinnon 1991). Each of these subunits is composed of six transmembrane domains (S1-S6), which are connected by intra- or extracellular loops (Fig. 2A, B). These helices form two structurally and functionally different parts of the tetrameric channel: 1) a potassium ion-conducting domain (pore domain) – helices S5–S6 located in the channel center, and 2) a domain sensible to changes in the membrane potential (voltage- sensing domain, VSD) – helices S1–S4 located on the channel periphery (Jiang et al. 2002; Jiang et al. 2003; Long et al. 2005; Long et al. 2007; Tao et al. 2009). The pore part includes a channel gate and a selective filter that does not allow ions other than K^+ to penetrate through the channel. The channel gate is formed by crossing C-termini of the S6 helices that block passage of ions when the channel is closed (Sokolova et al., 2003). A conserved fragment (P-region) and a S5–S6 loop participate in the formation of the selectivity filter of the channel.

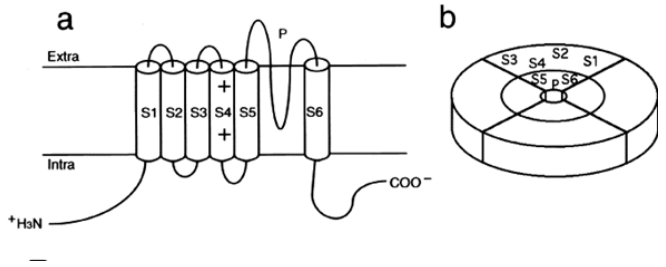

Figure 2. (A) Putative Kv1.3 single α subunit containing six transmembrane segments with the pore region formed between S5 and S6 segments. (B) Structure of the tetrameric assembly (Fujita and Kurachia, 2000).

1.1.2. Biogenesis and trafficking of Kv channels

The intracellular forward trafficking of ion channels is a key regulatory step in controlling the current density of specific ion channels. Newly synthesized plasma membrane proteins, such as Kv channels, must pass from the cytosol through the ER-Golgi trafficking machinery and be packaged in vesicles to be transported to their final destination (Palade, 1975). Kv channels are synthesized and assembled as tetrameric complexes in the ER (Schulteis et al. 1998; Papazian 1999; Lu et al. 2001). However, Kv channels do not possess the typical ER targeted signal sequence. Kv undergo ER targeting by an S2 transmembrane domain, found in Kv1.3 (Tu et al. 2000). Kv complexes are further subjected to a quality control checkpoint (Braakman and Bulleid 2011), which allows tetrameric configurations to exit the ER. Importantly, the ER-Golgi checkpoint regulates both exit of ion channels from the ER and channel degradation, as subunits failing to traffic (e.g. due to misfolding)

may be redirected to an ER-associated degradation pathway (Hesketh et al. 2009)

The appropriate folding of Kv may require the action of chaperones such as Heat Shock Proteins (Hsp) or calnexin. For example, Kv1.5 stability increases when interacting with Hsp70 (Hirota et al. 2008) and Kv1.2 surface levels increases when co-expressed with calnexin (Manganas and Trimmer 2004). Often, regulatory subunits also play a role of chaperones. Kvβ2 stabilizes the Kv1.2 and also increases membrane surface targeting (Shi et al. 1996). Other regulatory subunits, which play a similar role to chaperones, are KChAP, KChIP and dipetidyl aminopeptidase (DPPL)-like proteins (Kuryshev et al. 2000; Kuryshev et al. 2001; Nadal et al. 2003; Shibata et al. 2003). Signal sequences, such as R-X-R, K-K-X-X and K-D-E-L, are responsible for ER retention of Kv (Zerangue et al. 1999; Ma et al. 2001; Kupershmidt et al. 2002). In most cases, their accessibility becomes hidden when the channels acquire their proper folding, allowing the channels to leave the ER. If these sequences are exposed, the channel is retained at the ER. In addition to these generic ER retention signals, some Kv also possess an anterograde trafficking signal (V-X-X-S-L or similar) in their C-terminal domain (Li et al. 2000, Steele et al. 2007). Furthermore, in some Kv members, ER retention signals located near the extracellular face of the pore, between S5 and S6, have also been described (Manganas et al. 2001; Zhu et al. 2003; Zhu et al. 2003; Zhu et al. 2005). The effects of this ER retention signal are dominant respect to other signals or even in association with regulatory subunits, such as Kvβ (Manganas et al. 2001). From the ER, Kv channel

complexes continue on their journey to the plasma membrane, passing through cis-, medial-, and trans-Golgi elements. Some membrane proteins need a selective transport from the ER to the Golgi apparatus, for example via COPII vesicles. This process is complex and requires the coordinated activity of different proteins such as Sec and SarI, the cytoskeleton, etc. In general, COPII recognition sites are characterized for containing di-hydrophobic (F-F, Y-Y, L-L, or F-Y) or di-acidic (D/E-X-D/E) motifs. Few potassium channels have been described to interact directly with COPII anterograde mechanisms (KAT1, K2P9.1) (Zuzarte et al. 2007; Sieben et al. 2008). Kv1.3 contains an anterograde signature motif (YMVIEE) in the C-terminus domain which involves COPII interaction (Martínez-Mármol et al. 2013).

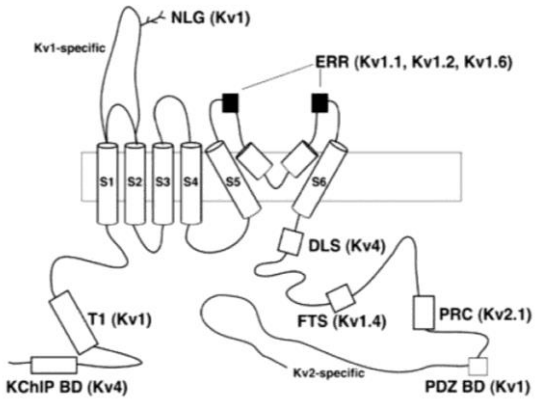

Figure 3. Cartoon summarizing trafficking signals on Kv α subunits. KChIP BD, KChIP binding domain; T1, tetramerization; NLG, N-linked glycosylation site; ERR, ER retention motif; DLS, dendritic localization signal; FTS, forward-trafficking signal; PRC, proximal dendritic clustering signal; PDZ BD, PDZ-binding domain (Misonou and Trimmer, 2004).

Moreover Kv channels go through some further modifications while trafficking to Golgi apparatus, such as N-linked glycosylation, tyrosine, serine and threonine's phosphorylation. Phosphorylation modifies not just channel's activity (Bowlby et al. 1997; Fadool et al. 1997; Nitabach et al. 2002; Misonou et al. 2004), but also surface membrane targeting (Misonou et al. 2004; Yang et al. 2007) and moreover the turnover of Kv channels (Sterling et al. 2002; Nesti et al. 2004). Finally, for several Kv channels, covalent ubiquitin conjugation has been described as a way to modify its membrane expression levels. ENaC, Kv1.5, Kv7.2, Kv7.3 and Kv7.5, for example, are ubiquitinated triggering endocytic signals and downregulating membrane abundance (Staub et al. 1997; Abriel et al. 2000; Ekberg et al. 2007; Boehmer et al. 2008).

1.2. Voltage-dependent potassium channel Kv1.3

Kv1.3 was cloned almost simultaneously from brain of different species (Christie et al. 1990; Grupe et al. 1990; Swanson et al. 1990) and human T lymphocytes (Grissmer et al. 1990; Attali et al. 1992; Cai et al. 1992). All these clones codified for the same protein of 575 amino acids (the human isoform). The distribution of this channel is mainly in the immune system, where is expressed in T, B lymphocytes and microglia (Cahalan et al. 2001), and in the nervous system (Ohno-Shosaku et al. 1996; Veh et al. 1995). Kv1.3 is a voltage gated potassium channel which is activated by depolarization of the membrane. The threshold of activation is around -50 mV, exhibiting a half activation voltage of -35

mV. Kv1.3 characterizes for reaching the maximum peak of conductance about 10 ms after a depolarizing stimulus. Kv1.3 exhibits a marked C-type inactivation, in front a sustained depolarization with a τ of inactivation between 200 and 400 ms (Fig.4). Kv1.3 is also characterized for presenting cumulative inactivation, which consists in a progressive decrease in the potassium current after the application of successive depolarizing pulse trains. The single-channel conductance of Kv1.3 is about 13 pS (Cahalan et al. 1985; Grissmer et al. 1990).

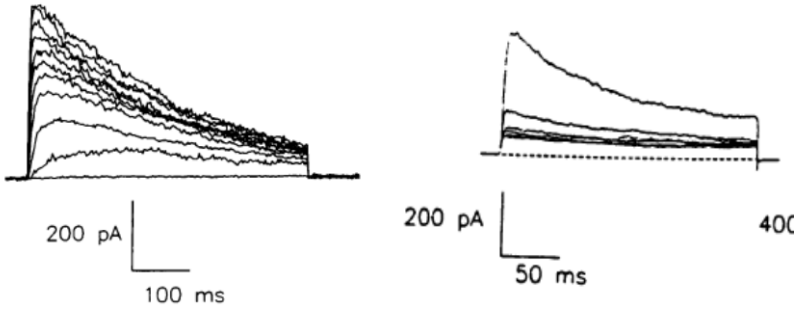

Figure 4. Kv1.3 inactivation. A. Characteristic Kv1.3 current, showing the C-type inactivation. B. Kv1.3 current density decreases in front of a repetitive depolarizing pulse train, due to cumulative inactivation. (Grissmer et al., 1990)

Kv1.3 forms heteromeric complexes with Kv1.1 Kv1.2 and Kv1.4, in the brain grey matter (Coleman et al. 1999), whereas in the bovine cortex, Kv1.3 hetero-oligomerizes with Kv1.6, Kv1.2, and Kv1.4 (Shamotienko et al. 1997). In the immune system, Kv1.3 forms hetero-tetramers in cells where Kv1.5 is also co-expressed such as macrophages

and microglia (Vicente et al. 2006; Villalonga et al. 2007). Kv1.3 is inhibited by general blockers of potassium channels such as quinidine, TEA and 4-aminopiridine (4-AP). Other Kv1.3 inhibitors are benzamide derivatives (Miao et al., 2003) or derivatives from 5-(4-phenyl-butoxy psoralen (Psora-4) (Vennekamp et al., 2004). Early Kv1.3 inhibitors come from venom scorpions such as margatoxin (Centruroides margaritatus) (Garcia-Calvo et al. 1993), which exhibits an IC50 in the pico-molar range. Another examples of Kv1.3 venom scorpion inhibitors are: Charybdotoxin (Leiurus quinquestriatus) (Miller et al., 1985; MacKinnon et al., 1988) and the Pi2 and Pi3 toxins (Pandimius imperator) (Peter et al. 2001). One of the most specific peptide toxins is Shk, from the sea anemone Stichodactyla helianthus, which blocks Kv1.3 in a nano-molar concentration, although some effect upon Kv1.1, Kv1.4 and Kv1.6 has also been described (Pennington et al. 1996). Different chemically and modified derivatives of ShK peptide have been developed, in order to increase selectivity and efficiency inhibiting Kv1.3 to target autoimmune diseases (Lanigan et al., 2002; Beeton et al., 2003; Beeton et al., 2005; Beeton et al., 2011; Chi et al., 2012).

As previously mentioned, Kv1.3 can be modulated by association with auxiliary subunits, such as the KCNE4 regulatory subunit (Grunnet et al., 2003; Solé et al., 2009). Other interacting regulatory subunits are Kvβ1.1 and Kvβ2.1, which enhance Kv1.3 currents (Autieri et al., 1997; McCormack et al., 1999; Vicente et al., 2005). Kv1.3 activity is also modulated by PKA and PKC which decrease the activity (Payet and Dupuis, 1992; Cai and Douglass, 1993). Kv1.3 can be also inhibited by

tyrosine kinase phosphorylation, such as by Src kinases (Holmes et al., 1996; Fadool et al., 1997) or tyrosine kinase-activity receptors (EGF or insulin receptors) (Bowlby et al., 1997). A Ca^{++}-dependent regulation of Kv1.3 was also suggested in lymphoblast together with an association with the type II CAM kinase (Chang et al., 2001), but no calmodulin association (Fanger et al., 1999). Recently, a Ca^{+}-dependent reduction of Kv1.3 inhibition in megakaryocytes and heterologous expression system has also been documented (Martínez-Pinna et al., 2012).

Kv1.3 plays an important role in nervous system during a restricted expression pattern in hippocampus, striatum corpus, piriform cortex and olfactory bulb (Swanson et al., 1990; Kues and Wunder, 1992; Mourre et al., 1999). In the immune system, Kv1.3 is ubiquosly present. In leukocytes, Kv1.3 is expressed in T and B lymphocytes and macrophages (Beeton and Chandy 2005). After TCR activation and subsequent release of endoplasmic reticulum calcium, Kv1.3, together with KCa3.1, plays a crucial role in providing the sufficient driving force for further Ca^{2+} to entry the cell via Ora1. The sustained calcium signal is needed for the T-cell activated transduction signal. Calcium signal is needed for activation of calcineurin and the NFAT translocation to the nucleus, which leads to the transcription of specific T-cell activation and proliferation genes.

Kv1.3 has also been related to many autoimmune diseases such as multiple sclerosis, diabetes mellitus, rheumatoid arthritis, etc. and for this reason there is a lot of effort in searching a specific inhibitor of Kv1.3 as an immunotherapeutic (Beeton and Chandy, 2005; Beeton et al., 2005; Varga et al., 2010; Beeton et al., 2011). Furthermore, Kv1.3

overreactivity has been also described in TEM cells from patients with autoimmune diseases (Rus et al., 2005; Varga et al., 2009). In this context, blocking Kv1.3 ameliorates the animal model EAE (Experimental autoimmune encephalomyelitis) for multiple sclerosis (Beeton et al. 2001). Kv1.3, as well as Kv1.5, plays also an important role in the maintenance of the membrane potential, proliferation and activation of macrophages (Vicente et al., 2006; Villalonga et al., 2007). In addition, Kv1.3 is also important for the production of ROS by microglia and the capacity for killing neurons (Khanna et al., 2001; Fordyce et al., 2005). In dendritic cells, both channels are involved in the regulation of inflammatory cytokines (Mullen et al., 2006).

As mentioned before, Kv1.3 is a channel that partially targets to lipid raft microdomains. In fact, lymphocytic Kv1.3 rearranges around the immunological synapse (IS), within lipid rafts, co-localizing with the TCR and CD3. An association between Kv1.3 and the TCR/CD3 receptor has been demonstrated by FRET experiments (Panyi et al., 2004). Also, molecular interactions between Kv1.3 and β1-integrin, SAP-97 and PSD-95 and Kvβ2 regulatory subunits have been also reported in these microdomains (Panyi et al. 2004; Cahalan and Chandy 2009; Szilagyi et al., 2013). Kv1.3 localization in lipid rafts is crucial, because methyl-beta-cyclodextrin treatment, which depletes the membrane from cholesterol, disrupts lipid rafts and causes a depolarizing shift of the Kv1.3 channel activation and inactivation and more than two-fold decrease in Kv1.3 currents (Pottosin et al., 2007). Furthermore, segregation of Kv1.3 channels into the IS modifies the gating properties (Toth et al., 2009). In

addition, an alteration in lipid raft formation in some autoimmune diseases such as Sistemic Lupus Erythematous (SLE) has been reported (Nicolaou et al., 2007; Nicolaou et al., 2010). Kv1.3 is also expressed in other tissues, but with less abundance (Bielanska et al., 2009), such as kidney (Yao et al., 1996), bladder (Davies et al., 2002), adipose tissue (Xu et al., 2003), smooth muscle (Cox et al. 2001; Miguel-Velado et al. 2005) and skeletal muscle (Villalonga et al. 2008), osteoclasts (Arkett et al. 1994), testis (Jacob et al. 2000), etc. Kv1.3 expression has been related to many cancers (Bielanska et al. 2009) and plays a role in apoptosis (Bock et al. 2002; Bock et al. 2003; Gulbins et al. 2010; Leanza et al. 2012). In fact, the presence of Kv1.3 in the mitochondrial membrane has been described (Szabo et al. 2005; 2008).

Kv1.3 knock-out mice present a hyperdeveloped olfactory sense and impaired action potentials in the bulb olfactory neurons (Fadool et al. 2004). Though, an enhancement of KNa currents (Slack channel) have been detected in olfactory bulb Kv1.3$^{-/-}$ mice, which may explain part of the olfactory phenotype of these mice (Lu et al. 2010). In addition, Kv1.3$^{-/-}$ presented a decreased body mass, and in the number of fat bodies, due to probably the enhanced nocturnal motor activity and metabolism which these mice exhibit. These mice also present higher longevity (Tucker et al. 2008). Furthermore, animals present an increased expression of some adaptor proteins such as PSD-95, Src, Grb, or 14-3-3, which some of them are involved directly or indirectly with the Kv1.3 activity (Fadool et al. 2004; Szilagyi et al. 2013). The immune system of Kv1.3 knock-out mice developed properly, because similar number of lymphocytes in the

spleen and thymus and no significant difference upon proliferation in response to anti-CD3 were initially found. However, a compensatory up-regulation of chloride currents (Koni et al. 2003) in lymphocytes was detected. Although more evidence demonstrate that $Kv1.3^{-/-}$ mice exhibited a decreased incidence and severity of experimental autoimmune encephalomyelitis (EAE) and a limited proliferative capacity of lymphocytes. $Kv1.3^{-/-}$ mice present significantly more naïve and TCM cells and fewer TEM cells in the lymph node at seven days after immunization than WT, despite of exhibiting similar percentages of $CD4^+$ and $CD8^+$ T cells in spleen and lymph node (Gocke et al., 2012).

1.3. Endocytosis of ion channels

Cellular endocytosis is classically a mechanism for protein internalization and degradation. However, multiple endocytic pathways which are able to define cellular destinations in many ways show that endocytosis means not just reduction of membrane proteins expression. Therefore, we see endocytosis as a mechanism of rapid recycling and redistribution of membrane proteins (Kirchhausen et al. 1996, McMahon et al. 2009, McMahon and Boucrot 2011). Endocytosis serves as a control mechanism of cell surface expression and function of many membrane proteins included ion channels.

Cell can use various mechanisms to internalize plasma membrane proteins (Fig.5), and many proteins are capable of being recruited to different endocytic pathways in response to environmental triggers or as a

result of constitutive or stimulated endocytosis (Trejo et al., 2011, Sigismund et al., 2008). The primary congregation point for most internalized proteins is the Rab5 (Ras-related GTPase 5) positive early endosome (Zhuang et al., 2006, Bonifacino and Traub, 2003). From here, proteins can either transit to recycling endosomes and back to the plasma membrane or are sorted to late endosomes and finally to the lysosome for degradation (Bonifacino and Traub, 2003; Bonifacino and Rojas, 2006; Platta and Stenmark, 2011). An ARF6 (a member of the family of ADP-ribosylation factor) positive compartment operates as an alternative route to direct delivery of cargo to the Rab5 positive early endosomes (Donaldson et al., 2001; Kobayashi and Fukuda, 2013; Chavrier et al., 2003; Radhakrishna and Donaldson, 1997). Proteins targeted to the ARF6 positive compartment can be recycled directly back to the cell surface or pass from there to early endosomes.

The endocytic routes and subsequent trafficking pathways (degradation versus recycling) are specified by structural features or sorting motifs within the cytoplasmic domains of cargo proteins (Bonifacino and Traub 2003; Traub and Bonifacino 2013). These endocytic signals enable binding partners to target the protein into specific pathways. While the molecular details of these processes are still emerging, recognized motifs and modifications have been defined.

The most extensively studied endocytic pathway is clathrin-mediated endocytosis (CME). However, a range of additional clathrin-independent endocytic pathways operate within different cell types and are proposed to account for a significant proportion of protein endocytosis

(Conner and Schmid 2003, Doherty and McMahon 2009, Hsu and Prekeris 2010). Adaptor proteins together with clathrin-associated sorting proteins (CLASPs) recruit cargo into clathrin-coated vesicles of the CME pathway (Ohno 2006, Perrais and Merrifield 2005, Traub 2005). Recruitment relies on recognition of sorting motifs predominantly within the cytosolic termini of cargo protein. A tyrosine motif (YXXϕ; using single amino acid code X represents a variable residue and ϕ a hydrophobic residue) and a di-leucine [DE]XXXL[LI] motif in channel c-termini are recognized by clathrin adaptor protein AP-2 (Bonifacino and Traub 2003). AP-2 binding facilitates recruitment to the clathrin bud and results in channel endocytosis and lysosomal targeting. AP-1 and AP-3 also recognize these motifs but play roles in bidirectional transport between TGN and endosomes and sorting to lysosome (for AP-3 recruited cargo) (Luzio et al 2002, Seaman 2008). A similar motif, DXXLL or acidic cluster/di-leucine motif, is recognised by another member of the ARF family (ARF1) which is localised to the TGN and endosomes and regulates membrane recruitment of AP1 and AP3 (Doray et al. 2012, Nakai et al. 2013). These motifs are thought not to be involved in cargo internalisation or recycling but likely enable sorting of transmembrane proteins from the TGN to endosomes. Cargo bearing an alternative tyrosine motif ([FX]NPXY[FX]), as seen in Kir1.1, are also endocytosed through the CME pathway (Bonifacino and Traub 2003, Chen et al. 1990, Fang et al. 2009). Here, recruitment into clathrin-coated vesicles appears to be independent of AP-2 but depends on CLASP proteins which either contain a phosphotyrosine-binding (PTB) domain and associate with either of PTB proteins, Disabled-2 (Dab2) and the autosomal recessive

hypercholesterolemia (ARH) protein which localize to clathrin-coated structures (Mishra et al. 2002). [FX]NPXY[FX] motifs are also recognized by sorting nexin (SNX) proteins, endocytic proteins which contain phox-homology (PX) domains selective for endosomal phosphatidylinositol 3-phosphate (PtdIns(3)P) and function in cargo internalization and endosomal sorting (Carlton et al. 2005, Teasdale and Collins 2012, van Vliet et al 2003).

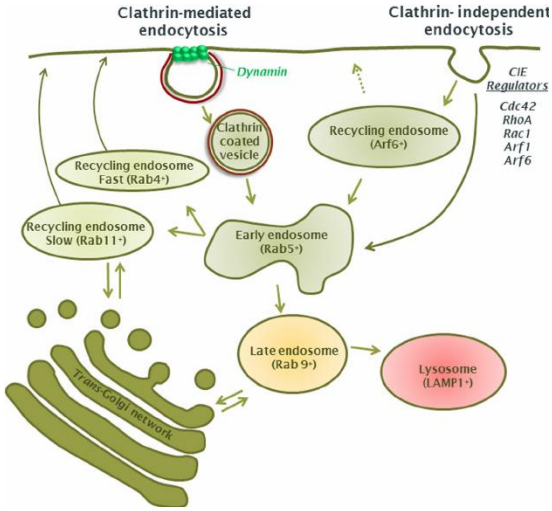

Figure 5. Ion channel endocytic pathways. Clathrin-mediated and clathrin-independent sorting pathways utilised by ion channels. Channels can be internalised by scission of clathrin-coated pits by action of dynamin to produce clathrincoated vesicles which can be sorted to endosomes, lysosomes and trans-Golgi network. Cargo internalised through clathrinin-dependent pathways can also be sorted to the same destinations following their shuffling to the early endosomes (Rab5+). Alternatively, cargo of the clathrin-independent pathway can enter ARF6+ recycling endosomes and return directly to the cell surface or transit to the early endosomes and into the endocytic pathway (recycling or late endosomes) from there. Prominent Rab proteins in each of the compartments are included. Arrows indicate possible direction of sorting between compartments (extracted from O'Kelly, 2014)

1.4. Ubiquitination of ion channels

Ubiquitination is a posttranslational modification that involves the covalent attachment of ubiquitin polypeptides to target proteins. Ubiquitin is a highly conserved polypeptide of 76 amino acids; it contains a diglycine motif at its COOH-terminal end, and it is ligated via this COOH terminus to lysine residues of target proteins (Fig.6). This modification was originally described as a signal that could target cellular proteins to rapid degradation by a cytosolic complex, the proteasome. It turned out to be a highly regulated system that is important for many cellular functions. Ubiquitination was later found to regulate numerous other processes in the cell (not just serving as a degradation signal for the proteasome), including protein trafficking.

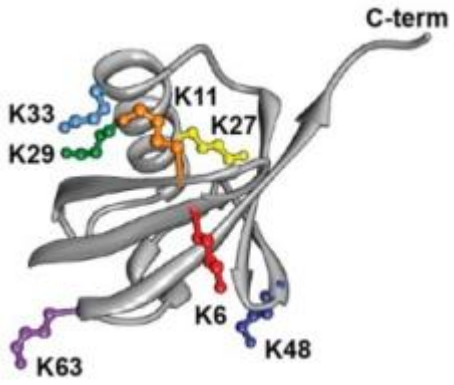

Figure 6. Structure of ubiquitin with seven lysines (adapted from Strieter et al. 2013)

The covalent ubiquitination of proteins is one of the most widespread regulatory posttranslational modifications of proteins. During the ubiquitination the C-terminus of ubiquitin is conjugated to target proteins by the action of three enzymes (Figure 7) a ubiquitin-activating enzyme (E1), a ubiquitin conjugating enzyme (E2), and a ubiquitin protein ligase (E3) (Pickart et al., 2004).

1) Activating enzymes (E1s). The first step consists of the ATP-dependent activation of the carboxyl terminus of ubiquitin (Ub) and its conjugation to the active-site of an E1 through a thiol-ester bond.
2) Conjugating enzymes (E2s). In the second step, Ub is transferred to a similar cysteine residue in the active site of one of more than twenty known E2 enzymes.
3) Ligases (E3s). The final step, which results in the formation of an isopeptide bond with the ε-amino group of a lysine residue in substrate proteins, is accomplished by E3 enzymes. Because E3s select substrates for modification at the correct time and place, there is a large diversity of E3 enzymes. Actually, ubiquitin ligases are emerging as a class of enzymes as important in cellular regulation as kinases.

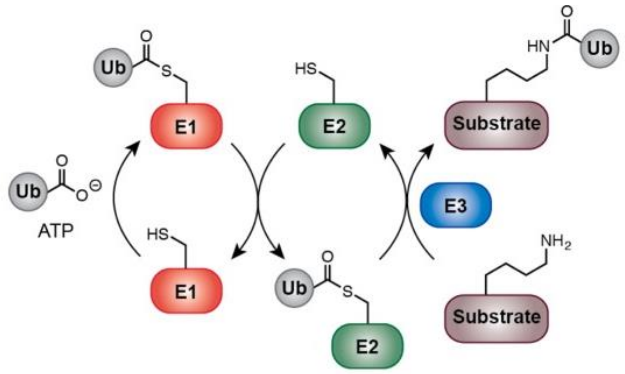

Figure 7. Diagram of ubiquitination process showing the three steps and the involved enzymes (adapted from Strieter et al. 2013)

Two main families of E3s are known: HECT-type (Homologous to the E6-AP Carboxyl Terminus) and RING-type (Really Interesting New Gene). In HECT-E3-mediated catalysis (shown on the right side of Figure 8) ubiquitin is transferred from the E2 to the HECT-E3 (always as a thiol-ester conjugate) and then by the E3 to the substrate (Rotin et al., 2001). In RING-E3-mediated catalysis (shown on the left side of Figure 8) ubiquitin is transferred directly from the E2 to the substrate while the RING-E3 (which is frequently a multisubunit complex) functions as an adaptor between them (Bhownick et al., 2013).

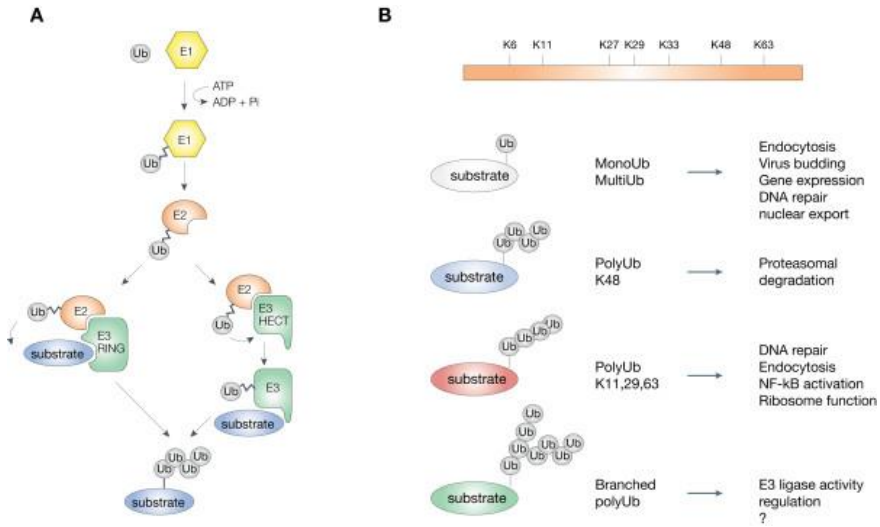

Figure 8. The ubiquitin pathway. (A) Schematic representation of the ubiquitination process. A hierarchical set of three types of enzyme is required for substrate ubiquitination: ubiquitin-activating (E1), ubiquitin-conjugating (E2) and ubiquitin-protein ligase (E3) enzymes. The two major classes of E3 ligases are depicted. (B) Schematic representation of the different Ub modifications with their functional roles (extracted from Polo et al. 2007)

Cellular proteins are modified by various ubiquitin signals: monoubiquitin, multiple monoubiquitin or polyubiquitin chains which can be of diverse length and linkage. There are seven lysine residues in ubiquitin (Lys6, Lys11, Lys27, Lys29, Lys33, Lys48 and Lys63), allowing for seven possible homotypic linkage types and multiple possible heterotypic chains. Each type of ubiquitination can lead the cell to a different destination (Figure 8B).

Ubiquitination plays a critical role in regulating the abundance and localization of many membrane proteins. Direct or indirect conjugation to

protein, such as ion channels, at the cell surface may function as a signal for internalization by triggering the assembly of endocytic machinery (Abriel et al., 2013). Alternatively, the internalization process may occur prior to conjugation, with ubiquitination instead serving to direct endocytosed channel toward a fate of degradation and prevent them from recycling to the surface.

Ion channel ubiquitination is well described for the epithelial sodium channel ENaC. This protein expressed in the distal part of the nephron is involved in sodium homeostasis and blood pressure control (Kellenberger et al., 2002). The channel consists of three subunits each containing two transmembrane domains, one extracellular loop and short intracellular N and C- terminals. Ubiquitination of ENaC targets the channel to lisosomal degradation through clathrin-mediated endocytosis (Rotin et al., 2000). Ubiqutination of ENaC channel occurs as a response of PKC activation which can be stimulated by phorbol esters (Chaibalin et al., 1999).

1.5. Protein Kinases involved in Kv1.3 internalization.

Protein kinases are important regulators of intracellular signal transduction pathways that mediate the development and regulation of many proteins. They play critical roles in cell growth, division, differentiation, adhesion, motility, and death. More than 500 protein kinases have been identified in the human genome (Sudarsanam et al. 2002). Based on their catalytic specificity, they can be subdivided into

tyrosine (Tyr, Y)- and serine (Ser, S)/threonine (Thr, T)-specific kinases. Their activity is usually highly regulated to mediate their cellular function and physiological responses. Normal cellular protein kinases can be positively upregulated by phosphorylation, dephosphorylation, protein cleavage, translocation, ligand/second-messenger or ion binding, dimerization or oligomerization, activating subunit interaction, and protein-protein or protein-lipid interactions. The activity of protein kinases is also governed by negative feedback systems, which can attenuate or terminate kinase activity and thus their induced downstream signals. Several mechanisms serve to negatively regulate kinase activity, including, in the case of ligand-induced receptor tyrosine kinase signaling, antagonistic ligands, heterooligomerization with truncated receptors, phosphorylation, dephosphorylation, endocytosis, protein degradation, and reduction of receptor mRNA, all of which serve as means of downregulation (Hunter, 2000).

1.5.1. Protein kinase C (PKC)

The protein kinase C (PKC) is a family of 11 isoenzymes. All PKC enzymes are single polypeptide composed of an N-terminal regulatory region and a C-terminal catalytic region (Newton et al., 1995). Most of PKC isoenzymes have a cysteine-rich C1 domain which forms the diacylglycerol/phorbol ester binding site. Diacylglycerol (DAG) is a PKC activator and phorbol esters, such as PMA (phorbol-12-myristate-13-acetate), can mimic it. Phorbol esters are stable in the cell therefore

effects last longer, which helps in the study of PKC signaling in vivo (Ron et al., 1999).

PKC is activated at the membrane and consequently induces increased membrane traffic. Its association with the membrane leads to its own movement along with the budding vesicles. The PKC is ultimately sorted and degraded. Catalytically inactive PKC is able to associate with membranes through functional regulatory domains and is passively drawn into the vesicle traffic and degraded. Activated PKC involves many cellular functions such as regulation of receptor desensitization and internalization, regulation of transcription, mediation in immune responses, regulation of cell growth and also regulation of endocytosis and trafficking (Alvi et al., 2007). PMA-induced PKC downregulation is observed in most cell types. Under action of PMA, PKC is regulating secretory and endocytic processes in mammalian cells. Kv1.3 is a target of PKC that upon activation reduces currents in Jurkat T cells (Kuras et al., 2012).

1.5.2. Protein kinase A (PKA)

PKA is the major intracellular target of cAMP. At low cAMP concentration, PKA exists mainly as an inactive tetrameric holoenzyme composed of two regulatory and two catalytic subunits. Activation of PKA occurs when four molecules of cAMP bind to the regulatory subunits, promoting the dissociation of the PKA holoenzyme into two active catalytic subunits and a dimer of regulatory subunits (Taylor et al., 2013). The two PKA isozymes differ in their regulatory subunits: PKA

type I (PKA-I) containing RIa or RIb and PKA type II (PKA-II) containing RIIa or RIIb. The importance of the relative cellular ratio between PKA-RI and PKA-RII has already been reported, supporting the idea that specific functions can be assigned to PKA isozymes mediating the distinct effects of cAMP in cellular processes such as growth and differentiation (Schwartz and Rubin, 1985; Ogreid et al., 1989; Rohlff et al., 1993; Cho-Chung et al., 1995; Kopperud et al., 2003; Ji et al., 2008; Pidoux and Tasken, 2010).

The cAMP/PKA signaling system constitutes an inhibitory pathway in T cells and, although its biochemistry has been thoroughly investigated, its possible effects on ion channels are still not fully understood. Kv1.3 channels play an important role in T-cell activation, and their inhibition suppresses T-cell function. It has been reported that PKA modulates Kv1.3 activity (Vang, et al., 2001). Two PKA isoforms are expressed in human T cells: PKAI and PKAII. PKAI has been shown to inhibit T-cell activation via suppression of the tyrosine kinase Lck (Ruppelt et al., 2007). 8-Bromoadenosine 3′,5′-cyclic monophosphate (8-BrcAMP), a nonselective activator of PKA, inhibited Kv1.3 currents both in primary human T and in Jurkat cells (Torgersen et al., 2002).

1.5.3. ERK1/2

Extracellular signal-regulated kinase 1 and 2 (Erk1/2) are central regulators of cellular proliferation, survival, and motility, and the mechanisms governing their activation have been extensively studied

(Cheung and Slack, 2004; Roux and Blenis, 2004; Viala and Pouyssegur, 2004). Erk1/2 is activated by phosphorylation, mediated by the dual-specificity kinase MEK, which in turn is activated by the Raf kinase (Torii et al., 2004b). Scaffold proteins play a key role in Erk activation by binding multiple components of the Raf MEK Erk module to promote signal transduction, amplification, and specificity.

ERK activation could dually regulate the Kv channel subunits at the transcriptional and post-translational levels (Berbard et al. 2004). ERK could directly phosphorylate the subunits of the ion channels, which were characterized by changes in the gating properties of the channels, such as upon acute regulation of the fast-transient outward K^+ current by growth factors (Dourado and Drye 1994, Yang et al. 2001).

1.5.4. Receptor Tyrosine Kinases

Receptor tyrosine kinases comprise over half of the 90 tyrosine kinases in the human genome (Manning et al. 2002). Most of them bind to specific protein ligands, such as growth factors and cytokines, via their extracellular domain, which results in activation of the cytoplasmic catalytic domain upon ligand-mediated oligomerization and phosphorylation of cytoplasmic proteins, thereby transducing extracellular signals across the plasma membrane (Hunter 2000). The EGF receptor family of tyrosine kinases has four members—EGFR, ErbB2, ErbB3, and ErbB4. EGFR, ErbB3, and ErbB4 bind ligands in the EGF family. EGFR, ErbB2, and ErbB4 are active kinases, whereas ErbB3

lacks catalytic activity. Upon ligand binding, these receptors can heterodimerize, thus generating distinct intracellular signals depending on the combination. For instance, ligand-induced interaction of any of the three active receptors in combination with ErbB3 results in activation of the PI3-K pathway (Blume-Jensen and Hunter 2001).

Receptor endocytosis is a regulatory mechanism that promotes constant and partial -regulated signaling by localizing receptors to signaling endosomes and by promoting receptor recycling to the cell surface (von Zastrow and Sorkin 2007, Schenck et al. 2008, Zoncu et al. 2009). Alternatively, endocytosis can lead to signal attenuation by culminating in receptor degradation. EGFR endocytosis is initiated by EGF binding to EGFR dimers at the plasma membrane (Chung et al. 2010). Stabilization of EGFR dimers promotes EGFR activation and trans-phosphorylation. Active EGFR is ubiquitinated by the E3 ligase Cbl, a posttranslational modification that recruits the endocytic machinery. Both clathrin-dependent (Goh et al. 2010) and clathrin-independent (Sigismund et al. 2005, Orth and McNiven 2006) pathways contribute to EGFR endocytosis. EGF mediates inhibition of the Shaker-type channels Kv1.2 and Kv1.3 (Bowlby et al. 1997; Tsai et al. 1997; Qiu et al. 2003). It is reported that EGF modulates Kv1.3 current (Holmes et al., 1997). EGF-mediated tyrosine phosphorylation decrease channel activity and reveal as potential modulator of Kv1.3 turnover.

2. Objectives

Kv1.3 channel plays a key role in a wide range of physiological phenomenon. For instance, the channel has been implicated in cell secretion, volume regulation, proliferation, T-lymphocyte activation and neuronal activity. In this work we focused on the Kv1.3 implication in the immune and nervous systems. We wanted to analyse whether an appropriate activity depends not only on the channel expression but also on the localization and abundance on the cell surface. The presence of Kv1.3 on the cell surface can be modulated by endocytosis. In this context, we aim to investigate mechanisms of Kv1.3 endocytosis.

Therefore, the specific objectives of the PhD dissertation were:

1. Mechanism of EGF-induced endocytosis of Kv1.3
2. PMA and Adenosine induced ubiquitin-mediated endocytosis of Kv1.3
3. Signaling pathways involved in the modulation and turnover of the channel
4. Deciphering the molecular determinants involved in the channel ubiquitination

3. Results

3.1. Part One:

Unconventional EGF-induced ERK1/2-mediated Kv1.3 endocytosis.

Published in final edited form as: Cell Mol Life Sci. 2016 Apr; 73(7): 1515–1528.
Published online 2015 Nov 5. doi: 10.1007/s00018-015-2082-0

Unconventional EGF-induced ERK1/2-mediated Kv1.3 endocytosis

Ramón Martínez-Mármol,[1,2] Núria Comes,[1] Katarzyna Styrczewska,[1] Mireia Pérez-Verdaguer,[1] Rubén Vicente,[3] Lluís Pujadas,[2] Eduardo Soriano,[2,4,5] Alexander Sorkin,[6] and Antonio Felipe[1,7]

[1]Molecular Physiology Laboratory, Departament de Bioquímica i Biologia Molecular, Institut de Biomedicina (IBUB), Barcelona, Spain

[2]Departament de Biologia Celular, Universitat de Barcelona, Barcelona, Spain

[3]Laboratory of Molecular Physiology and Channelopathies, Departament de Ciències Experimentals i de la Salut, Universitat Pompeu Fabra, Barcelona, Spain

[4]Centro de Investigación Biomédica en Red sobre Enfermedades Neurodegenerativas (CIBERNED), ISCIII, Madrid, Spain

[5]Vall *d* Hebron Institute of Research (VHIR) and Institució Catalana de Recerca i Estudis Avançats (ICREA), Barcelona, Spain

[6]Department of Cell Biology, University of Pittsburgh School of Medicine, Pittsburgh, PA, USA

[7]Departament de Bioquímica i Biologia Molecular, Universitat de Barcelona, Avda. Diagonal 643, 08028 Barcelona, Spain

Abstract

The potassium channel Kv1.3 plays roles in immunity, neuronal development and sensory discrimination. Regulation of Kv1.3 by kinase signaling has been studied. In this context, EGF binds to specific receptors (EGFR) and triggers tyrosine kinase-dependent signaling, which down-regulates Kv1.3 currents. We show that Kv1.3 undergoes EGF-dependent endocytosis. This EGF-mediated mechanism is relevant because is involved in adult neural stem cell fate determination. We demonstrated that changes in Kv1.3 subcellular distribution upon EGFR activation were due to Kv1.3 clathrin-dependent endocytosis, which targets the Kv1.3 channels to the lysosomal degradative pathway. Interestingly, our results further revealed that relevant tyrosines and other interacting motifs, such as PDZ and SH3 domains, were not involved in the EGF-dependent Kv1.3 internalization. However, a new, and yet undescribed mechanism, of ERK1/2-mediated threonine phosphorylation is crucial for the EGF-mediated Kv1.3 endocytosis. Our results demonstrate that EGF triggers the down-regulation of Kv1.3 activity and its expression at the cell surface, which is important for the development and migration of adult neural progenitors.

Report of the PhD student participation

Unconventional EGF-induced ERK1/2-mediated Kv1.3 endocytosis.

Katarzyna Styrczewska carried out the experiments and data analysis corresponding to the figure 5 A , 5 D-L, figure 7 A-D and 7 H in the article.

Antonio Felipe

PhD thesis director

Cell. Mol. Life Sci. (2016) 73:1515–1528
DOI 10.1007/s00018-015-2082-0

Cellular and Molecular Life Sciences

ORIGINAL ARTICLE

Unconventional EGF-induced ERK1/2-mediated Kv1.3 endocytosis

Ramón Martínez-Mármol[1,2] · Núria Comes[1] · Katarzyna Styrczewska[1] · Mireia Pérez-Verdaguer[1] · Rubén Vicente[3] · Lluís Pujadas[2] · Eduardo Soriano[2,4,5] · Alexander Sorkin[6] · Antonio Felipe[1,7]

Received: 28 April 2015 / Revised: 14 October 2015 / Accepted: 26 October 2015 / Published online: 5 November 2015
© Springer Basel 2015

Abstract The potassium channel Kv1.3 plays roles in immunity, neuronal development and sensory discrimination. Regulation of Kv1.3 by kinase signaling has been studied. In this context, EGF binds to specific receptors (EGFR) and triggers tyrosine kinase-dependent signaling, which down-regulates Kv1.3 currents. We show that Kv1.3 undergoes EGF-dependent endocytosis. This EGF-mediated mechanism is relevant because is involved in adult neural stem cell fate determination. We demonstrated that changes in Kv1.3 subcellular distribution upon EGFR activation were due to Kv1.3 clathrin-dependent endocytosis, which targets the Kv1.3 channels to the lysosomal degradative pathway. Interestingly, our results further revealed that relevant tyrosines and other interacting motifs, such as PDZ and SH3 domains, were not involved in the EGF-dependent Kv1.3 internalization. However, a new, and yet undescribed mechanism, of ERK1/2-mediated threonine phosphorylation is crucial for the EGF-mediated Kv1.3 endocytosis. Our results demonstrate that EGF triggers the down-regulation of Kv1.3 activity and its expression at the cell surface, which is important for the development and migration of adult neural progenitors.

Keywords Olfactory bulb · Sensory neurons · Map kinases · Tyrosine kinases · Endocytosis · Voltage-dependent potassium channels

Electronic supplementary material The online version of this article (doi:10.1007/s00018-015-2082-0) contains supplementary material, which is available to authorized users.

✉ Antonio Felipe
afelipe@ub.edu

[1] Molecular Physiology Laboratory, Departament de Bioquímica i Biologia Molecular, Institut de Biomedicina (IBUB), Barcelona, Spain

[2] Departament de Biologia Celular, Universitat de Barcelona, Barcelona, Spain

[3] Laboratory of Molecular Physiology and Channelopathies, Departament de Ciències Experimentals i de la Salut, Universitat Pompeu Fabra, Barcelona, Spain

[4] Centro de Investigación Biomédica en Red sobre Enfermedades Neurodegenerativas (CIBERNED), ISCIII, Madrid, Spain

[5] Vall dHebron Institute of Research (VHIR) and Institució Catalana de Recerca i Estudis Avançats (ICREA), Barcelona, Spain

[6] Department of Cell Biology, University of Pittsburgh School of Medicine, Pittsburgh, PA, USA

[7] Departament de Bioquímica i Biologia Molecular, Universitat de Barcelona, Avda. Diagonal 643, 08028 Barcelona, Spain

Introduction

The dentate gyrus of the hippocampal formation and the subventricular zone (SVZ) of the forebrain are considered the main loci of adult neurogenesis [1]. Cellular proliferation in the SVZ of healthy adult rodents supplies progenitor cells to the olfactory bulb (OB) via the rostral migratory stream (RMS), where they contribute to the replacement of granular and periglomerular neurons [2]. However, in response to injury, SVZ cells proliferate, migrate and differentiate into specific neuronal populations, astrocytes and oligodendrocytes [3]. Epidermal growth factor (EGF) is a mitogen involved in regulating neural stem cell proliferation and differentiation. Infusion of EGF into the lateral ventricle not only modulates proliferation but also results in SVZ cells altering their migration from their normal route and into adjacent areas

of the brain [4]. Therefore, the role of EGF-mediated effects in the neural precursors of the SVZ is essential for their final differentiation and function. The EGF receptor (EGFR) is expressed at high levels in the nervous system and exhibits regionalized patterns of distribution during the initial phases of development and in the adult [5]. EGFR activation initiates a downstream serine/threonine and tyrosine phosphorylation-based signaling cascade that modulates the activity of a wide range of heterogeneous proteins, including ion channels [6].

Voltage-gated potassium channels (Kv) have a crucial role in excitable cells by determining the resting membrane potential and controlling action potentials [7]. The Kv1.3 channel controls action potential firing of hippocampal and OB neurons, accounting for up to 60–80 % of the outward K^+ currents [8]. This channel is also predominantly expressed in the mitral and granule nerve cell layers and in postganglionic sympathetic neurons, as well as in brain progenitor cells [9]. Interestingly, the gene-targeted deletion of the Kv1.3 channel (Kv1.3$^{-/-}$) generates mice with altered interneuron populations of the cerebral cortex, and a highly developed olfactory function due to an increase of olfactory coding units in the OB [10]. The Kv1.3 channel is also critical in leukocytes participating in physiological responses such as cell proliferation, activation or migration [11, 12]. Kv1.3 can be phosphorylated by receptor (EGFR, TrkB and insulin receptor) and non-receptor tyrosine kinases (src and leukocyte-specific protein tyrosine kinase (Lck)), modulating channel kinetics and current amplitude [8, 10, 13–18]. In addition to kinase signaling, evidence has shown that the prevalence of Kv1.3 channels at the membrane surface have enormous consequences for cell physiology [19–22]; thus, ion channel-induced endocytosis mechanisms have attracted considerable attention. Ion channels, such as ENaC, K_{ATP} and CFTR, are internalized via clathrin-mediated endocytosis (CME) [23–25]. Furthermore, endocytosis is a mechanism for tyrosine kinase-dependent suppression of the neuronal Kv1.3-related channel Kv1.2 [26]. However, Kv1.3 tyrosine-phosphorylation is not accompanied by channel endocytosis [27]. Thus, it remains unclear whether Kv1.3 suppression may involve endocytosis as a relevant turnover mechanism.

Here, we report that suppression of Kv1.3 activity upon incubation with EGF was partially due to specific channel internalization. EGFR activation triggers channel endocytosis through a clathrin-dependent mechanism, which is independent of putative EGF-mediated Kv1.3 tyrosine phosphorylation. Interestingly, EGF mediates channel endocytosis via a novel ERK1/2-dependent threonine phosphorylation mechanism. This EGF-dependent Kv1.3 down regulation is crucial for the understanding of the proliferative and migratory behavior of specific neuronal populations of the forebrain.

Materials and methods

Animals, primary culture of SVZ explants and neuronal stem precursors cells (NSPCs) grown as neurospheres and immunohistochemistry

All of the experiments and surgical protocols were performed in accordance with the guidelines approved by the ethical committee of the Universitat de Barcelona following the European Community Council Directive 86/609 EEC. P5 newborn mice were anesthetized with 4 % halothane and were transcardially perfused with 4 % paraformaldehyde dissolved in phosphate buffer 0.12 M (pH 7.2–7.4). After perfusion, the brains were removed from the skull and postfixed in the same solution for an additional 12 h, cryoprotected in 30 % sucrose, and coronally sectioned on a freezing microtome (30 µm thick). Free-floating sections were permeabilized with PBS containing 0.5 % Triton X-100 and blocked with 10 % normal goat serum. The brain sections were incubated with anti-Kv1.3 (1:500 Alomone) and anti-EGFR (1:500, SantaCruz) antibodies and visualized using secondary fluorescent antibodies (Alexa 488 and 568, 1:1000, Invitrogen). Immunoreagents were diluted in PBS containing 0.5 % Triton X-100, 0.2 % gelatin, and 5 % pre-immune serum.

Experiments studying SVZ explant migration have been previously documented [28]. Briefly, SVZ explants were obtained as previously described [29]. P1–P3 newborn mice were anesthetized by hypothermia and then euthanized by rapid decapitation. Brains were removed and placed in ice-cold dissection medium (0.6 % glucose in PBS). After vibratome sectioning, the SVZ from the lateral wall of the anterior horn of the lateral ventricle was dissected out from the appropriate section and cut into pieces of 100–300 mm in diameter. The explants were mixed with Matrigel (BD Bioscience) and cultured in four-well dishes. After polymerization for 10 min, the gel was overlaid with 0.5 ml of growth medium (Neurobasal medium containing 0.5 mM L-glutamine and penicillin–streptomycin antibiotics and 2 % B-27). Cultures were maintained in a humidified, 5 % CO_2, 37 °C incubator for 7 days. EGF (10 ng/ml) and 30 nM Margatoxin, an inhibitor of Kv1.3, were added to the medium. After 7 days in vitro, tissue cultures were fixed with paraformaldehyde (4 % in 0.1 M PBS) and type-B astrocytes were visualized immunostaining against GFAP (1:1000, Dako), followed by Alexa 488 secondary antibodies (1:500, Invitrogen). Images were acquired using an Olympus Scan^R wide field microscope (10× objective lenses) and automated 5 × 6 mosaic acquisition was performed using Scan^R software. Mosaics were reconstructed using the FIJI Stitching plugin and the signal intensity was analyzed using the FIJI Radial Profile

Plot plugin. Plotted values represent the integrated intensity of concentric circles emerging from the center of the explants. Neuronal stem precursor cells (NSPC) grown as neurospheres were obtained from the SVZ of P1–P3 newborn mice as previously described [30] in growth medium supplemented with 2 % B27 and 20 ng/ml EGF and bFGF (R&D System). Twenty-four hours after the 3rd passage, neurospheres were transferred to poly-D-lysine-coated dishes, and electrophysiology of the adherent cells was performed 16 h later. For immunostaining, neurospheres were embedded in rat tail Collagen I (BD Biosciences), fixed with paraformaldehyde (4 % in 0.1 M PBS) and processed for immunodetection. Primary cultures of SVZ-derived cells were obtained by culturing SVZ-derived cells for 8–12 h in growth medium supplemented with 2 % B27. Finally, neurospheres and SVZ cells were immunostained against Kv1.3 (rabbit, Alomone 1:500; mouse, NeuroMab 1:250), EGFR (rabbit, SantaCruz 1:250) and Nestin (mouse, R&D Systems 1:500). Images were obtained using a Leica SP2 Spectral Confocal microscope.

Expression plasmids and site-directed mutagenesis

The rat Kv1.3 in pRcCMV construct was provided by T.C. Holmes (New York University, NY). The channel was subcloned into pEYFP-C1 (Clontech). The rKv1.3 construct that was externally tagged with HA between S3 and S4 was obtained from D.B. Arnold (University of Southern California, CA). All Kv1.3 mutants were generated in the pEYFP-Kv1.3 channel. Single and multiple Kv1.3 mutants were generated using the QuikChange and QuikChange multi-site-directed mutagenesis kits (Stratagene). All mutations were verified using automated DNA sequencing. The pEGFR-GFP construct has been extensively characterized by Sorkin's laboratory [31].

Cell culture, transfections and EGF incubations

HEK-293 and HeLa cells were grown in DMEM containing 10 % FBS and 100 U/ml penicillin/streptomycin. For the confocal analyses, cells cultured in the same medium were plated on poly-lysine-coated coverslips. Transfection was performed using Metafectene^{TM} Pro (Biontex) when cells reached nearly 80 % confluence. For transient transfection, the cells were washed in PBS (without K^+), fixed with 4 % paraformaldehyde in PBS for 10 min and mounted with Aqua Poly/Mount from Polysciences, Inc. at 24 h after transfection. Because HeLa cells express a high number of endogenous EGFR [32], a HeLa cell line with stable Kv1.3-YFP expression was generated. Twenty-four hours after transfection, cells were selected in the presence of 500 µg/ml G418. Geneticin-resistant clones were isolated and maintained in the presence 250 µg/ml G418. In some experiments, transiently transfected HEK-293 and HeLa cells were pre-incubated with 50 µM erbstatin or 10 µM U0126, respectively, for 1 h prior to incubation with EGF. Cells cultured for 24 h in the absence of serum were further incubated for 1 h at 4 °C in the presence of 10 ng/ml or 4 ng/ml EGF-rhodamine, for HEK and HeLa cells, respectively, and transferred to 37 °C for the desired times before analysis.

Protein extraction, co-immunoprecipitation, biotinylation of cell surface proteins and western blot analysis

Cells were washed twice in cold PBS. Next, they were lysed on ice with NHG solution (1 % Triton X-100, 10 % glycerol, 50 mM HEPES pH 7.2, 150 mM NaCl) supplemented with 1 µg/ml aprotinin, 1 µg/ml leupeptin, 1 µg/ml pepstatin and 1 mM phenylmethylsulfonyl fluoride to inhibit proteases. The homogenates were centrifuged at 16,000×*g* for 15 min, and the protein content was measured using the Bio-Rad Protein Assay (Bio-Rad).

The samples were pre-cleared with 30 µl of protein G-Sepharose beads for 2 h at 4 °C with gentle mixing as part of the co-immunoprecipitation procedure. The beads were then removed by centrifugation at 1000×*g* for 30 s at 4 °C. The sample was then incubated overnight with the desired antibody (4 ng/µg protein) at 4 °C with gentle agitation. Thirty microliters of protein G-Sepharose were added to each sample, and the samples were incubated for 4 h at 4 °C. The beads were removed by centrifugation at 1000×*g* for 30 s at 4 °C, washed four times in NHG, and resuspended in 80 µl of SDS sample buffer.

Cell surface biotinylation was carried out with the Pierce® Cell Surface Protein Isolation Kit (Pierce) following manufacturer's instructions. Cell surface proteins were labeled with sulfosuccinimidyl-2-(biotinamido)ethyl-1,3-dithiopropionate (Sulfo-NHS-SS-biotin; Pierce) as previously described. Briefly, cells were treated with lysis buffer and clear supernatant was reacted with immobilized NeutrAvidin gel slurry in columns (Pierce) to isolate surface proteins. Surface proteins were resolved on a SDS-PAGE gel and analyzed by western blot analysis against Kv1.3.

Protein samples (50 µg) and immunoprecipitates were then boiled in Laemmli SDS loading buffer and separated by 10 % SDS-PAGE. Next, samples were transferred to nitrocellulose membranes (Immobilon-P, Millipore) and blocked in 5 % dry milk-supplemented with 0.05 % Tween 20 in PBS before the immunoreaction. Filters were then immunoblotted with antibodies against HA (1/200, Sigma), GFP (1/1000, Roche), T-ERK1/2, P-ERK1/2 and P-Thr (1/1000, Cell signaling), P-Tyr (1/2000, Sigma), Clathrin heavy chain (1/500, BD Bioscience), Dynamin II (1/1000, ABR) and β-actin (1/50,000, Sigma).

Confocal microscopy and subcellular compartment identification

Staining with specific markers to label subcellular compartments was performed on permeabilized cells. Cells fixed with 4 % paraformaldehyde in PBS for 10 min were further permeabilized using 0.1 % Triton for 10 min. After a 60 min incubation with a blocking solution (10 % goat serum/5 % non-fat dry milk/PBS), the cells were treated with anti-clathrin heavy chain (1/100, BD Bioscience) or anti-EEA1 (1/1000, BD Bioscience) in 10 % goat serum/0.05 % Triton and again incubated for 1 h. Next, the cells were further incubated for 45 min with an Alexa Fluor antibody (1/500, Molecular Probes) in PBS. All experiments were performed at room temperature. In some experiments, the cells were washed with PBS and stained with Lyso Tracker® red (1/1000, Molecular Probes) for 30 min at 4 °C. The amount of internalized Kv1.3-YFP channel (arbitrary units) was calculated by using a pixel by pixel analysis, taking into account the relative amount of intracellular signal versus the total signal in control experiments versus different conditions. Cells were examined with a 63× oil immersion objective on a Leica TCS SL laser scanning confocal microscope. All offline image analyses were performed using a Leica confocal microscope, Image J software and Sigma Plot.

siRNA transfections

Synthetic siRNAs for CHC and Dynamin II were purchased from Thermo Fisher Scientific. Duplexes were resuspended in 1 × siRNA universal buffer (Thermo Fisher Scientific) to 20 µM. HeLa cells expressing the stable Kv1.3-YFP channel were grown in six-well plates to 50 % confluence. Cells were transfected with siRNA duplexes at a final concentration of 120 nM in 5 µl DharmaFECT1 reagent (Thermo Fisher Scientific). After 36 h, a second transfection was performed, and the cells were replated in 12-well plates on the next day for internalization experiments. To assess the efficiency of knockdown, total cell lysates were resolved on 7.5 or 10 % SDS-PAGE depending on the protein of interest and probed by western blotting. Mock- or siRNA-transfected cells were processed for immunofluorescence as described above.

Antibody feeding endocytosis assay

Cells grown on glass coverslips or 96-well plates were incubated with 1–2 µg/ml of anti-HA11 (1/1000, Covance) in DMEM for 30–60 min at 18–20 °C, washed twice and incubated at 37 °C in the presence or in the absence of 4 ng/ml EGF-rhodamine for 30 min. The cells were then washed with ice-cold Ca^{2+}, Mg^{2+}-free PBS (CMF-PBS) and fixed with freshly prepared 4 % paraformaldehyde for 8 min at room temperature. The cells were stained with anti-mouse secondary antibody conjugated with Cy5 (5 µg/ml, saturating concentration) in CMF-PBS containing 0.5 % BSA at room temperature for 60 min to label the HA11 antibody on the surface. After washing, the cells were permeabilized in CMF-PBS containing 0.1 % Triton X-100 for 10 min at room temperature, and then incubated with the same secondary conjugated with Cy3 (1 µg/ml, non-saturating concentrations) for 60 min to stain internalized HA11. Both primary and secondary antibody solutions were precleared by centrifugation at 100,000×g for 20 min. After staining, cells were washed and the coverslips were mounted in Mowiol (Calbiochem).

Internalization of EGF-rhodamine

To highlight the intracellular EGF-enriched vesicles which colocalized with endocytosed Kv1.3 in HeLa cells, an acid wash protocol was performed as previously described [33]. As the acid wash removes completely the EGF-rhodamine attached to cell surface, only intracellular EGF-rhodamine remained in acid wash-treated cells. Briefly, cells cultured in 12-well dishes were incubated with EGF-rhodamine (4 ng/ml) in binding medium (DMEM, 20 mM HEPES, 0.1 % BSA) at 37 °C for 30 min. After incubation, the remaining EGF was removed from cell surface by a 5 min incubation with a prechilled mild acid wash (0.2 M sodium acetate, 0.5 M NaCl, pH 4.5) or binding medium wash (no acid). Samples were processed for fluorescence microscopy as above.

Electrophysiology

Whole-cell currents were recorded using the patch-clamp technique in the whole-cell configuration with a HEKA EPC10 USB amplifier (HEKA Elektronik). PatchMaster software (HEKA) was used for data acquisition. We applied a stimulation frequency of 50 kHz and a filter at 10 kHz. The capacitance and series resistance compensation were optimized. In most experiments, we obtained an 80 % compensation of the effective access resistance. Micropipettes were prepared from borosilicate glass capillaries (Harvard Apparatus) using a P-97 puller (Sutter Instrument) and fire polished. The pipettes had a resistance of 2–4 MΩ. For the stably transfected HeLa cells, pipettes were filled with a solution containing (in mM): 120 KCl, 1 $CaCl_2$, 2 $MgCl_2$, 10 HEPES, 10 EGTA, and 20 D-glucose (pH 7.3 and 280 mOsm/l). The extracellular solution contained (in mM): 120 NaCl, 5.4 KCl, 2 $CaCl_2$, 1 $MgCl_2$, 10 HEPES and 25 D-glucose (pH 7.4 and 310 mOsm/l). To record the currents of SVZ neurons we used an intracellular solution containing (in mM): 145 KF, 1 $MgCl_2$, 10 HEPES,

10 EGTA (pH 7.2). The extracellular solution for the native currents contained (in mM): 160 NaCl, 4.5 KCl, 2 $CaCl_2$, 1 $MgCl_2$, and 5 HEPES (pH 7.4). Cells were clamped at a holding potential of −60 mV. To evoke voltage-gated currents, all cells were stimulated with a 250-ms square pulse from −60 to +70 mV. The peak amplitude (pA) was normalized using the capacitance values (pF). Data analysis was performed using FitMaster (HEKA) and Sigma Plot 10.0 software (Systat Software). All recordings were performed at room temperature (21–23 °C).

Results

EGFR and Kv1.3 are expressed in SVZ-derived neurons and cooperate in their differentiation

The SVZ of the forebrain supplies progenitor cells to OB where EGF is a major growth factor [5]. Furthermore, the genetic depletion of Kv1.3 produces a super-smeller phenotype, which would suggest that EGF-dependent down-regulation of Kv1.3 would be an important determinant for olfactory capacities [10, 13]. Therefore, we first confirmed Kv1.3 expression in the OB (Fig. 1a). In addition, Kv1.3 partially colocalized with EGFR in the SVZ, which is a main locus of adult neurogenesis, (Fig. 1b). To gain further insights, we cultured isolated NSPCs and confirmed the co-expression of EGFR and Kv1.3 (Fig. 1c, d) in Nestin-positive SVZ-derived progenitor cells. Nestin was used to identify multipotent neuronal stem cells. Next, we generated SVZ-derived neurospheres, which were subsequently allowed to differentiate. Neurosphere-derived neurons were heavily stained for Kv1.3 (Fig. 1e). In addition, K^+ currents elicited in neurospheres diminished upon EGF incubation (Fig. 1f). Surprisingly, K^+ currents, in the absence but not in the presence of EGF, were efficiently blocked by 100 nM MgTx, suggesting that Kv1.3 plays a major role in neuronal stem cells (NSC). We next studied the relevance of Kv1.3 and EFG in SVZ explant migration and differentiation by GFAP staining (Fig. 1g). We found that both 10 ng/ml EGF (0.37 ± 0.04, $p < 0.001$) and 100 nM MgTx (0.20 ± 0.02, $p < 0.01$) notably increased neuronal migration and differentiation (vs control, 0.13 ± 0.02; Student's t test at 500 µm) (Fig. 1h, i). Furthermore, incubation with both EGF and MgTx further enhanced the areas containing SVZ-derived migrating cells, suggesting synergistic cooperation of both pathways (0.50 ± 0.06, $p < 0.001$). Together, our results demonstrate that Kv1.3 and EGFR are co-expressed in the SVZ in vivo as well as in SVZ-derived NSPCs and that the suppression of Kv1.3 channel activity leads to a marked increase in both neurogenesis and migration in the SVZ.

EGF-mediated Kv1.3 endocytosis in HEK-293 cells

Although tyrosine kinase receptor activation triggers the endocytosis of channels and EGF efficiently inhibits Kv1.3 currents, their ability to induce Kv1.3 endocytosis remains controversial [13, 26]. Therefore, we incubated EGFR and Kv1.3 co-transfected HEK-293 cells with EGF (10 ng/ml). EGF activated the EGFR as demonstrated by the detection of tyrosine phosphorylated EGFR (Supplementary Fig. 1A). As expected, EGFR also underwent endocytosis in these cells (Supplementary Fig. 1B). Supplementary Fig. 1C and D demonstrated that Kv1.3 currents were diminished by EGF and that the blockade of the tyrosine kinase-EGFR activity by Erbstatin abolished this effect. EGF reduced Kv1.3 activity via a tyrosine kinase-dependent mechanism without affecting the abundance of the Kv1.3 protein (Supplementary Fig. 1E).

Next, we monitored the time course of Kv1.3 distribution in the presence of EGF. Figure 2 demonstrated that EGF caused Kv1.3 endocytosis. In the absence of EGF, Kv1.3 and EGFR were primarily localized at the cell surface (Fig. 2a–c); EGF incubation triggered the co-internalization of Kv1.3 and the EGFR (Fig. 2d–o). After 2 min of EGF incubation, only a few vesicles containing Kv1.3/EGFR/EGF were observed (Fig. 2d–g). However, longer periods of time triggered a massive increase in the number of intracellular vesicles with Kv1.3, EGFR and EGF colocalization (Fig. 2h–o). Co-immunoprecipitation studies (Fig. 2p) demonstrated that although Kv1.3 and EGFR shared intracellular compartments, the proteins did not associate. Similar negative results were obtained by Fluorescence Resonance Energy Transfer (FRET) studies between EGFR-CFP and Kv1.3-YFP.

EGF-dependent Kv1.3 endocytosis via clathrin-coated pits targeted the channel to lysosomes

To further investigate EGF-mediated Kv1.3 endocytosis, we used the HeLa cell line. HeLa cells express a significant amount of endogenous EGFR; therefore, the EGF-dependent signal transduction pathway is well preserved [32]. In addition, we generated a Kv1.3 stable HeLa cell line. Because Kv1.3 turnover is very rapid, we first wanted to decipher whether Kv1.3-containing vesicles were indeed a consequence of EGF-dependent endocytosis. Some intracellular Kv1.3 staining was observed in the absence of EGF (Supplementary Fig. 2A-B). When cells were incubated with non-saturating EGF concentrations (4 ng/ml), endocytic vesicles containing Kv1.3 were detected (Supplementary Fig. 2C-H). A mild acid wash eliminates excess unbound EGF at the cell surface and facilitates the analysis of the intracellular distribution of EGF and Kv1.3 (Supplementary Fig. 2F–H). Thus, the acid-wash magnified the Kv1.3-YFP/EGF-rhodamine colocalization

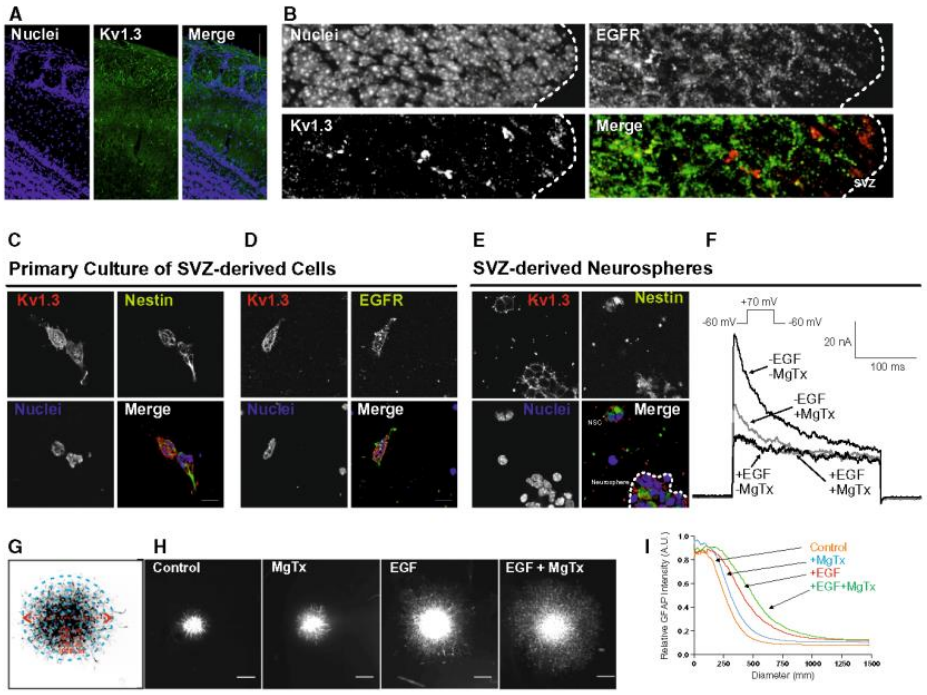

Fig. 1 Kv1.3 and EGFR colocalized in the brain and neuronal precursor cells. **a** Kv1.3 is present in the OB. OB slices were obtained and stained for Kv1.3 (*green*) and DAPI (*blue*). *Bar* represents 20 μm. **b** Kv1.3 colocalized with EGFR in the SVZ of the forebrain. SVZ explants were analyzed for Kv1.3 and EGFR. The *merge panel* indicates colocalization (*yellow*) within the SVZ. **c**, **d** Kv1.3 and EGFR colocalized in primary cultures of SVZ-derived cells. **c** Kv1.3 colocalized with Nestin, a marker of neuronal precursors. **d** Kv1.3 colocalized with EGFR in Nestin-positive cells. The *merge panels* indicate colocalization of these proteins in the same cell. **e** Expression of Kv1.3 in SVZ-derived neurospheres. Neurospheres were obtained from SVZ-derived cells and cultured as described in the "Materials and Methods". Nestin was used as a marker for NSCs. The *merge panel* highlights the expression of Kv1.3 in Nestin-positive neurospheres. **f** Voltage-dependent K^+ currents were evoked in neurospheres, incubated with or without EGF, as indicated by pulse protocols. Currents were inhibited by 100 nM Margatoxin only in the absence of EGF. **g**–**i** Effects of EGF and MgTx on the migration and differentiation of SVZ astrocytes. **g** GFAP intensity and distance from the core of the spot was used as a marker of differentiation and migration. **h** $GFAP^+$ cells ($n = 10$–15) were incubated in the presence and the absence of EGF and MgTx and images were captured for quantification. *Bars* represent 500 μm. **i** Quantification of the relative GFAP intensity from the core of the spot. Note that the incubation of EGF plus MgTx (*green*) was additive over EGF (*red*) or MgTx (*blue*) alone

because a notable decrease in the background signal corresponding to non-internalized rhodamine fluorophore was observed (compare Supplementary Fig. 2E and H). An "antibody feeding" assay paradigm has proven to be critical for deciphering the PKC-dependent endocytosis of the dopamine transporter (DAT) [34]. In HeLa cells transfected with HA-Kv1.3, the channels stained with Cy5-labeled antibodies were distributed as numerous small clusters throughout the plasma membrane (Supplementary Fig. 2I, L). In the absence of EGF, some Cy3-labeled intracellular vesicles were observed, which may correspond to endosomes containing constitutively internalized channels (Supplementary Fig. 2J). However, upon EGF incubation, an increase of Kv1.3 containing Cy3-labeled vesicles was noted (Supplementary Fig. 2M). Our results indicated that the intracellular complexes of the channel were inaccessible to the Cy5-labeled secondary antibodies applied to non-permeabilized cells, thereby confirming that the internal Cy3-labeled channels were indeed triggered by EGF (Supplementary Fig. 2L-N).

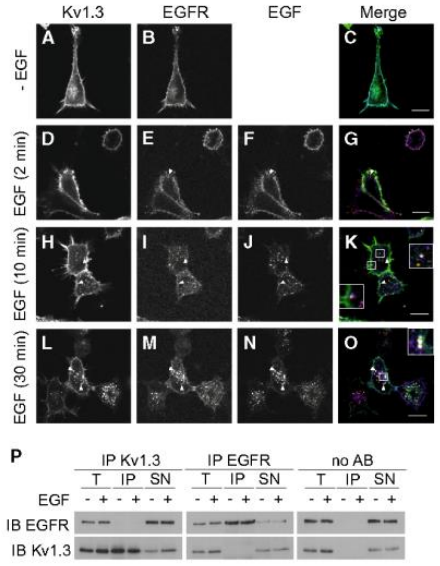

Fig. 2 EGF steadily increased Kv1.3 colocalization, but did not promote association with endocytosed EGFR. **a**–**o** Representative confocal images of HEK293 cells that were transiently co-transfected with Kv1.3-YFP (**a**, **d**, **h**, **l**, and *green in merge panels*) and EGFR-CFP (**b**, **e**, **i**, **m**, and *blue in merge panels*). Cells were incubated with 10 ng/ml EGF-rhodamine (**f**, **j**, **n**, and *red in merge panels*) for 2, 10 and 30 min at 37 °C. EGF-dependent EGFR endocytic vesicles (*pink*) were seen after 2 min (*arrowheads* in **e**–**g**). However, triple EGF-dependent EGFR and Kv1.3-containing vesicles (*white*) were observed after longer times of EGF incubation (*arrowheads* in **k** and **o**). *Insets* show magnification areas. *Bars* represent 10 µm. **p** Kv1.3 did not co-immunoprecipitate with EGFR. Cells were co-transfected with HA-Kv1.3 and EGFR-CFP and incubated in the presence (+) or in the absence (−) of 10 ng/ml EGF for 15 min. Lysates were immunoprecipitated (IP) with anti-HA (Kv1.3) and anti-GFP (EGFR) antibodies. No AB, absence of antibody. Filters were immunoblotted (IB) with anti-HA (Kv1.3) and anti-GFP (EGFR) antibodies. No co-IP was observed between the channel and the receptor. *T* total lysate, *IP* immunoprecipitate, *SN* supernatant

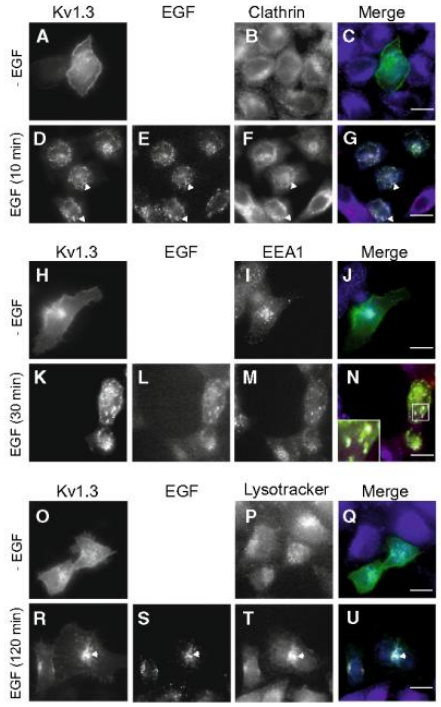

Fig. 3 Deciphering the steadily EGF-dependent Kv1.3 internalization pathway with endocytic markers in HeLa cells. Representative confocal images of HeLa cells that stably express Kv1.3-YFP. Cells were incubated in the absence (−EGF) or presence (+EGF) of EGF-rhodamine (4 ng/ml) at 37 °C during different times. (**a**–**g**) Cells were incubated for 10 min and stained with antibodies against CHC. (**h**–**n**) Cells were incubated for 30 min and stained with an anti-EEA1 antibody. (**o**–**u**) Cells were incubated with EGF-rhodamine for 120 min and with 50 nM LysoTracker for 30 min. Upon EGF incubation, triple colocalization was observed in structures containing Kv1.3, EGF and clathrin (**d**–**g**, *arrowheads*); Kv1.3, EGF and EEA1 (**n**, *inset*); and Kv1.3, EGF and LysoTracker (**r**–**u**, *arrowhead*). Color code in *merge panels*: Kv1.3 (*green*), EGF (*red*) and markers (*blue*). *Bars* represent 10 µm

EGF activation caused accumulation of Kv1.3 in vesicular endocytic structures moving from peripheral to perinuclear areas. This occurred concomitantly with a decrease in the plasma membrane fluorescence (Fig. 3a, g). To further characterize the EGF-dependent Kv1.3 endocytic mechanisms, markers of each intracellular compartment were used. Thus, after 10 min, Kv1.3 and EGF colocalized with CHC, a marker of clathrin-coated pits (CCP) (Fig. 3a–g). After 30 min of EGF incubation, Kv1.3 and EGF distributed within early endosomes, which were labelled with EEA1 (Fig. 3h–n). Similar results were obtained with other markers such as AP2 and Transferrin Receptor (TfnR). Finally, to examine whether Kv1.3 is targeted to the late endosomes and lysosomes due to EGFR activation, the localization of the channel was compared with that of the late endosome marker, Lyso Tracker® Red (Fig. 3o–u). Our results demonstrated that EGF triggered a down regulation of the Kv1.3 channel on the membrane surface via CCP that facilitated Kv1.3 turnover through lysosomal degradation.

To decipher the mechanisms involved in clathrin-mediated EGF-dependent Kv1.3 endocytosis, we incubated the HeLa cells with siRNAs against CHC and dynamin II (Fig. 4). Both clathrin and dynamin II are crucial for the CME of TfnR, EGFR and DAT [35, 36]. Both siRNAs effectively depleted CHC and dynamin II (Fig. 4a, b), although depletion was not complete (estimated more than 95 %) as shown in Fig. 4o (clathrin-positive staining encircled the cell). Under these conditions, HeLa cells stably expressing Kv1.3 and transfected with CHC siRNA were incubated without (Fig. 4j–l) or with (Fig. 4m–p) EGF for 30 min at 37 °C. No significant EGF-dependent internalization of Kv1.3 was observed in siRNA-depleted CHC cells (compare Fig. 4m, f). In addition, TfnR internalization is typically halted by Dynamin II depletion (Fig. 4r, v). Concomitantly, EGFR activation-induced Kv1.3 endocytosis was also abolished with a specific siRNA for dynamin II (Fig. 4q–w; compare Fig. 4t, f). Together, the efficient inhibition of Kv1.3 endocytosis in CHC- and dynamin II-depleted cells demonstrated that CCP-mediated endocytosis is the main pathway for EGFR-induced Kv1.3 internalization.

EGF-mediated Kv1.3 endocytosis via ERK1/2 threonine phosphorylation

EGF triggered CCP-mediated Kv1.3 endocytosis, targeting the channel to the lysosomes and thereby controlling Kv1.3 turnover. Therefore, we wanted to decipher the structural elements responsible for this event. We first confirmed that EGFR-tyrosine kinase activity was responsible for the Kv1.3 endocytosis. Thus, Erbstatin efficiently inhibited the EGF-dependent endocytosis of Kv1.3 (Supplementary Fig. 3A-E). The role of several important tyrosines in the Kv1.3 channel activity has been analyzed, and raised controversial results because the evidence suggests that those residues were not related to the channel internalization [27]. To decipher whether Kv1.3 tyrosines may be involved in the EGF-dependent endocytosis, we mutated all of the internal tyrosines of the channel. The Kv1.3-Yless channel was fully functional and, similar to Kv1.3 wild-type, EGF inhibited K^+ currents, although to a lesser extent (Supplementary Fig. 3F,G). This diminished effect confirmed the role of Tyr phosphorylation on the Kv1.3 activity. Surprisingly, Kv1.3-Yless underwent EGF-dependent endocytosis, as observed by colocalization with intracellular EGF (Supplementary Fig. 3H–L). Therefore, our results confirm that the tyrosines within Kv1.3, which are involved in the EGF-dependent down regulation of the Kv1.3 activity, are not responsible for channel internalization. Accordingly, we also studied other Kv1.3 structural elements (Supplementary Fig. 4). Kv1.3 contains

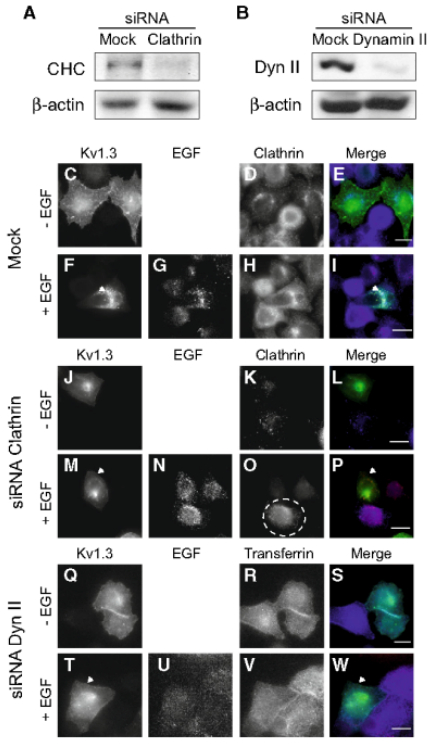

Fig. 4 EGF-dependent Kv1.3 internalization is governed by clathrin-mediated endocytosis. Confocal images and western blot analysis of HeLa cells stably expressing Kv1.3-YFP. Cells were transfected without (Mock) or with siRNAs against Clathrin Heavy Chain (CHC) and Dynamin II (Dyn II). Cell lysates were blotted with antibodies against Clathrin, Dyn II, and β-actin. Western blots demonstrated the depletion of CHC (**a**) and Dyn II (**b**). (**c**–**w**) Cells mock transfected (**c**–**i**) or transfected with siRNAs to CHC (**j**–**p**) or Dyn II (**q**–**w**) were incubated with (+EGF) or without (−EGF) 4 ng/ml EGF-rhodamine for 30 min at 37 °C. **c**–**p** Cells were stained with anti-Clathrin antibodies. **q**–**w** Cells were also incubated in the presence of Transferrin-Texas Red (5 μg/ml). As observed in **a**, low numbers of clathrin-positive cells were found and *circled* in **o**. Color code in *merge panels*: Kv1.3 (*green*), EGF (*red*) and clathrin/transferrin (*blue*). *Arrowheads* highlight Kv1.3 either intracellular (**f**–**i**) or at the membrane (**m**–**p** and **t**–**w**). *Bars* represent 10 μm

two proline-rich stretches (^{38}PLPPALP^{44} and ^{493}PQTP^{496}), which interact with SH3-containing signaling molecules in the EGFR pathway. In addition, Kv1.3 possesses a PDZ domain at the distal C-terminal end that has been implicated in targeting the channel to membrane raft

microdomains [37]. Both, the Kv1.3-Pless (no prolines, Supplementary Fig. 4F–J) and the Kv1.3T523X (no PDZ domain, Supplementary Fig. 4K–O) channels were endocytosed upon EGF incubation, similar to Kv1.3 wt (Supplementary Fig. 4A-E), demonstrating that those elements are not involved in EGF-mediated Kv1.3 endocytosis.

Activation of the EGF signaling cascade elicits a rapid phosphorylation of p42/44 MAPK (ERK1/2) [38]. ERK1/2 kinases participate in the suppression of ENaC activity [39]. To date, no ERK1/2 phosphorylation sites have been described in Kv1.3, although the channel contains a putative ERK phosphorylation consensus motif (^{493}PQTP^{496}). Therefore, we wondered whether a new, and not yet identified, ERK1/2 mechanism was responsible for the EGF-mediated Kv1.3 endocytosis (Fig. 5). We first analyzed ERK1/2 activation in the Kv1.3 HeLa cell line. The presence of EGF induced ERK1/2 phosphorylation (p42/44 MAPK) without varying their total amount (Fig. 5a). In this context, U0126, an inhibitor of ERK1/2, decreased the levels of P-ERK1/2 and counteracted the EGF-dependent decrease of biotinylated Kv1.3 at the cell surface. Concomitantly, U0126 blocked the EGF-dependent down regulation of Kv1.3 currents (Fig. 5b, c). These results indicate that ERK1/2 is indeed involved in the down-regulation of Kv1.3 by EGF. As mentioned above, the down-regulation of Kv1.3 by EGF has dual roles: (i) tyrosine kinase-dependent inhibition of K^+ currents and (ii) tyrosine kinase-independent mediated endocytosis. Therefore, we analyzed the role of ERK1/2 in EGF-dependent Kv1.3 endocytosis. EGF-dependent Kv1.3 endocytosis was efficiently neutralized by U0126 (Fig. 5d–m). Whether ERK1/2 kinases participated in the EGF-dependent Kv1.3 endocytosis was further analyzed in primary culture SVZ-derived cells (Fig. 6). ERK1/2 kinases were phosphorylated by EGF concomitantly to an increase of endocytosed Kv1.3 (Fig. 6a–f). In addition, EGF triggered the internalization of the EGFR which notably colocalized with endocytosed Kv1.3 (Fig. 6g–l). Finally, we mutated T495 within the putative ERK1/2 consensus motif of Kv1.3. The T495A mutation did not affect the Kv1.3 distribution in the absence of EGF (Fig. 7a). However, the EGF-mediated Kv1.3 (T495A) endocytosis was absent in the presence of EGF (Fig. 7b–e). Similar results were obtained with a glutamate mutation of the T495 (not shown). Concomitantly, Kv1.3 (T495A) currents were not down-regulated by EGF (Fig. 7f–g). Furthermore, unlike Kv1.3 wt, the T495A mutant underwent no Thr-phosphorylation upon EGF incubation (Fig. 7h). Our data demonstrated that ERK1/2 kinases specifically mediate the EGF-dependent Kv1.3 endocytosis through T495 phosphorylation, which is located at the C-terminal domain of the channel.

Discussion

Evidence indicates that the abundance of ion channels at the cell membrane is a crucial factor controlling their signal intensity. Thus, deciphering the mechanisms regulating the balance between forward traffic and internalization are essential. Ion channels, such as ENaC, Kv1.2, Kir1.1 and CFTR, undergo endocytosis via CCP through tyrosine kinase-dependent and -independent phosphorylation, and this mechanism is involved in controlling channel surface levels and activity [23, 25, 26, 40]. In this scenario, although Kv1.3 tyrosine kinase phosphorylation and its consequences have been extensively studied in lymphocytes and neurons, no internalization evidence had been observed. Using an extensive repertoire of complementary techniques, we demonstrate here that Kv1.3 undergoes notable EGF-induced CME via a novel mechanism that involves p42/44 MAPK (ERK1/2) kinases. EGF and Kv1.3 inhibition act synergistically in the proliferative behavior of NSC from the SVZ. Kv1.3 activity is reduced by EGFR activation in an unconventional dual pathway, comprising both tyrosine phosphorylation-dependent inhibition of channel activity and threonine phosphorylation-dependent internalization of the channel. Together, these results suggest that Kv1.3 activity is quickly reduced by EGF with important consequences in neurogenesis.

The adult mammalian brain contains NSC that generate neurons and glia cells throughout the whole life of an organism [41]. NSC reside in at least two proliferative niches in the adult brain, the SVZ of the lateral ventricles and the subgranular zone of the hippocampus [41]. EGF is a potent mitogen that triggers the proliferation, survival, migration and differentiation of neurons and SVZ type-B astrocytes [4]. Cell proliferation in the SVZ supplies new neurons that eventually become incorporated into the existing functional brain networks [41]. The EGF-stimulated progenitors are highly migratory, which facilitates neural tissue repair [42]. On the other hand, Kv1.3 is implicated in cell growth and differentiation of a wide diversity of cells [11, 43]. Kv1.3 is selectively distributed in the OB, the cerebral cortex, the dentate gyrus of the hippocampus and in brain progenitor cells [44]. The involvement of Kv1.3 in controlling the proliferation of adult neural precursor cells (NPC) remains controversial. Although some authors could not confirm the pharmacological expression of Kv1.3 in adult NPC, others identified gene and protein expression in adult rat mesencephalic-derived neurospheres, NPCs and oligodendrocyte progenitor cells (OPCs) [43, 45–47]. We found Kv1.3 in both the SVZ in vivo and in NSCs derived from the SVZ. We also detect functional Kv1.3 channels in progenitor cells from

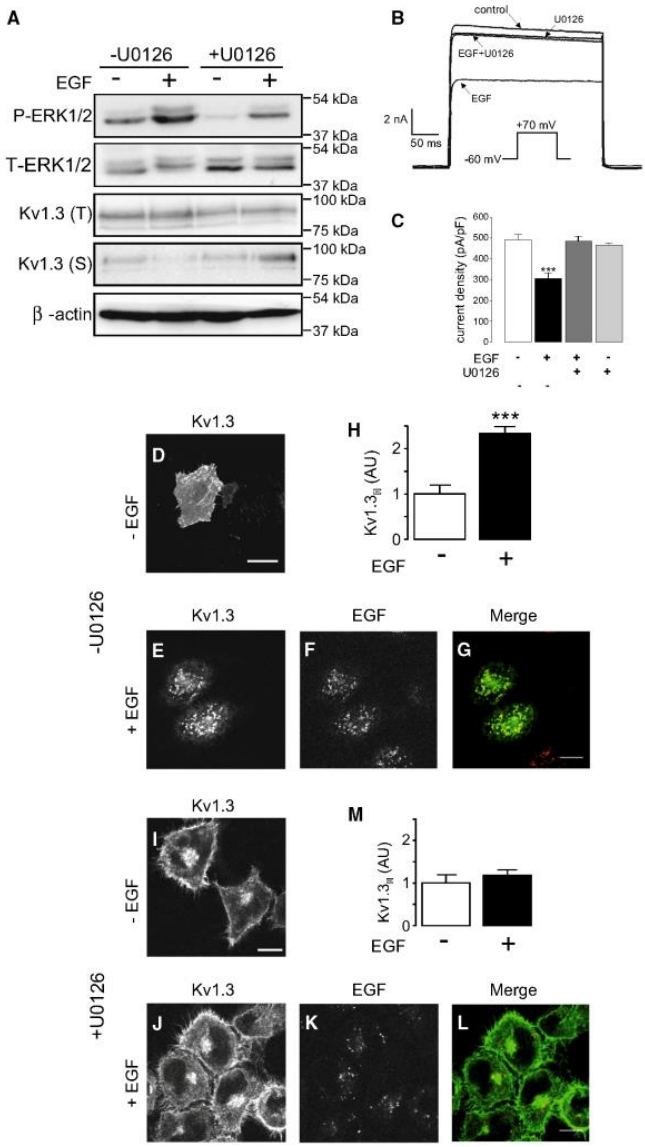
A
-U0126
+U0126
EGF
P-ERK1/2
T-ERK1/2
Kv1.3 (T)
Kv1.3 (S)
β -actin
54 kDa
37 kDa
100 kDa
75 kDa
B
control
U0126
EGF+U0126
EGF
2 nA
50 ms
+70 mV
-60 mV
C
current density (pA/pF)
EGF
U0126
D
Kv1.3
- EGF
H
Kv1.3β (AU)
EGF
-U0126
+ EGF
E
F
G
EGF
Merge
I
M
Kv1.3α (AU)
+U0126
J
K
L

◀**Fig. 5** Effect of ERK1/2 activity on EGF-dependent Kv1.3 endocytosis. HeLa cells stably expressing Kv1.3-YFP were treated for 15 min prior to and during EGF stimulation with (+) or without (−) 10 μM U0126. Cells were incubated with (+EGF) or without (−EGF) 4 ng/ml EGF-rhodamine for 30 min at 37 °C. **a** Western blot analysis for active/phosphorylated ERK (p-ERK1/2) and biotinylated Kv1.3 at the cell surface in the presence (+) or the absence (−) of U0126 with (+) or without (−) EGF. Filters were further reprobed for total ERK (T-ERK1/2) and β-actin as loading controls. Note that upon EGF incubation, the induction of P-ERK1/2 was notably affected by presence of U0126. Furthermore, while the total expression of Kv1.3 (T) remained similar, the amount of Kv1.3 at the surface (S) was reduced by EGF in the absence of U0126. **b** Voltage-dependent K^+ currents were evoked by a 250 ms depolarizing pulse from −60 to +70 mV. U0126 halted the EGF-dependent inhibition of K^+ currents. **c** Current density in pA/pF. ***$P < 0.001$ vs—EGF (*white column*) (Student's *t* test). The results are the mean ± SEM of 8–10 cells. (**d**–**m**) Representative images of Kv1.3 HeLa cells in the presence (+) or the absence (−) of EGF with (+) or without (−) U0126. **d**–**g** EGF-dependent Kv1.3 endocytosis in the absence of U0126. **i**–**m** EGF-dependent Kv1.3 endocytosis in the presence of U0126. **g**, **l** Kv1.3 (*green*) and EGF (*red*) in *merge panels*. (**h**, **m**) Relative quantification of intracellular Kv1.3 ($Kv1.3_{(i)}$) in the absence (*white column*) or the presence (*black column*) of EGF with (**m**) and without (**h**) U0126. ***$P < 0.001$ vs absence of EGF (Student's *t* test). The results are the mean ± SEM of 15–20 cells. Note that U0126 impaired the EGF-dependent Kv1.3 endocytosis. *Bars* represent 10 μm

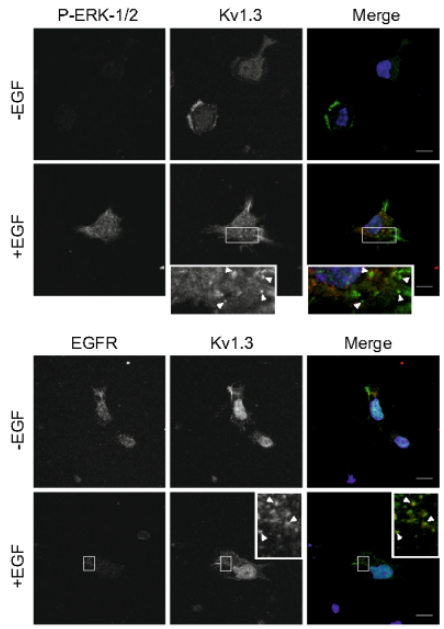

Fig. 6 EGF-dependent ERK1/2 phosphorylation, EGFR internalization and Kv1.3 endocytosis in primary culture SVZ-derived cells. Cells were incubated with (+EGF) or without (−EGF) 10 ng/ml EGF for 15 min at 37 °C. **a**–**f** Representative images of P-ERK1/2 and Kv1.3. In the presence of EGF, activated form of ERK1/2 (P-ERK1/2) was homogeneously distributed throughout the cell whereas Kv1.3 concentrated in intracellular vesicles (see *inset* for details). **g**–**l** EGFR and Kv1.3 colocalized in intracellular vesicles in the presence of EGF (see *inset* for magnification). Color in *merge panels*: Kv1.3 in *green* (**c**, **f**, **i**, **l**), P-ERK1/2 in *red* (**c**, **f**) and EGF in *red* (**i**, **l**). *Arrow heads* highlight Kv1.3 enriched vesicles. *Bars* represent 10 μm

neurospheres derived from the posterior SVZ (pSVZ). Selective blockage of Kv1.3 increased adult murine mesencephalic NPC proliferation, using the model of long-term cultured neurospheres under non-differentiating conditions. Furthermore, granzyme B (GrB) released by T cells increased the expression of Kv1.3 within NPC, inhibiting proliferation and neuronal differentiation [48]. Our results showed a reinforcement of the EGF effect by blocking Kv1.3 on SVZ-derived explants. This suggests that EGFR activation and down-regulation of Kv1.3 acts synergistically to promote NSC proliferation and migration.

In agreement with the EGFR/Kv1.3 colocalization in the SVZ of the brain, receptor tyrosine kinases, such as EGFR and the insulin receptor, target Kv1.3 activity by tyrosine phosphorylation of the channel without endocytosis [27]. The balance between forward traffic and internalization fine tunes ion channel surface abundance and function [22]. The specific molecular mechanisms mediating K^+ channel endocytosis are poorly understood. In this vein, a dominant negative form of dynamin blocks Kv1.2 internalization, and Kir1.1 is also regulated by tyrosine kinases in a process involving dynamin and clathrin-dependent endocytosis [26, 40]. Furthermore, ENac is present in CCP and co-immunoprecipitates with clathrin adaptor proteins [23].

We observed a major colocalization between Kv1.3 and EGFR in internalized vesicles after EGF addition, and the depletion of dynamin II and CHC with specific siRNAs supported a CCP-dependent mechanism of Kv1.3 internalization. As we demonstrated, Kv1.3 current reduction in the presence of EGF is also partially due to CCP-mediated channel endocytosis, but unlike Kv1.2 and Kir1.1, this mechanism was independent of tyrosine kinase phosphorylation of the channel [26, 40]. Thus, an Y132F mutation within the N-terminus of Kv1.2 confers resistance to phosphorylation-dependent suppression of Kv1.2 ionic currents and to channel endocytosis. Although Kv1.3 has several tyrosines, only Y479 has been described as being responsible for EGFR-mediated Kv1.3 current suppression, and non-specific channel internalization was postulated as a potential accompanying mechanism [8]. Phosphorylated tyrosines could be recognized by a variety of src homology 2 (SH2) domain-containing proteins. The adaptor protein

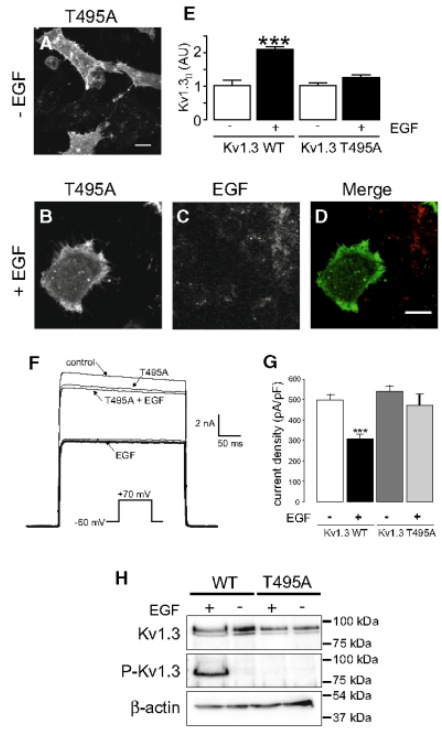

Fig. 7 The Kv1.3 (T495A) mutant did not undergo EGF-dependent endocytosis. HeLa cells were transiently transfected with the Kv1.3-YFP (T495A) mutant channel. Cells were incubated with (+EGF) or without (−EGF) 4 ng/ml EGF-rhodamine for 30 min at 37 °C. **a–d** Representative images of Kv1.3 (T495A) in the presence (+) or the absence (−) of EGF. **a** Kv1.3 (T495A) in the absence of EGF. **b–d** Kv1.3 (T495A) in the presence of EGF. **d** Kv1.3 (*green*) and EGF (*red*) in *merge panel*. *Bars* represent 10 μm. **e** Relative quantification in arbitrary units (AU) of intracellular ($Kv1.3_{(i)}$) Kv1.3 wt and Kv1.3 (T495A) in the absence (*white column*) or the presence (*black column*) of EGF. $***P < 0.001$ vs Kv1.3 wt in the absence of EGF (Student's *t*-test). The results are the mean ± SEM of 15–25 cells. Note that Kv1.3 (T495A) did not undergo EGF-dependent Kv1.3 endocytosis. **f** Voltage-dependent K^+ currents were evoked by a 250 ms depolarizing pulse from −60 to +70 mV. **g** Current density in pA/pF. $***P < 0.001$ vs Kv1.3 wt in the absence of EGF (*white column*) (Student's *t* test). The results are the mean ± SEM of 8–10 cells. **h** Western blot analysis for total Kv1.3 and Thr-phosphorylated-Kv1.3 (P-Kv1.3) in the presence (+) or the absence (−) of EGF. Filters were further reprobed for β-actin as loading control. Note that Kv1.3 (T495A) underwent no phosphorylation in Thr (P-Kv1.3) in the presence of EGF

nShc contains a SH2 domain and interacts with Kv1.3. However, our Kv1.3 (Y-less) mutant confirms and extents previous data indicating that SH2-interacting mechanisms are not involved in EGFR-dependent Kv1.3-mediated endocytosis. Several partners could link EGFR activation and downstream signaling cascades with channel endocytosis. Grb10 is a SH3 (Src homology 3) adaptor protein that co-immunoprecipitates with Kv1.3 in the OB and hippocampus [17]. SH3 domains mediate assembly of specific protein complexes by binding to proline-rich signatures in their targets. In this respect, Kv1.5 regulation by tyrosine kinases involves the SH3 domain-mediated physical interaction of src kinase with the channel protein [15]. Furthermore, PSD-95, an adaptor which contains PDZ and SH3 domains, interacts with Kv1.3 through a PDZ domain at the C-terminal end of the channel [37]. The PSD-95 SH3-guanylate kinase (GK) domain functionally modulates Kv1.3 and blocks the insulin-dependent channel phosphorylation [49]. However, our results indicate that these canonical Kv1.3 motifs, which interact with adaptor partners, were not involved in EGF-induced Kv1.3 endocytosis. Moreover, these experiments strongly reinforce that EGFR does not physically interact with Kv1.3. Alternatively, EGF controls sodium absorption, modulating ENaC surface expression via ERK1/2 activation in renal cells independent of tyrosine kinase activity [39]. Surprisingly, no ERK1/2 phosphorylation had been described for Kv1.3. Unlike other K^+ channels, Kv1.3 would be modulated by EGF similarly to ENaC, affecting neural stem cell fate. It is tempting to speculate that because Kv1.3 is the major K^+ channel entity in the sensory neuron physiology, EGF effectively regulates the channel in a dual unconventional pathway, which is comprised of both tyrosine phosphorylation-dependent inhibition of the activity, common to K^+ channels, and threonine phosphorylation-dependent internalization to fine tune cell responses.

In summary, we demonstrated that EGF triggers Kv1.3 current down-regulation by tyrosine phosphorylation and also a CME via a new, unconventional ERK1/2 kinase-dependent mechanism. Our results have important physiological significance. Kv1.3 is emerging as a promising target for developing new pharmacological agents against inflammation-associated neurodegenerative diseases, such as multiple sclerosis (MS) or brain infarction. Elevated levels of Kv1.3 may be associated with a negative prognosis in autoimmune neurodegenerative diseases [50, 51]. Moreover, EGFR signaling in vivo is involved in oligodendrocyte development and remyelination repair. Accordingly, EGF administration has been used therapeutically to counteract demyelination processes [52]. Our

results show an additive effect of EGF in SVZ-derived progenitors when Kv1.3 is also pharmacologically inhibited. It is tempting to speculate a putative synergistic role of EGF-signaling and Kv1.3 function in controlling the multiple and complementary pathways during the progression of demyelinating disorders. As a consequence, modulation of these two elements may control the progression of neurodegenerative diseases. Kv1.3 inhibition with therapeutic compounds, such as analogs of a sea anemone toxin or psoralene derivatives, would decrease the cytotoxic effect of MS-infiltrates acting simultaneously on activated lymphocytes and proliferating OPCs [53, 54]. Thus, EGF supplementation might be a useful adjunctive for Kv1.3 inhibition in the treatment of MS and brain damage (e.g., after hypoxia). Simultaneous control of EGF activity and Kv1.3 function may provide a more effective way to control the growth, proliferation and differentiation of stem cells used for the treatment of neurodegenerative disorders or regeneration of the CNS.

Acknowledgments Supported by the Ministerio de Economía y Competitividad (MINECO), Spain (BFU2014-54928-R and CSD2008-00005 to AF; SAF2013-42445-R to ES). MPV and KS hold fellowships from the MINECO. RMM and NC were supported by the Juan de la Cierva program (MINECO). AS was supported by NIH grants DA014204 and CA089151.

References

1. Lledo PM, Alonso M, Grubb MS (2006) Adult neurogenesis and functional plasticity in neuronal circuits. Nat Rev Neurosci 7:179–193
2. Menezes JR, Smith CM, Nelson KC, Luskin MB (1995) The division of neuronal progenitor cells during migration in the neonatal mammalian forebrain. Mol Cell Neurosci 6:496–508
3. Lichtenwalner RJ, Parent JM (2006) Adult neurogenesis and the ischemic forebrain. J Cereb Blood Flow Metab 26:1–20
4. Doetsch F, Petreanu L, Caille I, Garcia-Verdugo JM, Alvarez-Buylla A (2002) EGF converts transit-amplifying neurogenic precursors in the adult brain into multipotent stem cells. Neuron 36:1021–1034
5. Wong RW, Guillaud L (2004) The role of epidermal growth factor and its receptors in mammalian CNS. Cytokine Growth Factor Rev 15:147–156
6. Sashihara S, Tsuji S, Matsui T (1998) Oncogenes and signal transduction pathways involved in the regulation of Na+ channel expression. Crit Rev Oncog 9:19–34
7. Hille B (2001) Ion channels of excitable membranes, 3rd edn. Sinauer, Sunderland
8. Fadool DA, Levitan IB (1998) Modulation of olfactory bulb neuron potassium current by tyrosine phosphorylation. J Neurosci 18:6126–6137
9. Doczi MA, Morielli AD, Damon DH (2008) Kv1.3 channels in postganglionic sympathetic neurons: expression, function, and modulation. Am J Physiol Regul Integr Comp Physiol 295:R733–R740
10. Fadool DA, Tucker K, Perkins R, Fasciani G, Thompson RN, Parsons AD, Overton JM, Koni PA, Flavell RA, Kaczmarek LK (2004) Kv1.3 channel gene-targeted deletion produces "Super-Smeller Mice" with altered glomeruli, interacting scaffolding proteins, and biophysics. Neuron 41:389–404
11. Vicente R, Escalada A, Coma M, Fuster G, Sanchez-Tillo E, Lopez-Iglesias C, Soler C, Solsona C, Celada A, Felipe A (2003) Differential voltage-dependent K+ channel responses during proliferation and activation in macrophages. J Biol Chem 278:46307–46320
12. Villalonga N, David M, Bielanska J, Gonzalez T, Parra D, Soler C, Comes N, Valenzuela C, Felipe A (2010) Immunomodulatory effects of diclofenac in leukocytes through the targeting of Kv1.3 voltage-dependent potassium channels. Biochem Pharmacol 80:858–866
13. Bowlby MR, Fadool DA, Holmes TC, Levitan IB (1997) Modulation of the Kv1.3 potassium channel by receptor tyrosine kinases. J Gen Physiol 110:601–610
14. Holmes TC, Fadool DA, Levitan IB (1996) Tyrosine phosphorylation of the Kv1.3 potassium channel. J Neurosci 16:1581–1590
15. Holmes TC, Fadool DA, Ren R, Levitan IB (1996) Association of Src tyrosine kinase with a human potassium channel mediated by SH3 domain. Science 274:2089–2091
16. Fadool DA, Tucker K, Phillips JJ, Simmen JA (2000) Brain insulin receptor causes activity-dependent current suppression in the olfactory bulb through multiple phosphorylation of Kv1.3. J Neurophysiol 83:2332–2348
17. Cook KK, Fadool DA (2002) Two adaptor proteins differentially modulate the phosphorylation and biophysics of Kv1.3 ion channel by SRC kinase. J Biol Chem 277:13268–13280
18. Colley B, Tucker K, Fadool DA (2004) Comparison of modulation of Kv1.3 channel by two receptor tyrosine kinases in olfactory bulb neurons of rodents. Receptors Channels 10:25–36
19. Vicente R, Villalonga N, Calvo M, Escalada A, Solsona C, Soler C, Tamkun MM, Felipe A (2008) Kv1.5 association modifies Kv1.3 traffic and membrane localization. J Biol Chem 283:8756–8764
20. Villalonga N, Escalada A, Vicente R, Sanchez-Tillo E, Celada A, Solsona C, Felipe A (2007) Kv1.3/Kv1.5 heteromeric channels compromise pharmacological responses in macrophages. Biochem Biophys Res Commun 352:913–918
21. Sole L, Roura-Ferrer M, Perez-Verdaguer M, Oliveras A, Calvo M, Fernandez-Fernandez JM, Felipe A (2009) KCNE4 suppresses Kv1.3 currents by modulating trafficking, surface expression and channel gating. J Cell Sci 122:3738–3748
22. Martinez-Marmol R, Perez-Verdaguer M, Roig SR, Vallejo-Gracia A, Gotsi P, Serrano-Albarras A, Bahamonde MI, Ferrer-Montiel A, Fernandez-Ballester G, Comes N, Felipe A (2013) A non-canonical di-acidic signal at the C-terminus of Kv1.3 determines anterograde trafficking and surface expression. J Cell Sci 126:5681–5691
23. Shimkets RA, Lifton RP, Canessa CM (1997) The activity of the epithelial sodium channel is regulated by clathrin-mediated endocytosis. J Biol Chem 272:25537–25541
24. Mankouri J, Taneja TK, Smith AJ, Ponnambalam S, Sivaprasadarao A (2006) Kir6.2 mutations causing neonatal diabetes prevent endocytosis of ATP-sensitive potassium channels. EMBO J 25:4142–4151
25. Lukacs GL, Segal G, Kartner N, Grinstein S, Zhang F (1997) Constitutive internalization of cystic fibrosis transmembrane conductance regulator occurs via clathrin-dependent endocytosis and is regulated by protein phosphorylation. Biochem J 328(Pt 2):353–361
26. Nesti E, Everill B, Morielli AD (2004) Endocytosis as a mechanism for tyrosine kinase-dependent suppression of a voltage-gated potassium channel. Mol Biol Cell 15:4073–4088

27. Fadool DA, Holmes TC, Berman K, Dagan D, Levitan IB (1997) Tyrosine phosphorylation modulates current amplitude and kinetics of a neuronal voltage-gated potassium channel. J Neurophysiol 78:1563–1573
28. Gonzalez-Perez O, Quinones-Hinojosa A (2010) Dose-dependent effect of EGF on migration and differentiation of adult subventricular zone astrocytes. Glia 58:975–983
29. Chazal G, Durbec P, Jankovski A, Rougon G, Cremer H (2000) Consequences of neural cell adhesion molecule deficiency on cell migration in the rostral migratory stream of the mouse. J Neurosci 20:1446–1457
30. Fontana X, Nacher J, Soriano E, del Rio JA (2006) Cell proliferation in the adult hippocampal formation of rodents and its modulation by entorhinal and fimbria-fornix afferents. Cereb Cortex 16:301–312
31. Carter RE, Sorkin A (1998) Endocytosis of functional epidermal growth factor receptor-green fluorescent protein chimera. J Biol Chem 273:35000–35007
32. Fortian A, Sorkin A (2014) Live-cell fluorescence imaging reveals high stoichiometry of Grb2 binding to the EGF receptor sustained during endocytosis. J Cell Sci 127:432–444
33. Llado A, Tebar F, Calvo M, Moreto J, Sorkin A, Enrich C (2004) Protein kinaseCdelta-calmodulin crosstalk regulates epidermal growth factor receptor exit from early endosomes. Mol Biol Cell 15:4877–4891
34. Sorkina T, Miranda M, Dionne KR, Hoover BR, Zahniser NR, Sorkin A (2006) RNA interference screen reveals an essential role of Nedd4-2 in dopamine transporter ubiquitination and endocytosis. J Neurosci 26:8195–8205
35. Huang F, Khvorova A, Marshall W, Sorkin A (2004) Analysis of clathrin-mediated endocytosis of epidermal growth factor receptor by RNA interference. J Biol Chem 279:16657–16661
36. Sorkina T, Hoover BR, Zahniser NR, Sorkin A (2005) Constitutive and protein kinase C-induced internalization of the dopamine transporter is mediated by a clathrin-dependent mechanism. Traffic 6:157–170
37. Szilagyi O, Boratko A, Panyi G, Hajdu P (2013) The role of PSD-95 in the rearrangement of Kv1.3 channels to the immunological synapse. Pflugers Arch 465:1341–1353
38. Galperin E, Abdelmoti L, Sorkin A (2012) Shoc2 is targeted to late endosomes and required for Erk1/2 activation in EGF-stimulated cells. PLoS ONE 7:e36469
39. Booth RE, Stockand JD (2003) Targeted degradation of ENaC in response to PKC activation of the ERK1/2 cascade. Am J Physiol Renal Physiol 284:F938–F947
40. Zeng WZ, Babich V, Ortega B, Quigley R, White SJ, Welling PA, Huang CL (2002) Evidence for endocytosis of ROMK potassium channel via clathrin-coated vesicles. Am J Physiol Renal Physiol 283:F630–F639
41. Ming GL, Song H (2011) Adult neurogenesis in the mammalian brain: significant answers and significant questions. Neuron 70:687–702
42. Gonzalez-Perez O, Romero-Rodriguez R, Soriano-Navarro M, Garcia-Verdugo JM, Alvarez-Buylla A (2009) Epidermal growth factor induces the progeny of subventricular zone type B cells to migrate and differentiate into oligodendrocytes. Stem Cells 27:2032–2043
43. Chittajallu R, Chen Y, Wang H, Yuan X, Ghiani CA, Heckman T, McBain CJ, Gallo V (2002) Regulation of Kv1 subunit expression in oligodendrocyte progenitor cells and their role in G1/S phase progression of the cell cycle. Proc Natl Acad Sci U S A 99:2350–2355
44. Kues WA, Wunder F (1992) Heterogeneous expression patterns of mammalian potassium channel genes in developing and adult rat brain. Eur J Neurosci 4:1296–1308
45. Yasuda T, Bartlett PF, Adams DJ (2008) K(ir) and K(v) channels regulate electrical properties and proliferation of adult neural precursor cells. Mol Cell Neurosci 37:284–297
46. Lieban S, Propper C, Beckers T, Lehmann-Horn F, Storch A, Grissmer S, Wittekindt OH (2006) Selective blockage of Kv1.3 and Kv3.1 channels increases neural progenitor cell proliferation. J Neurochem 99:426–437
47. Tegla CA, Cudrici C, Rozycka M, Soloviova K, Ito T, Singh AK, Khan A, Azimzadeh P, Andrian-Albescu M, Niculescu F, Rus V, Judge SI, Rus H (2011) C5b-9-activated, K(v)1.3 channels mediate oligodendrocyte cell cycle activation and dedifferentiation. Exp Mol Pathol 91:335–345
48. Wang T, Lee MH, Johnson T, Allie R, Hu L, Calabresi PA, Nath A (2010) Activated T-cells inhibit neurogenesis by releasing granzyme B: rescue by Kv1.3 blockers. J Neurosci 30:5020–5027
49. Marks DR, Fadool DA (2007) Post-synaptic density perturbs insulin-induced Kv1.3 channel modulation via a clustering mechanism involving the SH3 domain. J Neurochem 103:1608–1627
50. Rus H, Pardo CA, Hu L, Darrah E, Cudrici C, Niculescu T, Niculescu F, Mullen KM, Allie R, Guo L, Wulff H, Beeton C, Judge SI, Kerr DA, Knaus HG, Chandy KG, Calabresi PA (2005) The voltage-gated potassium channel Kv1.3 is highly expressed on inflammatory infiltrates in multiple sclerosis brain. Proc Natl Acad Sci U S A 102:11094–11099
51. Varga Z, Csepany T, Papp F, Fabian A, Gogolak P, Toth A, Panyi G (2009) Potassium channel expression in human CD4+ regulatory and naive T cells from healthy subjects and multiple sclerosis patients. Immunol Lett 124:95–101
52. Scalabrino G, Tredici G, Buccellato FR, Manfridi A (2000) Further evidence for the involvement of epidermal growth factor in the signaling pathway of vitamin B12 (cobalamin) in the rat central nervous system. J Neuropathol Exp Neurol 59:808–814
53. Vennekamp J, Wulff H, Beeton C, Calabresi PA, Grissmer S, Hansel W, Chandy KG (2004) Kv1.3-blocking 5-phenylalkoxypsoralens: a new class of immunomodulators. Mol Pharmacol 65:1364–1374
54. Norton RS, Pennington MW, Wulff H (2004) Potassium channel blockade by the sea anemone toxin ShK for the treatment of multiple sclerosis and other autoimmune diseases. Curr Med Chem 11:3041–3052

Supplementary Figures:

Supplementary Figure 1. EGFR phosphorylation inhibited Kv1.3 activity without altering Kv1.3 protein levels. (A and B) Cells were transfected with EGFR-CFP and incubated with 10 ng/ml EGF for 15 minutes at 37ºC. (A) EGFR were immunoprecipitated (IP) with anti-phospho-tyrosine (PTyr) or anti-GFP (GFP) antibodies. No AB, absence of antibody. The membranes were blotted (IB) against phospho-tyrosine (PTyr) or GFP (GFP). (B) EGF triggered the appearance of endocytic vesicles containing EGFR-CFP (inset). (C-E) HEK-293 cells were co-transfected with Kv1.3-HA and EGFR-CFP and treated with or without EGF, as indicated above, in the presence or in the absence of 50 □M Erbstatin. (C) Voltage-dependent K^+ currents were evoked in cells using a 250 ms depolarizing pulse from -60 to +70 mV. Erbstatin prevented the EGF-dependent inhibition of K^+ currents. (D) Current density in pA/pF. *** $p<0.001$ vs control in the absence of EGF and Erbstatin (Student's t test). The results are the mean±SEM of 8-10 cells. (E) Total lysates from Kv1.3 expressing cells either co-transfected (+EGFR) or not (-EGFR) with EGFR in the presence (+) or the absence (-) of EGF were immunoblotted against Kv1.3 and EGFR. Western blot analysis demonstrated that Kv1.3 expression is not altered upon EGF incubation in the presence of EGFR.

Supplementary Figure 2. EGF-dependent Kv1.3 endocytosis in HeLa cells. Representative images of HeLa cells stably expressing Kv1.3-YFP.

(A-H) Cells were incubated in the absence (A,B) or the presence (C-H) of EGF-rhodamine (4 ng/ml) for 30 min at 37ºC. (F-H) After incubation, EGF was removed by an ice-cold mild-acid wash (+ ACID) or (C-E) binding medium wash (- ACID). As a result, the extracellular EGF-rhodamine background signal was reduced and the intracellular Kv1.3/EGF-containing vesicles were highlighted (inset in H). (I-N) Antibody feeding endocytosis assay targeting Kv1.3-HA external epitope. Representative confocal images of HeLa cells transiently transfected with HA-Kv1.3. Live cells, incubated with anti-HA antibody for 1 h at 4°C, were further treated with (+EGF) or without (-EGF) EGF for 30 min at 37°C. (I-K) Basal HA-Kv1.3 distribution in the absence of EGF. (I) Extracellular Cy5-stained HA-Kv1.3. (J) Intracellular Cy3-stained HA-Kv1.3. (L-N) EGF-dependent HA-Kv1.3 endocytosis. (L) Extracellular Cy5-stained HA-Kv1.3. (M) Intracellular Cy3-stained EGF-dependent HA-Kv1.3 endocytosis. (K,N) Merge panels in the absence or the presence of EGF, respectively. Bars represent 10 μm.

Supplementary Figure 3. Effect of EGF-dependent tyrosine kinase activity on Kv1.3 endocytosis. Images of HeLa cells transiently expressing Kv1.3-YFP wt and Kv1.3-YFP Yless channels. (A-D) Kv1.3-YFP wt cells were pretreated for 1 h prior to and during stimulation with (+) or without (-) 50 μM Erbstatin and were incubated with (+) or without (-) EGF-rhodamine (4 ng/ml) for 30 min. (E) $Kv1.3_{[i]}$, intracellular Kv1.3 wt in arbitrary units (AU) relative to the control (white column, no additions). *** $P < 0.001$ vs control with no incubations (Student's *t*-test). (F-L) HeLa cells transfected with the Kv1.3-YFP ($Y^{111\text{-}113,137,449,479}F$)

mutant channel (Kv1.3 Yless). (F) Voltage-dependent K^+ currents evoked in cells by a 250 ms depolarizing pulse from -60 to +70 mV. The lack of tyrosines in the Kv1.3-YFP Yless channel partially counteracted the EGF-dependent inhibition of K^+ currents. (G) Current density in pA/pF. *** $p<0.001$, * $p<0.05$ vs - EGF for Kv1.3 wt and Kv1.3 Yless channels, respectively (Student's t test). Note a significant current density decrease in the Kv1.3 Yless channel. The results are the mean±SEM of 8-10 cells. (H-L) Representative images of Kv1.3 Yless HeLa cells in the presence (+) or the absence (-) of EGF. (H) Kv1.3 Yless in the absence of EGF. (I-K) Kv1.3 Yless in the presence of EGF. (K) Kv1.3 (green) and EGF (red) in merge panel. (L) $Kv1.3_{[i]}$, intracellular Kv1.3 Yless in arbitrary units (AU) relative to the control (white column, -EGF). Black column, +EGF. *** $P < 0.001$ vs absence of EGF (Student's *t*-test). The results are the mean±SEM of 15-20 cells. Note a notable EGF-dependent Kv1.3 Yless channel endocytosis. Bars represent 10 μm.

Supplementary Figure 4. Effect of different mutations of relevant Kv1.3 signatures on channel endocytosis. HeLa cells were transiently transfected with Kv1.3-YFP wt (Kv1.3 wt), Kv1.3-YFP_P37G, P39A, $P^{40,493,496}L$ (Kv1.3 Pless) and Kv1.3-YFP_T523X (Kv1.3 T523X) channels. Cells were incubated with (+ EGF) or without (- EGF) 4 ng/ml EGF-rhodamine for 30 min at 37ºC. (A-E) Kv1.3 wt. (F-J) Kv1.3 Pless. (K-O) Kv1.3 T523X. (D, I, N) Color code in merge panels: Kv1.3, green; EGF, red. (E,J,O) $Kv1.3_{[i]}$, intracellular Kv1.3 in arbitrary units (AU) relative to the control (white column, -EGF). Black column, + EGF. ***

$p<0.001$ vs the absence of EGF (Student's t-test). The results are the mean±SEM of 15-25 cells. Bars represent 10 μm

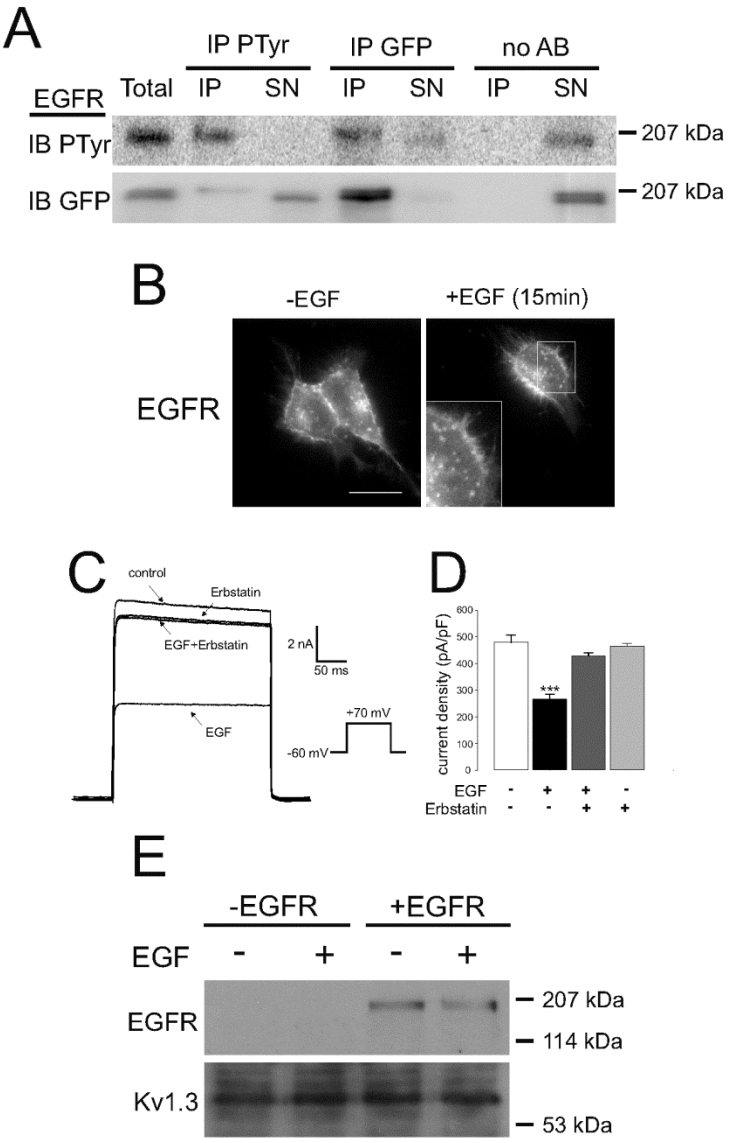

Supplementary Figure 1

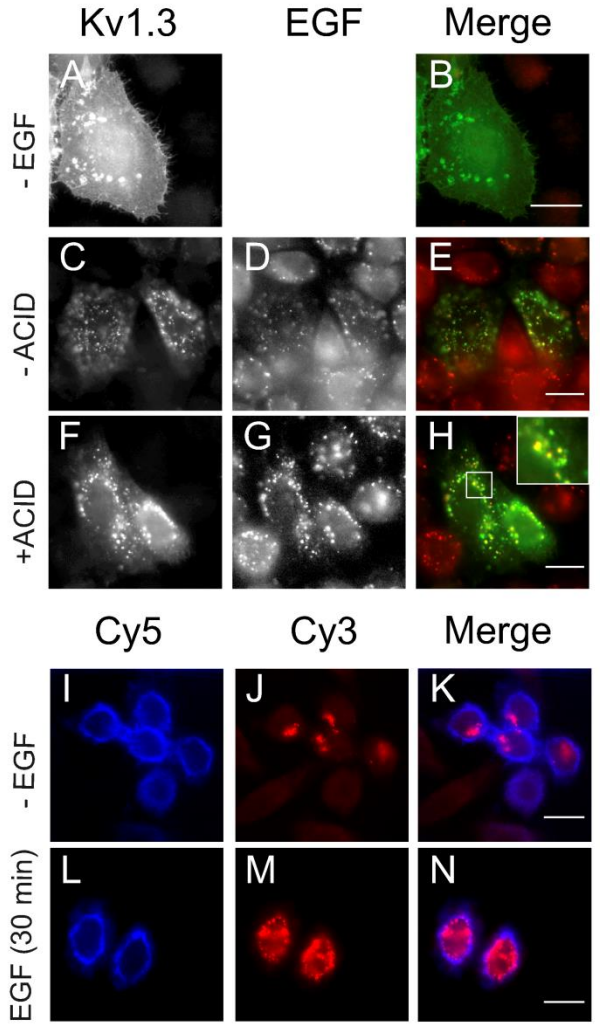

Supplementary Figure 2

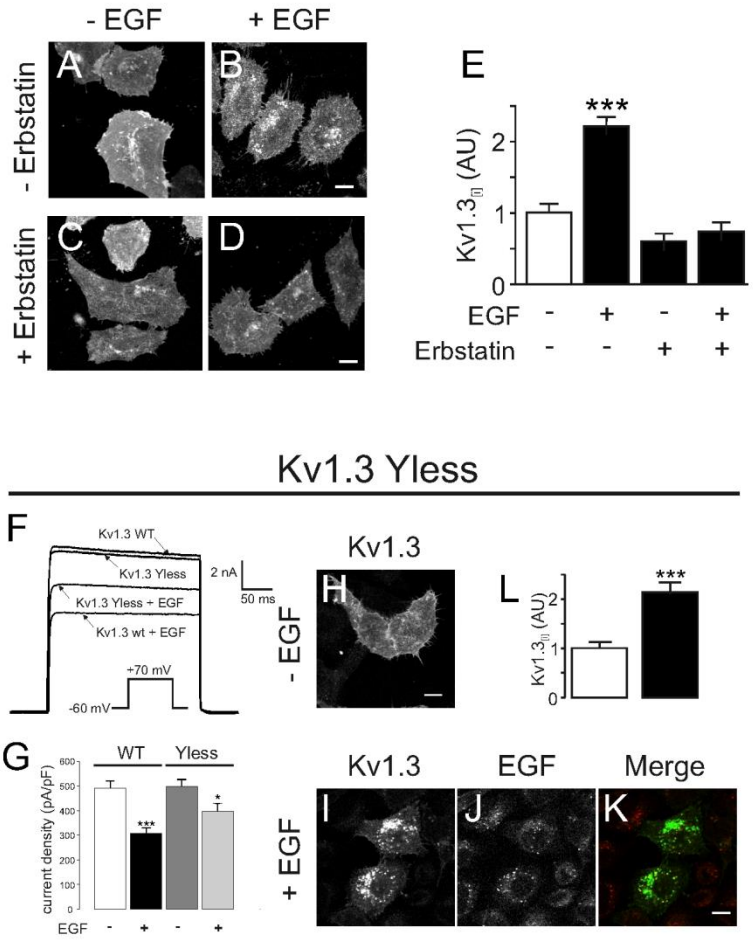

Supplementary Figure 3

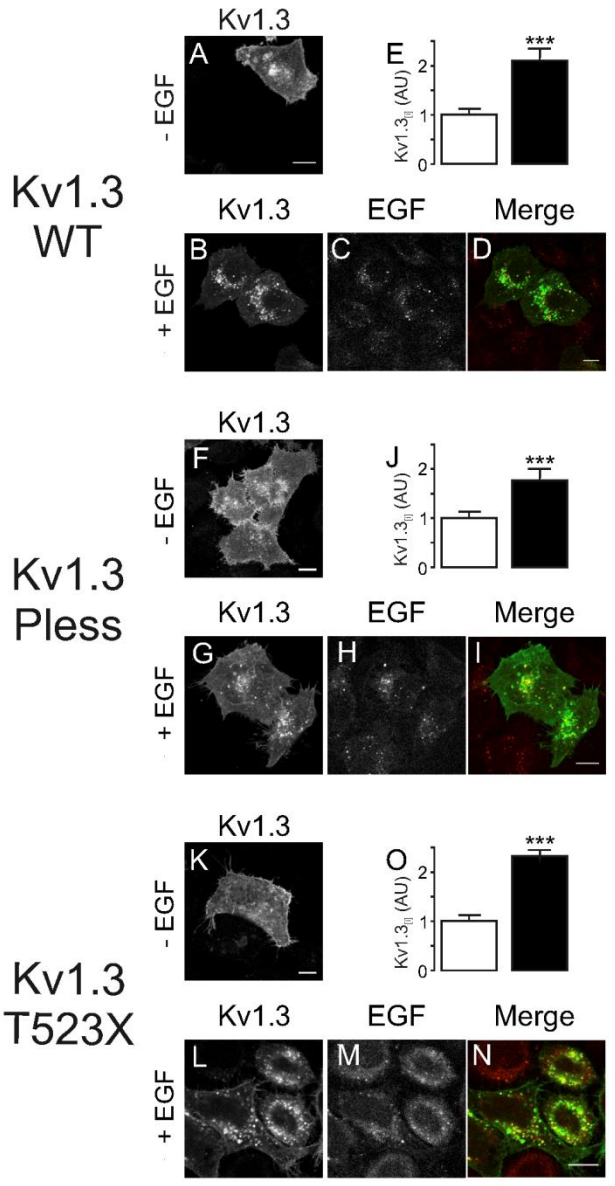

Supplementary Figure 4

3.1. Part Two:

Ubiquitination mediates Kv1.3 endocytosis as a mechanism for protein kinase C- dependent modulation

Sci Rep. 2017; 7: 42395.
Published online 2017 Feb 10. doi: 10.1038/srep42395

Ubiquitination mediates Kv1.3 endocytosis as a mechanism for protein kinase C- dependent modulation

Ramón Martínez-Mármol,[1,2,*] Katarzyna Styrczewska,[1,*] Mireia Pérez-Verdaguer,[1] Núria Comes,[1,3] Alexander Sorkin,[4] and Antonio Felipe[1]

[1]Molecular Physiology Laboratory, Departament de Bioquímica i Biologia Molecular, Institut de Biomedicina (IBUB), Barcelona, Spain

[2] Clem Jones Centre for Ageing Dementia Research, Queensland Brain Institute, The University of Queensland, Brisbane, Queensland 4072, Australia .

[3] Laboratory of Neurophysiology, Universitat de Barcelona and Institut d'Investigacions Biomèdiques August Pi i Sunyer (IDIBAPS), 08036 Barcelona, Spain.

[4]Department of Cell Biology, University of Pittsburgh School of Medicine, Pittsburgh, PA,15261, USA

*These authors contributed equally to this article

Abstract

The voltage-dependent potassium channel Kv1.3 plays essential physiological functions in the immune system. Kv1.3, regulating the membrane potential, facilitates downstream Ca^{2+} -dependent pathways and becomes concentrated in specific membrane microdomains that serve as signaling platforms. Increased and/or delocalized expression of the channel is observed at the onset of several autoimmune diseases. In this work, we show that adenosine (ADO), which is a potent endogenous modulator, stimulates PKC, thereby causing immunosuppression. PKC activation triggers down-regulation of Kv1.3 by inducing a clathrin-mediated endocytic event that targets the channel to lysosomal-degradative compartments. Therefore, the abundance of Kv1.3 at the cell surface decreases, which is clearly compatible with an effective anti-inflammatory response. This mechanism requires ubiquitination of Kv1.3, catalyzed by the E3 ubiquitin-ligase Nedd4-2. Postsynaptic density protein 95 (PSD-95), a member of the MAGUK family, recruits Kv1.3 into lipid-raft microdomains and protects the channel against ubiquitination and endocytosis. Therefore, the Kv1.3/PSD-95 association fine-tunes the anti-inflammatory response in leukocytes. Because Kv1.3 is a promising multi-therapeutic target against human pathologies, our results have physiological relevance. In addition, this work elucidates the ADO-dependent PKC-mediated molecular mechanism that triggers immunomodulation by targeting Kv1.3 in leukocytes.

Report of the PhD student participation

Ubiquitination mediates Kv1.3 endocytosis as a mechanism for protein kinase C- dependent modulation

Katarzyna Styrczewska carried out the experiments corresponding to the Figure 1 A-D, Figurw 2 A-I and 2 O-P, Figure 8 M-Q , Figure 4 , and data analysis corresponding to the figure Figure 4,Figure 6 and 7 in the article.

Antonio Felipe

PhD thesis director

www.nature.com/scientificreports

SCIENTIFIC REPORTS

OPEN

Ubiquitination mediates Kv1.3 endocytosis as a mechanism for protein kinase C-dependent modulation

Received: 12 July 2016
Accepted: 09 January 2017
Published: 10 February 2017

Ramón Martínez-Mármol[1,2], Katarzyna Styrczewska[1], Mireia Pérez-Verdaguer[1], Albert Vallejo-Gracia[1], Núria Comes[1,3], Alexander Sorkin[4] & Antonio Felipe[1]

The voltage-dependent potassium channel Kv1.3 plays essential physiological functions in the immune system. Kv1.3, regulating the membrane potential, facilitates downstream Ca^{2+}-dependent pathways and becomes concentrated in specific membrane microdomains that serve as signaling platforms. Increased and/or delocalized expression of the channel is observed at the onset of several autoimmune diseases. In this work, we show that adenosine (ADO), which is a potent endogenous modulator, stimulates PKC, thereby causing immunosuppression. PKC activation triggers down-regulation of Kv1.3 by inducing a clathrin-mediated endocytic event that targets the channel to lysosomal-degradative compartments. Therefore, the abundance of Kv1.3 at the cell surface decreases, which is clearly compatible with an effective anti-inflammatory response. This mechanism requires ubiquitination of Kv1.3, catalyzed by the E3 ubiquitin-ligase Nedd4-2. Postsynaptic density protein 95 (PSD-95), a member of the MAGUK family, recruits Kv1.3 into lipid-raft microdomains and protects the channel against ubiquitination and endocytosis. Therefore, the Kv1.3/PSD-95 association fine-tunes the anti-inflammatory response in leukocytes. Because Kv1.3 is a promising multi-therapeutic target against human pathologies, our results have physiological relevance. In addition, this work elucidates the ADO-dependent PKC-mediated molecular mechanism that triggers immunomodulation by targeting Kv1.3 in leukocytes.

Voltage-dependent potassium channels participate in propagating electrical impulses in excitable cells such as myocytes and neurons[1]. In addition, ion channels control leukocyte physiology[2]. The voltage-dependent potassium channel Kv1.3 modulates membrane potential and drives Ca^{2+} influx in immune cells, including T-cells, dendritic cells and macrophages, thereby regulating activation, proliferation and migration[3]. Altered Kv1.3 expression is associated with multiple autoimmune diseases and changes in sensory discrimination. Therefore, Kv1.3 is an emerging therapeutic target in T-cell-mediated diseases such as multiple sclerosis, rheumatoid arthritis, type 1 diabetes mellitus and psoriasis[3].

Kv1.3 signaling relies on the activity, abundance and proper localization of channels at the cell surface. In this respect, Epidermal growth factor receptor (EGFR) activity regulates Kv1.3 by both tyrosine phosphorylation and ERK1/2-dependent endocytosis, with consequences for neuronal fate[4,5]. Kv1.3 is also regulated by PKC, modulating T-cell activation[6]. In this context, adenosine (ADO), a potent endogenous anti-inflammatory mediator in leukocytes, activates PKC-dependent signaling pathways[7,8]. Also physiologically relevant is the spatial regulation of ion channels within specific membrane lipid raft domains[9]. Raft microdomains are cell platforms that concentrate signaling molecules, such as PKC and their targets[9,10]. Lipid rafts recruit Kv1.3 in macrophages and in the immunological synapse (IS) of cytotoxic T lymphocytes[11]. The localization of Kv1.3 in rafts and caveolae is dependent on the accessibility of a caveolin-binding domain near the T1 domain and of the Kvβ subunit recognition motif at

[1]Molecular Physiology laboratory, Departament de Bioquímica i Biomedicna Molecular, Institut de Biomedicina (IBUB), Universitat de Barcelona, 08028 Barcelona, Spain. [2]Clem Jones Centre for Ageing Dementia Research, Queensland Brain Institute, The University of Queensland, Brisbane, Queensland 4072, Australia. [3]Laboratory of Neurophysiology, Universitat de Barcelona and Institut d'Investigacions Biomèdiques August Pi i Sunyer (IDIBAPS), 08036 Barcelona, Spain. [4]Department of Cell Biology, University of Pittsburgh School of Medicine, Pittsburgh, PA, 15261, USA. Correspondence and requests for materials should be addressed to A.F. (email: afelipe@ub.edu)

the N-terminal of the channel[12]. Evidence demonstrates that the control of Kv1.3 surface abundance takes place at multiple stages, balancing forward trafficking mechanisms to the cell membrane and the internalization of fully functional channels[4,13]. These results strongly support the idea that the prevalence of Kv1.3 channels at the membrane surface has enormous consequences for cell physiology.

In the present study, we show the clathrin-mediated PKC-induced internalization of Kv1.3. ADO, activating PKC, down-regulates Kv1.3 by increasing the endocytosis and lysosomal degradation of the channel. This mechanism is mainly mediated via the ubiquitination of Kv1.3 by the E3 ubiquitin ligase Nedd4–2 (neural precursor cell expressed, developmentally downregulated 4–2) and is essential for fine-tuning the immunological response. Moreover, PSD-95 protects Kv1.3 from the PKC-induced internalization and ubiquitination by inducing the clustering of the channel in membrane raft microdomains. This PKC-dependent Kv1.3 downregulation is crucial for understanding the anti-inflammatory effect of ADO in leukocytes. Overall, our results elucidate the complex interactions between Kv1.3 and scaffolding proteins within the channelosome, which are essential for the proper establishment of the immunological synapse between T lymphocytes and antigen-presenting cells during the adaptive immune response.

Results

Adenosine hampers the LPS-dependent activation of macrophages and dendritic cells concomitantly with a down-regulation of Kv1.3. Kv1.3 is crucial during proliferation and activation in leukocytes. Bacterial lipopolysaccharide (LPS) activates macrophages, thereby inducing the expression of iNOS (inducible nitric oxide synthase). LPS also increases Kv1.3 activity through transcriptional and translational controls. Pharmacological blockage of Kv1.3 decreases the iNOS expression, demonstrating that this channel participates in the LPS-dependent macrophage activation[14]. ADO, an endogenous anti-inflammatory agent, modulates various functional activities such as the antimicrobial responses of immune cells[15]. In this context, we cultured murine bone marrow derived macrophages (BMDM) and CY15 cells, a histiocytic tumor cell line that phenotypically mimics immature dendritic cells, with LPS in the presence of ADO. LPS triggered iNOS expression in both mononuclear phagocyte cell models (Fig. 1A,C). However, ADO hampered iNOS induction as well as the LPS-dependent Kv1.3 increase (Fig. 1A–D). ADO also slightly, but statistically non-significant, decreased the basal levels of Kv1.3 in control cells (BMDM, 2 over 4 experiments; CY15, 3 over 5 experiments). These effects were also observed in the Kv currents elicited from CY15 dendritic cells (Fig. 1E,F). Thus, while LPS increased outward K^+ currents, the presence of ADO halted this induction (Fig. 1E,F). Kv currents were slightly, but statistically non-significant, diminished by ADO in control cells, which is consistent with the minor effects on Kv1.3 (Fig. 1D) and a notable contribution of Kv1.5 in dendritic cells[16,17], which expression was not altered under any situation.

Adenosine triggers PKC-dependent Kv1.3 endocytosis in HEK-293 cells. ADO, which stimulates PKC and PKA[18], decreased the expression and activity of Kv1.3 in activated macrophages and CY15 dendritic cells. Although PKC mostly triggers internalization of channels and transporters[19–22], ADO stabilizes KATP channels at the membrane surface in a PKC-dependent manner[23]. With this debate in mind, we investigated whether the modulation of Kv1.3 was consequence of a specific PKC-mediated endocytosis. HEK-293 cells, similarly to macrophages[24–26], endogenously express the A_{2B} subtype of adenosine receptors[27]. Therefore, this cell line is a good model for dissecting the ADO-dependent PKC signaling.

We further analyzed the participation of a PKC-dependent mechanism by using the PKC agonist phorbol 12-myristate 13-acetate (PMA). The presence of the PKC inhibitor bisindolylmaleimide (BIM) hampered the internalization of channels (Fig. 2A–D,G), indicating that ADO triggered Kv1.3 endocytosis via stimulation of PKC. Similarly, specific PMA-dependent PKC activation also promoted the redistribution of Kv1.3 from the cell surface to vesicular structures (Fig. 2E–G). BIM abolished this effect, indicating that, similar to ADO-induced endocytosis, PMA-associated endocytosis was dependent on PKC (Fig. 2B,D,F,G). This mechanism was indeed concomitant to an activation of the PKC. We analyzed the phosphorylation of PKCε because this isoform participates in TNF-α-dependent pro-inflammatory responses in HEK cells[28] and during the LPS-induced and MCSF-dependent activation in macrophages[29–31]. ADO (Fig. 2H) and PMA (Fig. 2I) augmented the phosphorylation of PKCε (~2 fold increase), without changes in total PKC. Again BIM effectively hampered (~50% decrease) PKC phosphorylation in both cases. Next, we monitored the time-course of Kv1.3 distribution under persistent PKC activation. PMA steadily induced the endocytosis of Kv1.3 ($p < 0.0001$, One-way ANOVA), which was almost completely internalized within 30 minutes (Fig. 2J–N). Supporting HEK 293 cells, similar mechanisms functioned in mononuclear phagocytes (see Fig. 1), because a 30 min incubation with ADO (Fig. 3O–Q) vesicularized Kv1.3 in CY15 dendritic cells.

The "antibody-feeding assay" was essential to unequivocally decipher the PKC-dependent endocytosis of the dopamine transporter (DAT) and the EGFR-dependent internalization of Kv1.3[4,21]. HA-Kv1.3-YFP channels that simultaneously contain an extracellular HA tag and an intracellular YFP fluorophore were expressed in HEK-293 cells. Total (YFP) and extracellular (Cy5) Kv1.3 channels were observed under non-permeabilizing conditions. In the absence of PMA, cells showed surface HA-Kv1.3-YFP channels when stained with Cy5-labeled anti-HA antibodies (Fig. S1A,B). In addition, some Cy3-labeled intracellular vesicles were also observed (Fig. S1C). Because Kv1.3 recycling is rapid, this would correspond to constitutively internalized HA-Kv1.3-YFP channels in early endosomes. PMA increased intracellular Kv1.3-containing Cy3-stained vesicles (Fig. S1G). Intracellular channels were inaccessible to Cy5-labeled secondary antibodies applied to non-permeabilized cells, both a decrease in extracellular Cy5 channels and an increase in internal Cy3-stained channels were observed upon PKC activation (Fig. S1E–H).

We next analyzed whether the Kv1.3 internalization was associated with changes in Kv currents in Kv1.3-YFP stable HEK-293 cells. Depolarizing pulses elicited K^+ currents, and 30 min incubation with PMA reduced those currents by 49%. BIM counteracted this effect, demonstrating a specific dependence on the PKC stimulation

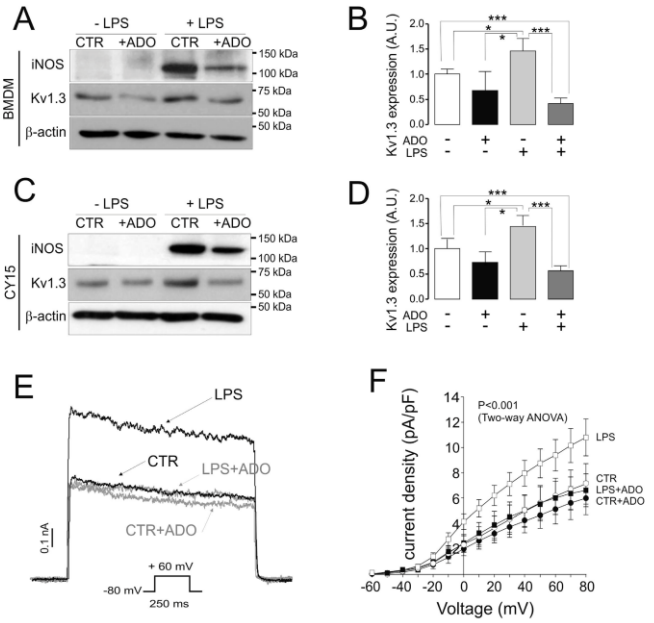

Figure 1. Adenosine counteracts the LPS-dependent activation and Kv1.3 induction in macrophages and dendritic cells. Murine bone marrow-derived macrophages (BMDM) and CY15 dendritic cells were incubated with (+) or without (−) LPS (100 ng/ml) in the presence (+ADO) or the absence (control, CTR) of 200 μM adenosine for 24 h. (A-D) Cells were lysed, and protein expression of Kv1.3 and iNOS was analyzed. (**A**,**B**) BMDM; (**C**,**D**) CY15 dendritic cells. (**A**,**C**) Representative western blots; (**B**,**D**) Kv1.3 expression in arbitrary units (A.U.). β-Actin was used as a control reference. Values are mean ± SE of 4–5 independent experiments. Statistical analysis by One-Way ANOVA ($P < 0.001$) with a Tuckey post-test (*, $p < 0.05$; ***, $p < 0.001$). (**E**) CY15 cells were held at −80 mV, and voltage-dependent K^+ currents were elicited by a 250 ms depolarizing pulse from −80 mV to +60 mV. Black traces, CY15 cells in the absence of ADO; grey traces, cells in the presence of ADO. (**F**) Current density vs. voltage for outward K^+ currents in CY15 cells. Currents were elicited by 250 ms pulses from −60 mV to +80 mV in 10 mV steps. Circles, control cells in the absence (○) or the presence (●) of ADO. Squares, LPS-treated cells in the absence (□) or the presence (■) of ADO. Statistical analysis was performed by Two-Way ANOVA ($p < 0.001$, LPS vs control, CTR + ADO and LPS + ADO) with a Bonferroni post-test ($p < 0.05$, LPS vs all other groups at −10 mV; $p < 0.01$, LPS vs all other groups at 0 mV; $p < 0.001$, LPS vs all other groups from 10 to 80 mV). Values are shown as the mean ± SE (n = 5–10 independent cells).

(Fig. 3A). The I–V plots showed that PKC activation efficiently reduced current densities at all activation voltages (Fig. 3B) ($p < 0.001$, two-way ANOVA). We further analyzed the specific Kv1.3 C-type inactivation (Fig. 3C–F). This hallmark, which is the result of the cooperative interaction of all subunits within the complex, remained unaltered[32]. Thus, the τ of current decay (in ms) was similar being 720 ± 14, 698 ± 14, 742 ± 30 and 741 ± 11 for Control (Fig. 3C), PMA (Fig. 3D), Control + BIM (Fig. 3E) and PMA + BIM (Fig. 3F) respectively. Taken together, these results further supported the down-regulation of Kv1.3, mostly governed by a PKC-mediated decrease of channel subunits at the cell surface, rather than major changes in Kv1.3 biophysics upon PKC activation.

PKC-dependent Kv1.3 endocytosis is a clathrin-mediated mechanism. We next dissected the mechanisms of PKC-dependent Kv1.3 endocytosis (Fig. 4). After 5 minutes of PMA incubation, Kv1.3 colocalized with AP2 (Adaptor-related Protein complex 2) and Clathrin, components of the clathrin-coated pit (CCP)

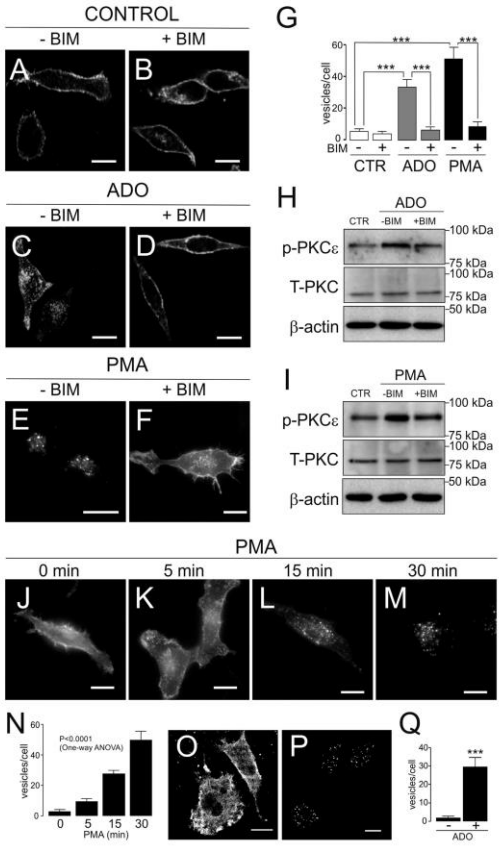

Figure 2. ADO- and PMA-dependent PKC stimulation triggered Kv1.3 endocytosis. Representative confocal images of HEK-293, with stable expression of Kv1.3-YFP, and CY15 dendritic cells incubated in the presence or the absence of 200 μM Adenosine and 1 μM PMA at the indicated times. (**A–F**) HEK-293 cells cultured for 30 min at 37 °C in the absence (**A**,**B**) or the presence of ADO (**C**,**D**) and PMA (**E**,**F**) with (**B**,**D**,**F**) or without (**A**,**C**,**E**) 1 μM BIM. (**G**) Quantification of Kv1.3 intracellular vesicles from representative images on panels A–F. Values are mean ± SE of n = 20–25 cells. A One-Way ANOVA analysis revealed differences vs treatment ($p < 0.001$). A further Tuckey post-test among groups is indicated (***, $p < 0.001$). (**H**,**I**) Adenosine and PMA-dependent PKCε phosphorylation (p-PKCε. HEK cells were incubated during 30 min in the absence (CTR, Control) or in the presence (ADO and PMA) of any insult without (−) or with (+) BIM. β-Actin was used as a reference control. Note that total PKC abundance (T-PKC) was not altered. (**J–M**) Time-dependent Kv1.3 endocytosis in the presence of PMA. (**N**) Quantification of Kv1.3 intracellular vesicles from representative images on panels J–M. Values are mean ± SE of n = 20–25 cells. Statistical analysis was performed by One-Way ANOVA (***, $p < 0.0001$ vs time). (**O**,**P**) Representative images of Kv1.3 staining in CY-15 dendritic cells incubated during 30 min without (**O**) or with (**P**) 200 μM ADO. (**Q**) Quantification of intracellular vesicles from representative images on panels O and P. Values are mean ± SE of n = 10–15 cells. ***, $p < 0.001$ vs the absence of ADO (–) by the Student's *t* test. Bars represent 10 μm.

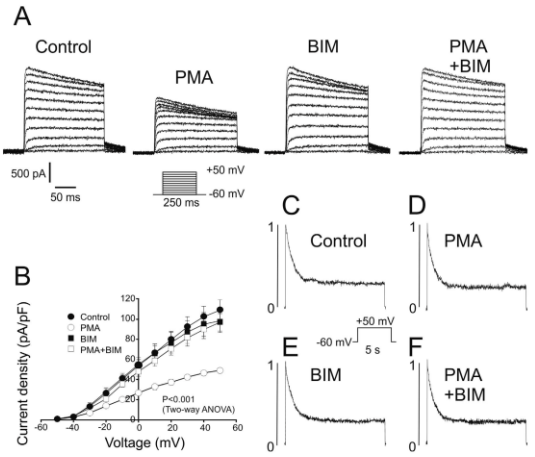

Figure 3. PKC-dependent stimulation decreases Kv1.3 currents. HEK-293 cells stably transfected with Kv1.3-YFP were incubated for 30 min with or without 1 μM PMA at 37 °C in the presence or the absence of 1 μM BIM. Cells were held at −60 mV, and voltage-dependent K^+ currents were elicited by 250 ms depolarizing pulses from −60 mV to +50 mV in 10 mV steps. (**A**) Representative current traces from cells preincubated with or without BIM in the presence or the absence of PMA. (**B**) Current density versus voltage plot of K^+ currents. ●, control cells with no treatment; ○, PMA-treated cells; ■, cells preincubated with BIM; □, cells treated with PMA and preincubated with BIM. Values are shown as the mean ± SE (n = 6–10 independent cells). Statistical analysis was performed by Two-Way ANOVA ($p < 0.001$ PMA vs Control, BIM and PMA + BIM) with a Bonferroni post-test ($p < 0.01$, PMA vs all other groups at −20 mV; $p < 0.001$, PMA vs all other groups from −10 to 50 mV). (**C**–**F**) C-type inactivation of Kv1.3 currents. Cells were held at –60 mV, and a 5 s depolarizing pulse of +50 mV was applied. Representative traces from 6–8 independent cells are shown and normalized to 1 in order to better compare the inactivation kinetics. (**C**) Control, 720 ± 14 ms. (**D**) PMA, 698 ± 14 ms. (**E**) BIM, 743 ± 30 ms. (**F**) PMA + BIM, 741 ± 11 ms. No statistical significance was found by Mann-Withney U test.

internalization machinery (Fig. 4A–H). Thus, a pixel by pixel analysis indicated that Kv1.3 followed a intracellular pattern that overlaid with that of Clathrin and AP2 (Fig. 4D,H). To further decipher this mechanism, stable Kv1.3 HEK cells were transfected with siRNAs against dynamin II (Dyn II) and Clathrin (Fig. 4I–Q), both crucial for the EGFR-mediated clathrin-dependent endocytosis of Kv1.3[4]. Under effective Clathrin and Dyn II depletion (Fig. 4I,J), cells were incubated without (Fig. 4K–M) or with (Fig. 4N–P) PMA for 30 min. Unlike mock treated cells, no significant PMA-dependent internalization of Kv1.3 was observed in Clathrin- or Dyn II-depleted cells (Fig. 4Q). Clathrin and Dyn II also participate in the exocytic pathway of membrane proteins[33]; therefore, some perinuclear Kv1.3 accumulation was observed (arrowheads in Fig. 4L,M,O,P). Altogether, this evidence supports that CCP-mediated endocytosis was the main pathway for PKC-dependent Kv1.3 internalization.

Kv1.3 is targeted to sphingolipid- and cholesterol-enriched lipid rafts[34]. Caveolae/raft-dependent endocytosis upon PKC stimulation may be relevant for some ion channels located in such specialized microdomains[35]. Therefore, we investigated whether this endocytic mechanism was also involved in the PKC-dependent Kv1.3 internalization. Filipin and Nystatin inhibit lipid raft- and caveolae-dependent internalization[36]. However, neither treatment affected the PKC-dependent Kv1.3 endocytosis (Fig. S2A–C,E–G). In addition, lipid rafts are profoundly affected by cholesterol-modifying agents such as methyl-β-cyclodextrin (MβCD)[34]. Although MβCD alters the raft targeting of Kv1.3, it did not affect the endocytosis of Kv1.3 (Fig. S2D,H). To further exclude the involvement of caveolae-dependent internalization, we used a caveolin 1-null ($Cav1^-$) HEK-293 cell line[12]. Whether $Cav1^-$ cells were treated with or without MβCD, Kv1.3 always underwent endocytosis in the presence of PMA (Fig. S2I–L). Therefore, PKC-dependent Kv1.3 endocytosis is a clathrin-mediated but caveolin-independent mechanism.

PSD-95 association stabilizes Kv1.3 at membrane raft microdomains and prevents PKC-mediated channel endocytosis. PKC and Kv1.3 are recruited into the IS, fine-tuning the T-cell activation[10,11]. Moreover, the IS concentrates lipid raft microdomains as signaling platforms[10]. Kv1.3 interacts with proteins from the MAGUK family such as PSD-95, which recruits the channel into the IS[37]. Impaired IS

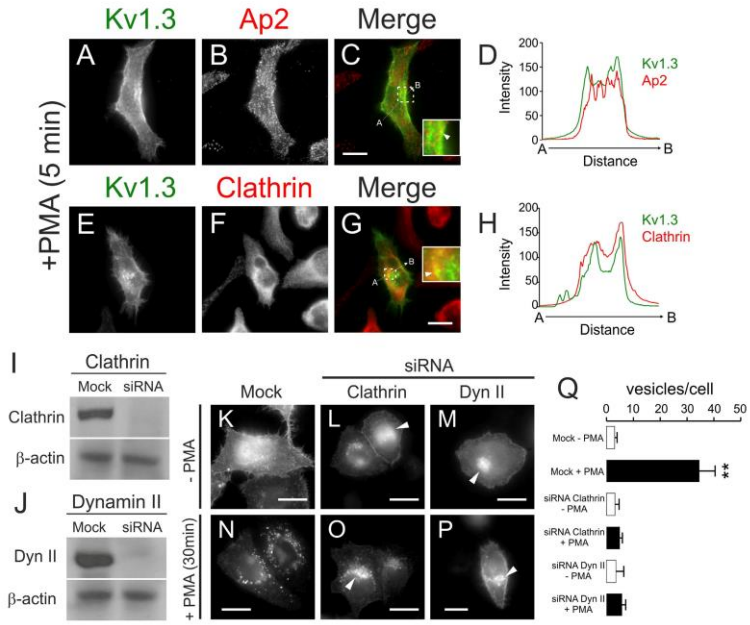

Figure 4. PMA-dependent Kv1.3 internalization is governed by clathrin-mediated endocytosis. Confocal images and western blot analysis of cells stably transfected with Kv1.3-YFP. (**A–H**) Cells were stained for AP2 (**A–D**) and Clathrin (**E–H**) after 5 min of 1 μM PMA incubation at 37 °C. Insets in merged panels highlight the intracellular colocalization in discrete vesicles pointed by arrowheads. Arrowheads in C, G indicate channels that colocalized with AP2 and Clathrin, respectively. (**D**,**H**) Histogram showing the results of the pixel-by-pixel analysis of the section indicated by the arrow in the merged images ($n > 25$ independent cells for each condition). Color code in panels: Kv1.3 (green), AP2/Clathrin (red), merge (yellow). (I and J) Cells were transfected with siRNAs scramble (Mock) or with siRNAs targeting Clathrin Heavy Chain (Clathrin) and Dynamin II (Dyn II). Cell lysates were blotted with antibodies against Clathrin, Dyn II, and β-actin. Western blots demonstrated the depletion of Clathrin (**I**) and Dyn II (**J**). (**K–Q**) Cells mock transfected (**K**,**N**) or transfected with siRNAs targeting Clathrin (**L**,**O**) or Dyn II (**M**,**P**) were incubated with (+PMA) or without (−PMA) 1 μM PMA for 30 min. Arrowheads in L, M, O, P highlight intracellular accumulated Kv1.3. Bars represent 10 μm. (**Q**) Quantification of intracellular vesicles from cells in panels K-P in the absence (white bars) or in the presence (black bars) of PMA. Values are the mean ± SE of $n = 24–30$ cells. **, $p < 0.01$ vs Mock −PMA (Student's t test).

localization of Kv1.3 is associated with lupus erythematosus[38]. Therefore, PKC-mediated internalization of Kv1.3 would affect the immune response. Thus, we analyzed whether PSD-95 protects Kv1.3 against PKC-dependent endocytosis. PSD-95 associated with Kv1.3 in HEK-293 cells (Fig. 5A), affecting the channel membrane distribution (Fig. 5B–J). Kv1.3 evenly decorated the cell membrane (Fig. 5B,F), whereas the presence of PSD-95 induced the formation of discrete clusters that colocalized with lipid raft markers (Fig. 5F–J). To further demonstrate the effect of PSD-95 on the cell membrane targeting of Kv1.3, we performed fluorescence recovery after photobleaching (FRAP) experiments in the presence of PSD-95 (Fig. 5K–Q). FRAP values indicated that the presence of PSD-95 increased about 2-fold the half-life ($p < 0.01$) and decreased by 50% the mobile fraction ($p < 0.001$) of Kv1.3 (Fig. 5O–Q). These results suggested that PSD-95 recruited Kv1.3 to less-mobile membrane microdomains.

Because PSD-95 redistributed Kv1.3 at the cell surface, we next analyzed whether PSD-95 could modify the PKC-dependent Kv1.3 internalization. PMA shifted Kv1.3 out of low-buoyancy fractions, suggesting that the CCP internalization delocalized the channel from lipid raft microdomains (Fig. 6A,P). However, PSD-95

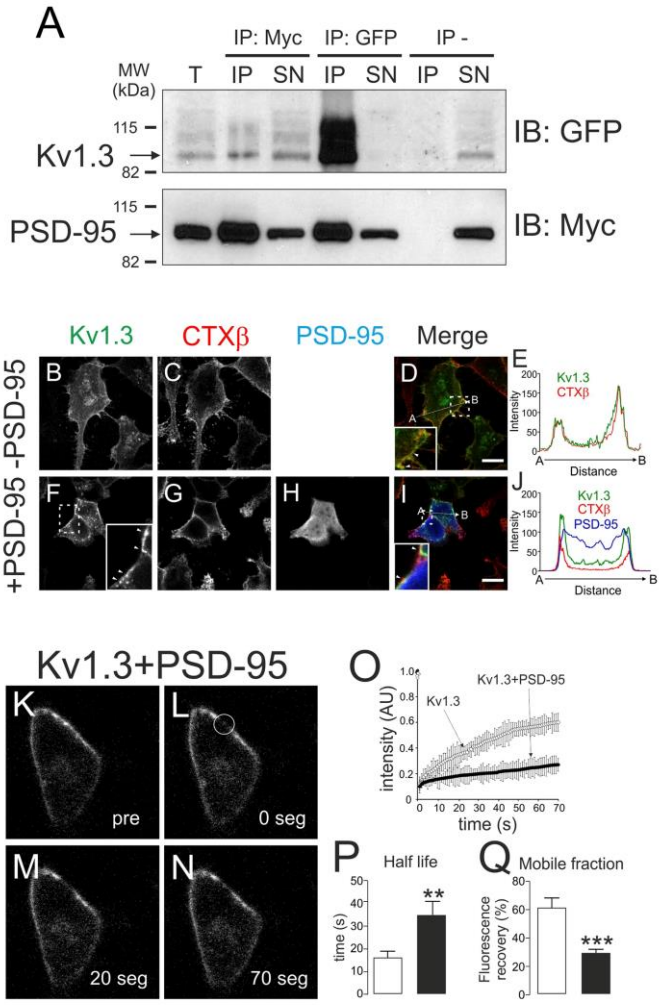

Figure 5. Interaction with PSD-95 recruits Kv1.3 into less-mobile membrane structures. HEK-293 cells with stable expression of Kv1.3-YFP were cotransfected with PSD-95-myc for 24 h. (**A**) Co-immunoprecipitation of Kv1.3 and PSD-95. Cell lysates were immunoprecipitated (IP) for PSD-95 (Myc) and Kv1.3 (GFP), and membranes were blotted (IB) for Kv1.3 (GFP, top panel) and PSD-95 (Myc, bottom panel). T, total lysates; IP, immunoprecipitates; SN, supernatants; IP−, absence of antibody. (B-J) PSD-95 recruits Kv1.3 into discrete membrane clusters. (**B–E**) Kv1.3 colocalized evenly with cholera toxin β subunit (CTXβ), which

stains lipid raft microdomains. (F-J) PSD-95 recruited Kv1.3 to discrete cell surface clusters that are also positive for CTXβ. Insets in D, F and I highlight areas of interest. Arrowheads indicate clusters (**F**) and colocalization spots (**I**). Bars represent 10 μm. (**E,J**) Histogram showing a pixel-by-pixel analysis of the section indicated by the arrow in the merged images. Color code in panels: green, Kv1.3; red, CTXβ; blue, PSD-95; yellow, merge of Kv1.3 and CTXβ; white, triple merge of Kv1.3, CTXβ and PSD-95. (**K–Q**) FRAP experiments indicate that PSD-95 targets Kv1.3 to less-mobile membrane microdomains. (**K–N**) Representative FRAP images of Kv1.3 in the presence of PSD-95. The membrane surface was bleached at discrete ROIs (regions of interest) in the circle (**L**), and the fluorescence recovery was analyzed at the indicated times (in seconds). Pre, pre-bleaching. (**O**) Intensity of Kv1.3-YFP recovery after photobleaching, in arbitrary units (AU), versus time (s) in the absence (○) or the presence (●) of PSD-95. (**P**) Half time (s) and (**Q**) Mobile fraction (%) analysis of the fluorescence recovery after photobleaching. Values are the mean ± SE of n >25 cells. White bars, Kv1.3; black bars, Kv1.3 + PSD-95. **, $p < 0.01$; ***, $p < 0.001$ vs Kv1.3 in the absence of PSD-95 (Student's t test).

stabilized Kv1.3 in floating fractions in the presence of PMA (Fig. 6B,P). In addition, PSD-95 protected Kv1.3 against the PKC-dependent internalization triggered by PMA (Fig. 6C–H). While Kv1.3 was endocytosed in PSD-95-negative cells (circled cell, Fig. 6F–H), Kv1.3 remained at the surface in the presence of PSD-95 (unmarked cell, Fig. 6F–H).

To further demonstrate that PSD-95 protected Kv1.3 against PKC-dependent endocytosis, we used the HA-Kv1.3-YFP channel. In this experiment, while PMA elevated Kv1.3-YFP-positive intracellular vesicles, it almost completely abolished Kv1.3-HA extracellular staining (Fig. S3A–F). However, the presence of PSD-95 prevented the loss of the Kv1.3 extracellular HA signaling (Fig. S3G–N). In the absence of PSD-95, PKC activation triggered strong colocalization of Kv1.3 with EEA1 (Early Endosomal Antigen 1) (circled cell, Fig. S3S–U; inset, Fig. S3V). However, PSD-95 reduced the colocalization between Kv1.3 and EEA1, further demonstrating that the MAGUK protein stabilized the channel at the cell surface.

Kv1.3 interacts with PSD-95 through a C-terminal PDZ-binding domain, defined by the last three residues of the channel (Thr^{523}-Asp^{524}-Val^{525})[37]. Therefore, we used Kv1.3(T523X), a truncated channel that lacks this motif and thus cannot bind PSD-95[37]. Consequently, PSD-95 did not protect Kv1.3(T523X) from targeting out of floating-raft-enriched fractions upon PKC-dependent stimulation (Fig. 6I,P). Moreover, Kv1.3(T523X) did not cluster in the presence of PSD-95 under basal conditions, and it underwent PKC-dependent internalization (Fig. 6J–O, circled cell).

PKC-dependent Kv1.3 endocytosis targeted the channel for lysosomal degradation. Our results in macrophages and CY15 dendritic cells suggested that the abundance of Kv1.3 was decreased under ADO-dependent PKC stimulation (Fig. 1). Therefore, to study in more detail whether Kv1.3 clathrin-mediated internalization ends in a lysosomal-associated degradative intracellular compartment, the PKC-dependent Kv1.3 endocytic mechanisms were further analyzed. After 15 minutes, Kv1.3 colocalized with Transferrin Receptor (Trsf-R), which is used as a CCP marker (Fig. 7Aa–Bd). After 30 minutes of PMA incubation, Kv1.3 was distributed within early endosomes, identified by Early Endosomal Antigen 1 (EEA1) (Fig. 7Ca–Dd). Finally, 120 minutes of PKC activation targeted Kv1.3 to lysosomes stained with LysoTracker® Red (Fig. 7Ea–Fd). Concomitantly, 4 hours of PMA incubation in the presence of 100 μg/ml CHX triggered a massive decrease of Kv1.3 expression (Fig. 7Ga–Gc). Further, when also inhibiting lysosomal degradation using the vacuolar-type H^+-ATPase inhibitor BafA1 (20 μM), the rapid PKC-associated decrease in Kv1.3 abundance was halted (Fig. 7H). Overall, our results suggest that PKC activation, either by ADO or by PMA, triggered a down-regulation of cell-surface Kv1.3 via CCP that targets the channel for lysosomal degradation.

PKC activation induces ubiquitination-dependent Kv1.3 endocytosis mediated by Nedd4-2 ubiquitin ligase activity. Ubiquitin-dependent endocytosis targets channels and transporters to lysosome-dependent degradation[22,39,40]. In this context, the E3 ubiquitin ligase Nedd4-2 associates with Kv1.3 and downregulates the activity of the channel[41,42]. Therefore, we next evaluated whether PKC-dependent Kv1.3 endocytosis, and thus lysosome-dependent degradation, was associated with the channel ubiquitination. PMA triggered a notable PKC-dependent ubiquitination of Kv1.3, which was hampered by BIM (Fig. 8A,B). Kv1.3 was transiently ubiquitinated upon PMA incubation and exhibited maximum levels at 15-30 minutes (Fig. 8C,D). Similar to Kv1.3 endocytosis and raft microdomain displacement, PSD-95 protected Kv1.3 against ubiquitination (Fig. 8E,F). To assess whether Nedd4-2 was involved in Kv1.3 endocytosis via PKC activation, we blocked its expression by using specific siRNA against Nedd4-2 (Fig. 8G). Kv1.3-YFP HEK cells transfected with Nedd4-2 siRNA were incubated with PMA for 30 min at 37 °C. When Nedd4-2 was depleted, the internalization of Kv1.3 was negligible (Fig. 8H–L). To definitively demonstrate the role of ubiquitination on the PKC-dependent Kv1.3 endocytosis, we mutated all the intracellular lysines of the channel (Lys70, 80, 146, 270, 342, 467, 476, 498, 519 and 520) to arginines. In the presence of PMA, the Kv1.3(Kless) mutant was not ubiquitinated (Fig. 8M,N). Relatedly, the internalization of Kv1.3(Kless) was minor upon PMA incubation (Fig. 8O–Q). Altogether, our results demonstrate that Kv1.3 is ubiquitinated by Nedd4-2 upon PKC-activation, triggering channel endocytosis and lysosome-dependent degradation.

Discussion

Adenosine (ADO), which activates PKC signaling pathways, is an endogenous regulator in many physiological processes[7,8,43,44]. PKC modulates Kv1.3 activity, which is essential for a proper immune response[14,45]. Furthermore, both proteins are localized in the same membrane platforms, highlighting the importance of PKC-dependent

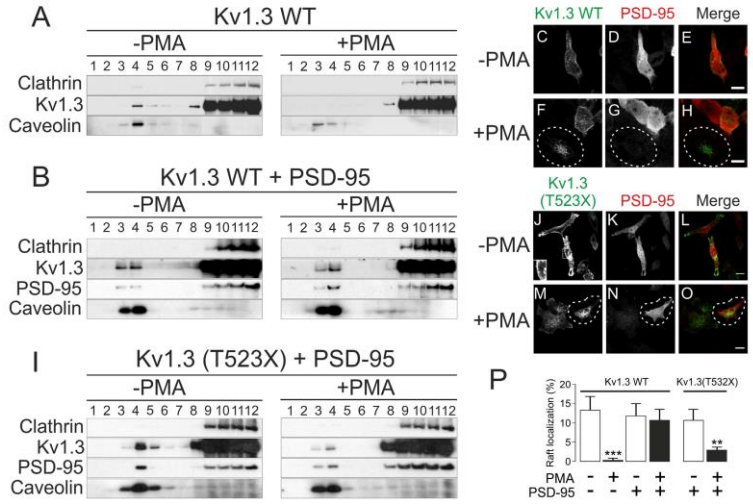

Figure 6. PSD-95 stabilizes Kv1.3 in lipid rafts and protects the channel against PMA-induced endocytosis. HEK-293 cells stably expressing Kv1.3-YFP wild-type (WT) or transiently transfected with Kv1.3(T523X)-YFP were cultured without (left panels) or with (right panels) 1 μM PMA for 30 min at 37 °C, in the absence (**A**) or presence (**B**,**I**) of PSD-95-myc. After the treatment, lipid raft localization and PMA-induced internalization of Kv1.3 were analyzed. (**A**) Representative lipid raft localization of Kv1.3 WT in the presence (+) or the absence (−) of PMA. A continuous sucrose gradient from low-density (1) to high-density (12) fractions was performed. Caveolin and clathrin indicated lipid raft and non-lipid raft fractions, respectively. (**B**) Lipid raft localization of Kv1.3 WT and PSD-95 in the presence (+) or the absence (−) of PMA. (**C**–**H**) PSD-95 protected Kv1.3 WT against PMA-induced internalization. Cells incubated in the absence (**C**–**E**) or the presence (**F**–**H**) of PMA. Note that Kv1.3 in the circled cell in panels F–H did not express PSD-95 and underwent internalization. Color code in merge panels: green, Kv1.3-YFP; red, PSD-95-myc; yellow, colocalization. (**I**–**O**) The mutant Kv1.3(T523X)-YFP channel was not protected by PSD-95 against lipid raft delocalization or PMA-induced endocytosis. (**I**) Lipid raft localization of Kv1.3(T523X) and PSD-95 in the presence (+) or the absence (−) of PMA. (**J**–**O**) PSD-95 did not protect Kv1.3(T523X) against PMA-induced internalization. Cells incubated in the absence (J-L) or the presence (**M**–**O**) of PMA. Inset in panel J shows that, like Kv1.3 WT (**C**), Kv1.3(T523X) is targeted evenly to the cell surface in the absence of PMA. Note that the presence of PSD-95 in the highlighted cell in panels M-O did not prevent Kv1.3 internalization. Color code in merge panels: green, Kv1.3-YFP; red, PSD-95-myc; yellow, colocalization. Bars represent 10 μm. Confocal images are representative from >25 cells analyzed in 3–5 independent experiments. (**P**) Quantitative analysis of the PSD-95 effects on the lipid raft expression of Kv1.3 WT and Kv1.3(T523X) in the presence or the absence of PMA. Floating raft fractions were defined by the expression of Caveolin. Values are the mean ± SE of 4 independent experiments. White bars, absence of PMA; black bars, presence of PMA. Statistical analysis was performed by using One-Way ANOVA with a Tuckey post-test. **, $p < 0.01$ Kv1.3(T532X) + PMA vs Kv1.3(T532X) − PMA; ***, $p < 0.001$ Kv1.3 WT + PMA vs Kv1.3 WT − PMA.

regulation of Kv1.3 in leukocyte physiology[10,34]. Because Kv1.3 participates in the onset of several immunological diseases[3,46], elucidating the mechanism by which ADO-dependent PKC-activation modulates this channel is essential for understanding the immune response. Therefore, we analyzed the PKC-based mechanisms that control the cell-surface levels of Kv1.3 as an efficient way to regulate the function of this ion channel. ADO, activating PKC, initiates a signaling cascade that modulates the cell-surface abundance of Kv1.3 by channel endocytosis. In addition, PSD-95 stabilizes Kv1.3 into lipid raft microdomains and protects the channel against internalization. Kv1.3 endocytosis is a CCP-dependent mechanism that drives the channel to lysosome-associated degradative intracellular compartments and requires previous ubiquitination by the E3 ubiquitin ligase Nedd4-2.

While activation of mononuclear phagocytes increases Kv1.3, anti-inflammatory agents decrease channel expression[14,16,47]. ADO, via A_{2A} and A_{2B} receptors, is a potent endogenous immunosuppressor[7,15], and it decreases Kv1.3 levels in macrophages and dendritic cells. In addition, ADO induced internalization of the channel in

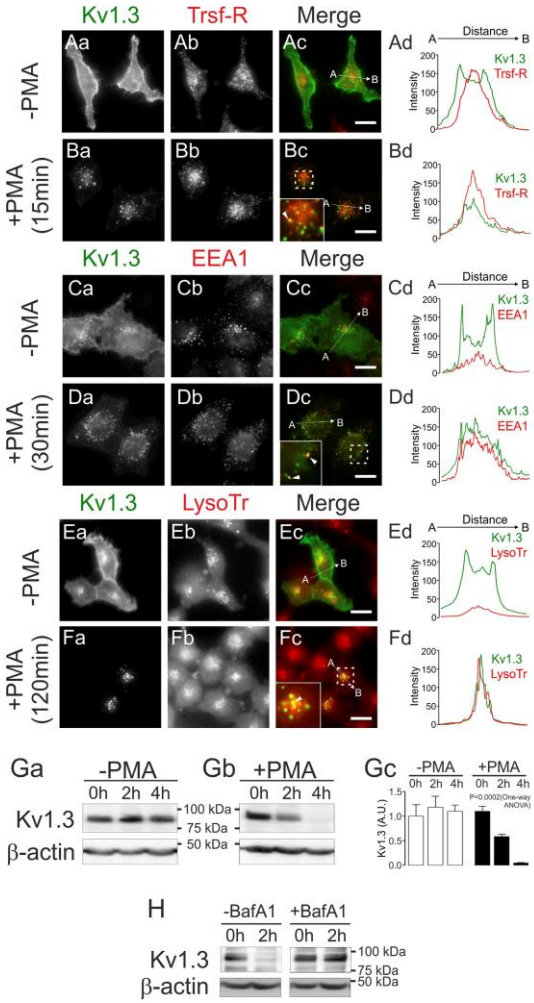

Figure 7. PKC-dependent endocytosis targets Kv1.3 to lysosomal degradation. HEK-293 cells stably expressing Kv1.3 were incubated with 1 μM PMA at 37 °C, and the endocytic pathway was evaluated. (Aa–Bd) Cells were untreated (Aa–Ad) or treated (Ba–Bd) with 1 μM PMA for 15 min, and the colocalization of Kv1.3-YFP and the transferrin receptor (Trsf-R), used as a marker of CCP, was analyzed. (Ca–Dd) Cells were cultured for 30 min without (Ca–Cd) or with (Da–Dd) PMA, and the distribution of Kv1.3-YFP and EEA1 was studied. (Ea–Fd) Cells were incubated for 120 min in the absence (Ea–Ed) or the presence (Fa–Fd) of PMA.

The localization of Kv1.3-YFP into lysosomes was confirmed by LysoTracker (LysoTr) staining. Color code: Kv1.3, green; intracellular compartment marker, red. Yellow in merge panels (Ac, Bc, Cc, Dc, Ec, Fc) indicates colocalization. Insets in panels Bc, Dc and Fc magnify specific regions of interest, indicated by square outlines. Arrowheads indicate colocalizing structures. Bars represent 10 μm. (Ad, Bd, Cd, Dd, Ed, Fd) Histograms showing the results of the pixel-by-pixel analysis of the section A-B indicated by the arrow in the merged images. Color code: green, Kv1.3; red, marker (Trsf-R, EEA1 or LysoTr). Confocal images are representative from >25 cells analyzed in 3–5 independent experiments. (Ga–Gc) PKC-dependent PMA stimulation decreases Kv1.3 expression. Cells were pre-incubated for 3 h with 100 μg/ml of CHX in the absence (−, Ga) or the presence (+, Gb) of PMA, and the Kv1.3 protein expression was analyzed at the indicated times. (Gc) Quantification of Kv1.3 abundance, in arbitrary units (A.U.), from results represented in Ga and Gb. Values are mean ± SE of 4 independent experiments. Statistical analysis was performed by using One-Way ANOVA ($P < 0.0002$, +PMA vs time) with a Tuckey post-test. ($p < 0.05$, +PMA 0 h vs +PMA 2 h and +PMA 2 h vs +PMA 4 h; $p < 0.001$ + PMA 0 h vs + PMA 4 h). (**H**) Further inhibition of the lysosomal function by the addition of 20 μM BafA1 to the CHX pre-incubation counteracted the PMA-dependent degradation of Kv1.3. A representative result from 3 independent experiments is shown.

HEK-293 cells, leading to PKC-mediated Kv1.3 lysosomal degradation. The presence of fewer channels at the cell surface results in less Kv1.3-driven signaling and thereby leads to immunosuppression in leukocytes[47]. In contrast, an ADO-mediated PKC-dependent mechanism stabilizes Kir6.2 channels at the myocyte plasma membrane[23]. However, PKC activation induces internalization of the epithelial sodium channel (ENaC) and the dopamine transporter (DAT) by the same clathrin-mediated endocytosis (CME) mechanism as Kv1.3[48–50]. CME also participates in the Kv1.2 and Kir1.1 endocytic pathways in neurons and renal cells[51,52]. Our results support that the down-regulation of Kv1.3 would trigger immunosuppression via PKC-dependent CME in leukocytes. This mechanism accelerates the degradation of the channel by targeting it to the lysosomal compartment after PKC-dependent stimulation. We further demonstrated that this process requires direct ubiquitination of Kv1.3 by the E3 ubiquitin ligase Nedd4-2. Recent evidence has shown that Nedd4-2 also drives Kv1.3 toward proteasomal degradation[41]. Thus, efficient Nedd4-2-dependent ubiquitination triggers the down-regulation of Kv1.3 via lysosomes and proteasomes, likely acting as redundant and complementary pathways. PKC activation triggers endocytosis and ubiquitination of proteins such as DAT, the glutamate transporter GLT1, the cationic amino acid transporter CAT-1 and aquaporin-2 (AQP2)[22,50,53,54]. Nedd4-2 downregulates Kv1.3 currents, but no direct ubiquitination of the channel had been demonstrated until now[41,42]. The absence of a canonical PY motif together with the irrelevance of a SH3 signature and several lysines within the C-terminal domain of Kv1.3 would suggest alternative mechanisms of association[41].

In T-cells and macrophages, Kv1.3 is targeted to lipid raft membrane microdomains, where it is concentrated upon cellular activation[11,55]. Altered raft-associated Kv1.3 localization in the IS occurs at the onset of the disease lupus erythematosus[38] and a minor raft targeting of Kv1.3 modifies the physiological response[34,47]. We demonstrated that PKC activation displaced Kv1.3 from lipid rafts, similar to what was described for the transporter NET[56]. However, unlike that of NET, the PKC-dependent endocytosis of Kv1.3 is independent of caveolae/lipid raft internalization. Several ion channels, such as TRPV5 and Kir6.1, use the caveolae-dependent internalization machinery[35,57]. TRPV5 endocytosis is inhibited by caveolin-1 knockdown[57]. However, similar to the cationic amino acid and dopamine transporters (CAT1 and DAT, respectively), Kv1.3 was internalized via CCP and independently of caveolae/rafts[22,50]. In this context, the localization of Kv1.3 in and out of rafts would have important physiological consequences. Therefore, recruitment and/or stabilization of the channel at the proper location by accessory proteins, such as caveolins and MAGUKs, would influence the immune response. PKC and Kv1.3 are distributed into lipid raft membrane microdomains within T-lymphocytes, and they are recruited to the IS during T-cell activation[11]. Moreover, PKC and Kv1.3 are part of a signalplex that also includes the tyrosine kinase p56lck, adaptor proteins such as Kvβ2 and hDlg (human homolog of the Drosophila discs large tumor suppressor protein), PSD-95 (postsynaptic density 95), ZIP-1 (Zrt/Irt-like protein) and ZIP-2, and the accessory protein CD4[58]. This cluster facilitates the phosphorylation of Kv1.3, thereby modulating its function. Our results show that PSD-95 association redistributes Kv1.3 into less-mobile membrane microdomains compatible with lipid rafts. In T-lymphocytes, PSD-95 interacts with Kv1.3, inducing clustering and recruiting Kv1.3 into the IS[57]. Similarly, PSD-95 recruits Kv1.4 into lipid rafts, inhibiting the internalization of Kv1.4[59]. A dynamic partitioning model would explain the behavior of raft proteins, suggesting movements in and out of raft domains in a steady-state equilibrium. This spatial distribution would permit proteins to transiently populate raft domains as well as to undergo diffusion outside of rafts. It is tempting to speculate that Kv1.3 would exit rafts being internalized via CCP during immunosuppression. In fact, Kv1.5, acting as an immunosuppresor, influences Kv1.3 by displacing heteromeric Kv1.3/Kv1.5 channels out of rafts in macrophages[34,47,60]. In this scenario, PKC would enhance the exit of Kv1.3 from raft areas and/or facilitate its distribution into clathrin-accessible regions to be endocytosed. In fact, PMA-induced PKC-activation in T-lymphocytes inhibits Kv1.3-dependent K^+ currents[6]. Therefore, a functional Kv1.3-PSD-95 interaction is required not only for correct Kv1.3 redistribution in the vicinity of IS formation but also to prevent a massive internalization of the channel as a consequence of PKC-dependent immunosuppressive insults.

New treatments targeting inflammation-mediated organ dysfunction associated with autoimmune diseases are worth investigation. After persistent activation, mononuclear phagocytes play a pivotal role, supporting the characterization of ADO as an immunomodulatory agent. Adenoreceptor stimulation attenuates inflammation-mediated damage by down-regulating phagocytic activity and preventing excessive respiratory burst activation. For example, the inflammatory response is partially responsible for the damage associated with

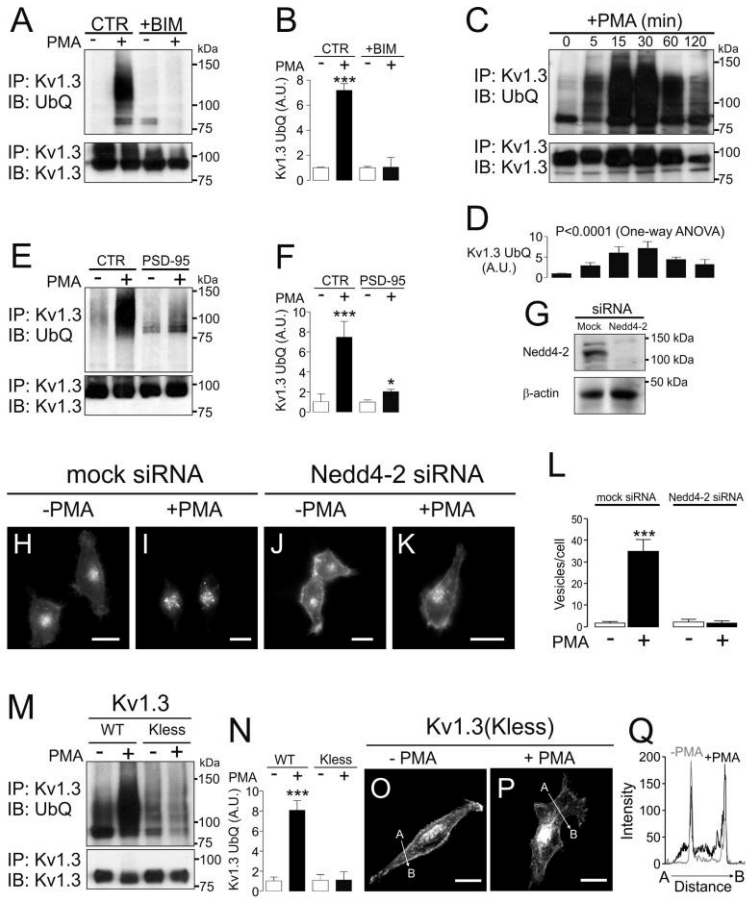

Figure 8. PKC-dependent internalization of Kv1.3 requires Nedd4-2-mediated ubiquitination of the channel. HEK cells with stable expression of Kv1.3-YFP were treated with 1 μM PMA for 30 min at 37 °C, and the ubiquitination of the channel was analyzed. (**A**,**B**) Ubiquitinated Kv1.3 expression in the absence (−) or the presence (+) of PMA with (+BIM) or without (CTR) BIM. (**C**,**D**) Time-course of Kv1.3 ubiquitination upon PMA incubation. Persistent PMA incubation was performed, and cell lysates were collected at the indicated times. (**E**,**F**) PSD-95 hampered the ubiquitination of Kv1.3 in the presence (+) of PMA. (**A**,**C**,**E**) Representative western blots. Total lysates immunoprecipitated against GFP (IP: Kv1.3) were immunoblotted using anti-GFP (IB: Kv1.3) or anti-ubiquitin (IB: UbQ) antibodies. (**B**,**D**,**F**) Expression of ubiquitinated Kv1.3 in arbitrary units (A.U.). Values are mean ± SE of 3–5 independent experiments. (**B**,**F**) White bars, −PMA; Black bars, +PMA. *, $p < 0.05$; ***, $p < 0.001$ vs −PMA, Student's t test. (**D**) Values are mean ± SE of 3 independent experiments. Statistical analysis: $p < 0.0001$ vs time, One-way ANOVA. (**G**) HEK-293 cells were transfected either with siRNA scramble (Mock) or with siRNA against Nedd4-2 to deplete the Nedd4-2 protein expression. Total lysates were blotted with anti-Nedd4-2 and anti-β-actin antibodies. (**H**–**L**) The depletion of Nedd4-2 hampered

the PKC-dependent PMA-induced Kv1.3 endocytosis. Confocal images are representative from >25 cells. (**L**) Quantification of Kv1.3 intracellular vesicles from representative images on panels H-K. Values are mean ± SE of >25 cells from 3 independent experiments. ***, $p < 0.001$ +PMA vs −PMA in mock transfected cells, Student's t test. (**M**,**N**) The absence of lysines in the Kv1.3(Kless) mutant prevents the ubiquitination of the channel in the presence (+) and in the absence (−) of PMA. HEK-293 cells were transiently transfected with Kv1.3 WT (wild type) or Kv1.3(Kless), and the ubiquitination of the channel was analyzed in the absence (−) or the presence (+) of PMA (see materials and methods for details). (**M**) Total lysates immunoprecipitated for GFP (IP: Kv1.3) were immunoblotted with anti-GFP (IB: Kv1.3) or anti-ubiquitin (IB: UbQ). (**M**) Representative western blot from 4 independent experiments. (N) Expression of ubiquitinated Kv1.3 in arbitrary units (A.U.). Values are mean ± SE of 4 independent experiments. White bars, −PMA; Black bars, +PMA. ***, $p < 0.001$ vs −PMA in the Kv1.3 WT channel, Student's t test. (**O**,**P**) Confocal images of HEK cells transfected with Kv1.3(Kless) in the presence (+, **O**) or the absence (−, **P**) of PMA. Kv1.3(Kless) was not internalized in the presence of PMA. Confocal images are representative from >25 cells. (**Q**) Histograms plotting the pixel-by-pixel analysis of the section A-B indicated by the arrow in panels O and P. Color code: grey, absence of PMA (−PMA); black, presence of PMA (+PMA). Note that in both cases Kv1.3 channels decorated the cell surface.

reperfusion of ischemic tissues. ADO modulation has been demonstrated in ischemia/reperfusion injury[61]. In this respect, selective inhibition of A_{2B} enhances intestinal inflammation and injury following ischemia/reperfusion, whereas specific A_{2B} agonist treatment protects against intestinal injury[62]. A_{2B} receptor agonists reduce myocardial ischemia/reperfusion damage by promoting anti-inflammatory M2 macrophages together with decreases in M1 macrophage and neutrophil infiltration in re-perfused hearts[63]. In this context, Kv1.3 is a viable pharmacological target for neuroinflammation associated with ischemia/reperfusion stroke[64]. Our results shed light on the molecular mechanism underlying the anti-inflammatory function of A_{2B} agonist therapy via the modulation of Kv1.3.

Methods

Expression plasmids and site-directed mutagenesis. The rat Kv1.3 in the pRcCMV construct was provided by T.C. Holmes (University of California, Irvine, CA). The channel was subcloned into pEYFP-C1 (Clontech). The rKv1.3 construct that was externally tagged with HA between S3 and S4 was obtained from D.B. Arnold (University of Southern California, CA). For some experiments, the HA-Kv1.3 channel was further subcloned into the pEYFP-C1 plasmid, generating the double-tagged HA-Kv1.3-YFP channel. All Kv1.3 mutants were generated in the pEYFP-Kv1.3 channel. Single and multiple Kv1.3 mutants were generated using the QuikChange site-directed and multi-site-directed mutagenesis kits (Stratagene). All mutations were verified using automated DNA sequencing. Myc-PSD-95 was a kind gift from Dr. F. Zafra (Centro de Biología Molecular Severo Ochoa, Madrid).

Cell culture, transfections and incubations. Unless specified, all reagents were purchased from Sigma-Aldrich. HEK-293 and CY15 mouse dendritic cells were cultured in DMEM and RPMI culture medium (Lonza), respectively, supplemented with 10% fetal bovine serum (FBS), 10,000 U/ml penicillin, 100 μg/ml streptomycin and 2 mM L-glutamine (GIBCO). Murine bone marrow-derived macrophages (BMDM) were isolated and cultured as previously described[14]. HEK-293 cells were incubated with 200 μM Adenosine (ADO) or 1 μM phorbol-12-myristate-13-acetate (PMA) in DMEM for the specified times. BMDM and CY15 cells were incubated for 24 h with or without 200 μM ADO in the presence or the absence of 100 ng/ml of lipopolysaccharide (LPS). Experiments and surgical protocols were performed in accordance with the guidelines approved by the ethical committee of the Universitat de Barcelona and following the European Community Council Directive 86/609 EEC.

Transfection was performed using Metafectene® Pro (Biontex) at approximately 80% confluence. Kv1.3-YFP experiments in HEK-293 cells were mainly performed using a cell line with stable Kv1.3-YFP expression. Briefly, 24 h after Kv1.3 transfection, cells were cultured in the presence of 500 μg/ml of G418 (Geneticin) for selection. Geneticin-resistant clones were maintained in the presence of 250 μg/ml G418. When required, transient transfections were performed 24 h to 48 h before the experiment. For the confocal analyses, cells cultured in the same medium were plated on poly-lysine-coated coverslips. Cells were incubated with 200 μM ADO or 1 μM PMA in DMEM for the specified times. DMSO (dilution 1:1,000) was used as a negative control. Cells were washed in PBS (without K^+), fixed with 4% paraformaldehyde in PBS for 10 min and mounted with Aqua Poly/Mount from Polysciences, Inc. In some experiments, cells were pre-incubated for 15 min in the presence of 1 μM bisindolylmaleimide (BIM) as a PKC inhibitor or with DMSO as vehicle or for 3 h in the presence of 100 μg/ml cycloheximide (CXM) with or without 2 μM bafilomycin A1 (BafA1), as the inhibitor of the lysosomal function. When indicated, cells were pre-incubated with Filipin (5 μM), Nystatin (15 μM) and methyl-β-cyclodextrin (5 mM, MβCD) for 45 min. The caveolin-deficient HEK-293 cell line (Cav1−) was also used[12].

Protein extraction, co-immunoprecipitation, raft isolation and western blot analysis. Cells were washed twice in cold PBS before being lysed on ice with NHG solution (1% Triton X-100, 10% glycerol, 50 mmol/L HEPES pH 7.2, 150 mmol/L NaCl) supplemented with 1 μg/ml aprotinin, 1 μg/ml leupeptin, 1 μg/ml pepstatin and 1 mM phenylmethylsulfonyl fluoride to inhibit proteases. Total lysates were centrifuged at 16,000 × *g* for 15 min at 4 °C, and the protein content was measured using the Bio-Rad Protein Assay (Bio-Rad).

Samples were precleared with 30 μl of protein G-Sepharose beads for 2 h at 4 °C with gentle mixing as part of the co-immunoprecipitation procedures. Beads were removed by centrifugation at 1,000 × *g* for 30 s at 4 °C.

Samples were incubated overnight with the specified antibody (4 ng/μg protein) at 4 °C with gentle agitation. Next, 30 μl of protein G-Sepharose 4 fast flow (GE Healthcare) was added to each sample, and the samples were incubated for 4 h at 4 °C. Beads were removed by centrifugation at 1,000 × *g* for 30 s at 4 °C, washed four times in NHG, and resuspended in 80 μl of SDS sample buffer.

Protein samples (50 μg) and immunoprecipitates were boiled in Laemmli SDS loading buffer and separated using 10% SDS-PAGE. Next, samples were transferred to nitrocellulose membranes (Immobilon-P, Millipore) and blocked in PBS supplemented with 5% dry milk and 0.05% Tween-20 before the immunoreaction. The filters were immunoblotted with antibodies against Kv1.3 (1/200, NeuroMab), iNOS (1/200, Santa Cruz), HA (1/200, Sigma), GFP (1/1,000, Roche), myc (1/1,000, Sigma), PAN-caveolin (1/250, BD Bioscience), clathrin heavy chain (1/500, BD Bioscience), dynamin II (1/1,000, ABR), total PKC (1/500, Santa Cruz), phosphorylated PKCε (1/200, Santa Cruz) and ubiquitin and Nedd4-2 (1/1,000, Santa Cruz) and β-actin (1/50,000, Sigma).

Lipid raft isolation was performed as previously described[34]. Briefly, samples were homogenized in MES (2-Morpholino ethanesulfonic acid)-buffered saline (24 mM MES, pH 6.5, and 0.15 mM NaCl) plus 1% Triton X-100 and centrifuged at 3,000 g for 5 min at 4 °C. Next, sucrose was added to achieve a final concentration of 40%. A 5–30% linear sucrose gradient was layered on top and further centrifuged (39,000 rpm) for 20–22 h at 4 °C in a Beckman SW41 Ti swinging bucket rotor. Gradient fractions (1 ml) were collected from the top and analyzed by Western blot.

Confocal microscopy and subcellular compartment identification. Cells fixed with 4% paraformaldehyde in PBS for 10 min were further permeabilized using 0.1% Triton X-100 for 10 min. After a 60 min incubation with a blocking solution (PBS, 10% goat serum, 5% non-fat dry milk), cells were incubated for 60 min with anti-Clathrin (clathrin heavy chain, 1/100, BD Bioscience), anti-α subunit of AP2 (Adaptor-related Protein complex 2, 1/500, AP.6, American Type Culture Collection), anti-Transferrin receptor (1/1,000, Abcam) or anti-EEA1 (Early Endosomal Antigen 1, 1/1,000, BD Bioscience) in PBS, 10% goat serum and 0.05% Triton. For the extracellular distribution of HA-Kv1.3-YFP, cells were incubated with anti-HA (1/1,000, Sigma) under non-permeabilizing conditions. Next, cells were further incubated for 45 min with an Alexa Fluor secondary antibody (1:500, Molecular Probes) in PBS and BSA (2%). All experiments were performed at 21–23 °C (RT). In some experiments, cells were washed with PBS at 4 °C and stained with LysoTracker® red (1/1,000, Molecular Probes) for 30 min at 4 °C. Staining with FITC-labeled cholera toxin β subunit (CTXβ) for lipid raft microdomains was performed under non-permeabilized conditions. Cells washed with PBS were stained with FITC-CTXβ for 30 min at 4 °C. Subsequently, cells were washed and fixed as above. Cells were examined with a 63x oil immersion objective on a Leica TCS SL laser-scanning confocal microscope. All offline image analyses were performed using a Leica confocal microscope, Image J software and Sigma Plot. The level of endocytosis was quantified analyzing the number of intracellular vesicle accumulation by using the automatic particle counting protocol of the Image J software and setting threshold around 75% to discard the membrane surface mask.

siRNA transfections. Synthetic siRNAs for Clathrin, dynamin II and the missense negative control (Mock) were purchased from Dharmacon. Duplexes were resuspended in 1x siRNA universal buffer (Dharmacon) to 20 μM. HEK-293 cells expressing the stable Kv1.3-YFP channel were grown in six-well plates to 50% confluence. Cells were transfected with siRNA duplexes to a final concentration of 120 nM in 5 μl DharmaFECT1 reagent (Dharmacon, Inc). After 36 h, a second transfection was performed, and the cells were replated into 12-well plates on the following day for internalization experiments. The efficiency of knockdown was evaluated by Western blotting. Mock- and siRNA-transfected cells were processed for immunofluorescence as described above.

Antibody-feeding endocytosis assay. Cells grown on glass coverslips were incubated with 1–2 μg/ml of anti-HA11 (1/1,000, Covance) in DMEM for 30–60 min at RT, washed twice and incubated at 37 °C in the presence or in the absence of 1 μM PMA for 30 min. The cells were then washed with ice-cold Ca^{2+}/Mg^{2+} -free PBS (CMF-PBS) and fixed with freshly prepared 4% paraformaldehyde for 8 min at room temperature. Cells were stained with secondary anti-mouse antibody conjugated with Cy5 (5 μg/ml, saturating concentration) in CMF-PBS containing 0.5% BSA at RT for 60 min to occupy surface HA11. After washings, the cells were permeabilized by 10 min of incubation in CMF-PBS containing 0.1% Triton X-100 at RT and then incubated with the same secondary antibody conjugated with Cy3 (1 μg/ml, non-saturating concentration) for 60 min to stain internalized HA11. Both primary and secondary antibody solutions were precleared by centrifugation at 100,000 × g for 20 min. After staining, cells were washed, and the coverslips were mounted in Mowiol (Calbiochem).

Electrophysiology. Whole-cell currents were recorded using the patch-clamp technique in the whole-cell configuration with a HEKA EPC10 USB amplifier (HEKA Elektronik). PatchMaster software (HEKA) was used for data acquisition. We applied a stimulation frequency of 50 kHz and a filter at 10 kHz. The capacitance and series resistance compensation were optimized. In most experiments, we obtained an 80% compensation of the effective access resistance. Micropipettes were made from borosilicate glass capillaries (Harvard Apparatus) using a P-97 puller (Sutter Instrument) and fire polished. The pipettes had a resistance of 2–4 MΩ. For the stably transfected HEK-293 cells, pipettes were filled with a solution containing the following (in mM): 120 KCl, 1 $CaCl_2$, 2 $MgCl_2$, 10 HEPES, 10 EGTA, 20 D-glucose (pH 7.3 and 280 mOsm/l). The extracellular solution contained the following (in mM): 120 NaCl, 5.4 KCl, 2 $CaCl_2$, 1 $MgCl_2$, 10 HEPES and 25 D-glucose (pH 7.4 and 310 mOsm/l). Cells were clamped at a holding potential of −60 mV. To evoke voltage-gated currents, cells were stimulated with 250 ms square pulses from −60 to +50 mV in 10 mV steps. To analyze the C-type inactivation of Kv1.3, a 5 s depolarizing pulse of +60 mV was applied. Electrodes for CY15 cells were filled with a solution containing the following (in mM): 84 K-aspartate, 36 KCl, 10 KH_2PO_4, 6 K_2ATP, 5 HEPES, 5 EGTA, and 3 $MgCl_2$, pH 7.2. The

extracellular solution contained the following (in mM): 136 NaCl, 4 KCl, 1.8 $CaCl_2$, 1 $MgCl_2$, 10 HEPES, and 10 D-glucose, pH 7.4. CY15 cells were clamped to a holding potential of −60 mV. To evoke voltage-gated currents, cells were stimulated with 250 ms square pulses ranging from −60 to +80 mV in 10 mV steps. The peak amplitude (pA) was normalized using the capacitance values (pF). Data analysis was performed using FitMaster (HEKA) and Sigma Plot 10.0 software (Systat Software). All recordings were performed at RT.

Statistics. Statistical analysis was performed where indicated by means of One-Way or Two-Way ANOVA with Tukey or Bonferroni post-test respectively, Mann-Whitney U test or Student *t* test by using GraphPad Prism 5 (Graphpad Software Inc.).

References

1. Hille, B. *Ion channels of excitable membranes* 3rd edn (Sinauer, Sunderland, Mass., 2001).
2. Feske, S., Wulff, H. & Skolnik, E. Y. Ion channels in innate and adaptive immunity. *Annu Rev Immunol* **33,** 291–353 (2015).
3. Perez-Verdaguer, M. *et al.* The voltage-gated potassium channel Kv1.3 is a promising multitherapeutic target against human pathologies. *Expert Opin Ther Targets* **20,** 577–591 (2016).
4. Martinez-Marmol, R. *et al.* Unconventional EGF-induced ERK1/2-mediated Kv1.3 endocytosis. *Cell Mol Life Sci* **73,** 1515–1528 (2016).
5. Bowlby, M. R., Fadool, D. A., Holmes, T. C. & Levitan, I. B. Modulation of the Kv1.3 potassium channel by receptor tyrosine kinases. *J Gen Physiol* **110,** 601–610 (1997).
6. Payet, M. D. & Dupuis, G. Dual regulation of the n type K+ channel in Jurkat T lymphocytes by protein kinases A and C. *J Biol Chem* **267,** 18270–18273 (1992).
7. Festugato, M. Adenosine: an endogenous mediator in the pathogenesis of psoriasis. *An Bras Dermatol* **90,** 862–867 (2015).
8. De Ponti, C. *et al.* Adenosine A2a receptor-mediated, normoxic induction of HIF-1 through PKC and PI-3K-dependent pathways in macrophages. *J Leukoc Biol* **82,** 392–402 (2007).
9. O'Connell, K. M., Martens, J. R. & Tamkun, M. M. Localization of ion channels to lipid Raft domains within the cardiovascular system. *Trends Cardiovasc Med* **14,** 37–42 (2004).
10. Bi, K. *et al.* Antigen-induced translocation of PKC-theta to membrane rafts is required for T cell activation. *Nat Immunol* **2,** 556–563 (2001).
11. Panyi, G. *et al.* Kv1.3 potassium channels are localized in the immunological synapse formed between cytotoxic and target cells. *Proc Natl Acad Sci USA* **101,** 1285–1290 (2004).
12. Perez-Verdaguer, M. *et al.* Caveolin interaction governs Kv1.3 lipid raft targeting. *Sci Rep* **6,** 22453 (2016).
13. Martinez-Marmol, R. *et al.* A non-canonical di-acidic signal at the C-terminus of Kv1.3 determines anterograde trafficking and surface expression. *J Cell Sci* **126,** 5681–5691 (2013).
14. Vicente, R. *et al.* Differential voltage-dependent K+ channel responses during proliferation and activation in macrophages. *J Biol Chem* **278,** 46307–46320 (2003).
15. Roger, T. *et al.* High expression levels of macrophage migration inhibitory factor sustain the innate immune responses of neonates. *Proc Natl Acad Sci USA* **113,** E997–1005 (2016).
16. Zsiros, E. *et al.* Developmental switch of the expression of ion channels in human dendritic cells. *J Immunol* **183,** 4483–4492 (2009).
17. Sole, L. *et al.* The C-terminal domain of Kv1.3 regulates functional interactions with the KCNE4 subunit. *J Cell Sci* **129,** 4265–4277 (2016).
18. Miras-Portugal, M. T., Gualix, J. & Pintor, J. The neurotransmitter role of diadenosine polyphosphates. *FEBS Lett* **430,** 78–82 (1998).
19. Sun, H. *et al.* Kainate receptor activation induces glycine receptor endocytosis through PKC deSUMOylation. *Nat Commun* **5,** 4980 (2014).
20. Kanda, V. A., Purtell, K. & Abbott, G. W. Protein kinase C downregulates I(Ks) by stimulating KCNQ1-KCNE1 potassium channel endocytosis. *Heart Rhythm* **8,** 1641–1647 (2011).
21. Miranda, M., Dionne, K. R., Sorkina, T. & Sorkin, A. Three ubiquitin conjugation sites in the amino terminus of the dopamine transporter mediate protein kinase C-dependent endocytosis of the transporter. *Mol Biol Cell* **18,** 313–323 (2007).
22. Vina-Vilaseca, A., Bender-Sigel, J., Sorkina, T., Closs, E. I. & Sorkin, A. Protein kinase C-dependent ubiquitination and clathrin-mediated endocytosis of the cationic amino acid transporter CAT-1. *J Biol Chem* **286,** 8697–8706 (2011).
23. Yang, H. Q. *et al.* Plasticity of sarcolemmal KATP channel surface expression: relevance during ischemia and ischemic preconditioning. *Am J Physiol Heart Circ Physiol* **310,** H1558–1566 (2016).
24. Xaus, J. *et al.* IFN-gamma up-regulates the A2B adenosine receptor expression in macrophages: a mechanism of macrophage deactivation. *J Immunol* **162,** 3607–3614 (1999).
25. Csoka, B. *et al.* Adenosine promotes alternative macrophage activation via A2A and A2B receptors. *FASEB J* **26,** 376–386 (2012).
26. Hasko, G. *et al.* Adenosine receptor agonists differentially regulate IL-10, TNF-alpha, and nitric oxide production in RAW 264.7 macrophages and in endotoxemic mice. *J Immunol* **157,** 4634–4640 (1996).
27. Cooper, I., Hill, S. J. & Alexander, S. P. An endogenous A2B adenosine receptor coupled to cyclic AMP generation in human embryonic kidney (HEK 293) cells. *Br J Pharmacol* **122,** 546–550 (1997).
28. Kellerer, M., Mushack, J., Mischak, H. & Haring, H. U. Protein kinase C (PKC) epsilon enhances the inhibitory effect of TNF alpha on insulin signaling in HEK293 cells. *FEBS Lett* **418,** 119–122 (1997).
29. Comalada, M. *et al.* PKC epsilon is involved in JNK activation that mediates LPS-induced TNF-alpha, which induces apoptosis in macrophages. *Am J Physiol Cell Physiol* **285,** C1235–1245 (2003).
30. Valledor, A. F., Xaus, J., Comalada, M., Soler, C. & Celada, A. Protein kinase C epsilon is required for the induction of mitogen-activated protein kinase phosphatase-1 in lipopolysaccharide-stimulated macrophages. *J Immunol* **164,** 29–37 (2000).
31. Valledor, A. F., Xaus, J., Marques, L. & Celada, A. Macrophage colony-stimulating factor induces the expression of mitogen-activated protein kinase phosphatase-1 through a protein kinase C-dependent pathway. *J Immunol* **163,** 2452–2462 (1999).
32. Panyi, G., Sheng, Z. & Deutsch, C. C-type inactivation of a voltage-gated K+ channel occurs by a cooperative mechanism. *Biophys J* **69,** 896–903 (1995).
33. Radulescu, A. E., Siddhanta, A. & Shields, D. A role for clathrin in reassembly of the Golgi apparatus. *Mol Biol Cell* **18,** 94–105 (2007).
34. Vicente, R. *et al.* Kv1.5 association modifies Kv1.3 traffic and membrane localization. *J Biol Chem* **283,** 8756–8764 (2008).
35. Jiao, J., Garg, V., Yang, B., Elton, T. S. & Hu, K. Protein kinase C-epsilon induces caveolin-dependent internalization of vascular adenosine 5′-triphosphate-sensitive K+ channels. *Hypertension* **52,** 499–506 (2008).
36. Ros-Baro, A. *et al.* Lipid rafts are required for GLUT4 internalization in adipose cells. *Proc Natl Acad Sci USA* **98,** 12050–12055 (2001).
37. Szilagyi, O., Boratko, A., Panyi, G. & Hajdu, P. The role of PSD-95 in the rearrangement of Kv1.3 channels to the immunological synapse. *Pflugers Arch* **465,** 1341–1353 (2013).
38. Nicolaou, S. A. *et al.* Altered dynamics of Kv1.3 channel compartmentalization in the immunological synapse in systemic lupus erythematosus. *J Immunol* **179,** 346–356 (2007).

39. Balut, C. M., Loch, C. M. & Devor, D. C. Role of ubiquitylation and USP8-dependent deubiquitylation in the endocytosis and lysosomal targeting of plasma membrane KCa3.1. *FASEB J* **25,** 3938–3948 (2011).
40. Sun, T. *et al.* The role of monoubiquitination in endocytic degradation of human ether-a-go-go-related gene (hERG) channels under low K+ conditions. *J Biol Chem* **286,** 6751–6759 (2011).
41. Velez, P., Schwartz, A. B., Iyer, S., Warrington, A. & Fadool, D. A. Ubiquitin ligase Nedd4-2 modulates Kv1.3 current amplitude and ion channel protein targeting. *J Neurophysiol* **116,** 671–685 (2016).
42. Henke, G., Maier, G., Wallisch, S., Boehmer, C. & Lang, F. Regulation of the voltage gated K+ channel Kv1.3 by the ubiquitin ligase Nedd4-2 and the serum and glucocorticoid inducible kinase SGK1. *J Cell Physiol* **199,** 194–199 (2004).
43. Kunduri, S., Dick, G., Nayeem, M. & Mustafa, S. Adenosine A1 receptor signaling inhibits BK channels through a PKCalpha-dependent mechanism in mouse aortic smooth muscle. *Physiol Rep* **1,** e00037 (2013).
44. Lasley, R. D. Adenosine receptors and membrane microdomains. *Biochim Biophys Acta* **1808,** 1284–1289 (2011).
45. Chung, I. & Schlichter, L. C. Native Kv1.3 channels are upregulated by protein kinase C. *J Membr Biol* **156,** 73–85 (1997).
46. Rangaraju, S., Chi, V., Pennington, M. W. & Chandy, K. G. Kv1.3 potassium channels as a therapeutic target in multiple sclerosis. *Expert Opin Ther Targets* **13,** 909–924 (2009).
47. Villalonga, N. *et al.* Immunomodulation of voltage-dependent K+ channels in macrophages: molecular and biophysical consequences. *J Gen Physiol* **135,** 135–147 (2010).
48. Eaton, A. F., Yue, Q., Eaton, D. C. & Bao, H. F. ENaC activity and expression is decreased in the lungs of protein kinase C-alpha knockout mice. *Am J Physiol Lung Cell Mol Physiol* **307,** L374–385 (2014).
49. Shimkets, R. A., Lifton, R. P. & Canessa, C. M. The activity of the epithelial sodium channel is regulated by clathrin-mediated endocytosis. *J Biol Chem* **272,** 25537–25541 (1997).
50. Sorkina, T., Hoover, B. R., Zahniser, N. R. & Sorkin, A. Constitutive and protein kinase C-induced internalization of the dopamine transporter is mediated by a clathrin-dependent mechanism. *Traffic* **6,** 157–170 (2005).
51. Nesti, E., Everill, B. & Morielli, A. D. Endocytosis as a mechanism for tyrosine kinase-dependent suppression of a voltage-gated potassium channel. *Mol Biol Cell* **15,** 4073–4088 (2004).
52. Lin, D. H. *et al.* POSH stimulates the ubiquitination and the clathrin-independent endocytosis of ROMK1 channels. *J Biol Chem* **284,** 29614–29624 (2009).
53. Barrera, S. P. *et al.* PKC-Dependent GlyT1 Ubiquitination Occurs Independent of Phosphorylation: Inespecificity in Lysine Selection for Ubiquitination. *PLoS One* **10,** e0138897 (2015).
54. Kamsteeg, E. J. *et al.* Short-chain ubiquitination mediates the regulated endocytosis of the aquaporin-2 water channel. *Proc Natl Acad Sci USA* **103,** 18344–18349 (2006).
55. Martinez-Marmol, R. *et al.* Multiple Kv1.5 targeting to membrane surface microdomains. *J Cell Physiol* **217,** 667–673 (2008).
56. Jayanthi, L. D., Samuvel, D. J. & Ramamoorthy, S. Regulated internalization and phosphorylation of the native norepinephrine transporter in response to phorbol esters. Evidence for localization in lipid rafts and lipid raft-mediated internalization. *J Biol Chem* **279,** 19315–19326 (2004).
57. Cha, S. K., Wu, T. & Huang, C. L. Protein kinase C inhibits caveolae-mediated endocytosis of TRPV5. *Am J Physiol Renal Physiol* **294,** F1212–1221 (2008).
58. Panyi, G., Vamosi, G., Bodnar, A., Gaspar, R. & Damjanovich, S. Looking through ion channels: recharged concepts in T-cell signaling. *Trends Immunol* **25,** 565–569 (2004).
59. Wong, W. & Schlichter, L. C. Differential recruitment of Kv1.4 and Kv4.2 to lipid rafts by PSD-95. *J Biol Chem* **279,** 444–452 (2004).
60. Vicente, R. *et al.* Association of Kv1.5 and Kv1.3 contributes to the major voltage-dependent K+ channel in macrophages. *J Biol Chem* **281,** 37675–37685 (2006).
61. Ham, I. & Rees, D. A. The adenosine a2b receptor: its role in inflammation. *Endocr Metab Immune Disord Drug Targets* **8,** 244–254 (2008).
62. Hart, M. L., Jacobi, B., Schittenhelm, J., Henn, M. & Eltzschig, H. K. Cutting Edge: A2B Adenosine receptor signaling provides potent protection during intestinal ischemia/reperfusion injury. *J Immunol* **182,** 3965–3968 (2009).
63. Tian, Y., Piras, B. A., Kron, I. L., French, B. A. & Yang, Z. Adenosine 2B Receptor Activation Reduces Myocardial Reperfusion Injury by Promoting Anti-Inflammatory Macrophages Differentiation via PI3K/Akt Pathway. *Oxid Med Cell Longev* **2015,** 585297 (2015).
64. Chen, Y. J. *et al.* The potassium channel KCa3.1 constitutes a pharmacological target for neuroinflammation associated with ischemia/reperfusion stroke. *J Cereb Blood Flow Metab* **36,** 2146–2161 (2015).

Acknowledgements

Supported by the Ministerio de Economía y Competitividad (MINECO), Spain (BFU2014-54928-R and BFU2015-70067-REDC) and Fondo Europeo de Desarrollo Regional (FEDER). AS was supported by NIH grants DA014204 and CA089151. KS, MPV and AVG holded fellowships from the MINECO. RMM and NC were supported by the Juan de la Cierva program (MINECO). RMM and KS contributed equally.

Author Contributions

R.M.M., K.S., M.P.V., A.V.G. and N.C. performed the experiments. R.M.M., A.S. and A.F. designed the experiments. A.F. directed the study. All authors participated in writing the manuscript.

Additional Information

Supplementary information accompanies this paper at http://www.nature.com/srep

Competing financial interests: The authors declare no competing financial interests.

How to cite this article: Martínez-Mármol, R. *et al.* Ubiquitination mediates Kv1.3 endocytosis as a mechanism for protein kinase C-dependent modulation. *Sci. Rep.* **7,** 42395; doi: 10.1038/srep42395 (2017).

Publisher's note: Springer Nature remains neutral with regard to jurisdictional claims in published maps and institutional affiliations.

This work is licensed under a Creative Commons Attribution 4.0 International License. The images or other third party material in this article are included in the article's Creative Commons license, unless indicated otherwise in the credit line; if the material is not included under the Creative Commons license, users will need to obtain permission from the license holder to reproduce the material. To view a copy of this license, visit http://creativecommons.org/licenses/by/4.0/

© The Author(s) 2017

Supplementary Information

Ubiquitination mediates Kv1.3 endocytosis as a mechanism for protein kinase C-dependent modulation

Ramón Martínez-Mármol, Katarzyna Styrczewska, Mireia Pérez-Verdaguer, Albert Vallejo-Gracia, Núria Comes, Alexander Sorkin and Antonio Felipe

Legend to Supplementary Figures

Supplementary Figure 1. PMA-dependent Kv1.3 endocytosis in HEK-293 cells. Confocal images of HEK cells transfected with HA-Kv1.3-YFP. Antibody-feeding endocytosis assay targeting the Kv1.3-HA external epitope. Live cells, incubated with anti-HA antibody for 1 h at 4°C, were further treated with (+PMA) or without (-PMA) PMA for 30 min at 37°C. HA-Kv1.3-YFP distribution in the absence (A-D) or the presence (E-H) of PMA. (A, E) Total HA-Kv1.3-YFP channel distribution. (B, F) Extracellular Cy5-stained HA-Kv1.3. (C, G) Intracellular Cy3-stained HA-Kv1.3. PMA-dependent (G) and independent (C) HA-Kv1.3-YFP endocytosis. (D, H) Merge panels in the absence or the presence of PMA, respectively. Confocal images are representative from >25 cells analyzed in 3 independent experiments. Bars represent 10 μm.

Supplementary Figure 2. Caveolae/lipid raft-independent Kv1.3 endocytosis upon PMA incubation. The internalization of Kv1.3 in HEK-293 cells stably transfected with the channel was induced by 30 min of incubation with 1 μM PMA at 37ºC. (A-H) Cells were pretreated for 45 min without (A, E) or with 5 μM Filipin (B, F), 15 μM Nystatin (C, G) or 5 mM MβCD (D, H) prior to incubation with PMA. (I-L) HEK-293 cells with lentiviral depletion of caveolin 1 ($Cav1^-$) were transfected with Kv1.3-YFP and preincubated with 5 mM MβCD for 45 min before treatment with (+) or without (-) 1 μM PMA at 37ºC. Confocal images are representative from >25 cells analyzed in 3 independent experiments. Bars represent 10 μm.

Supplementary Figure 3. PSD-95 protects Kv1.3 against PMA-dependent endocytosis. HEK-293 cells were cotransfected with HA-Kv1.3-YFP and PSD-95-myc and treated with 1 μM PMA for 30 min at 37ºC. (A-F) Cells were incubated without (-, A-C) or with (+, D-F) PMA. $Kv1.3_{TOTAL}$ (green) stands for the Kv1.3-YFP signal. $Kv1.3_{EXTRACEL}$ (red) refers to the extracellular HA staining under non-permeabilizing conditions. Colocalization (yellow) decorates the membrane in the merge panel without PMA (C) but not in (F). (G-N) PSD-95 preserved $Kv1.3_{EXTRACEL}$ in the presence of PMA. Color code in merge panels: green, $Kv1.3_{TOTAL}$; blue, $Kv1.3_{EXTRACEL}$; red, PSD-95; cyan, colocalization between $Kv1.3_{TOTAL}$ and $Kv1.3_{EXTRACEL}$; white, triple colocalization. (O-V) PSD-95 counteracted the targeting of Kv1.3 to early endosomes (EEA1) in the presence of PMA. Color code in merge panels: green, Kv1.3-YFP; red, EEA1; yellow, colocalization between Kv1.3 and EEA1. PSD-95 is not shown in the merge panels. Circled cells in S-U are not transfected with PSD-95-myc. Insets in panel V show distinct colocalization of Kv1.3 and EEA1 in the absence (cells in circle) or the presence of PSD-95-myc. Confocal images are representative from >25 cells analyzed in 3 independent experiments. Bars represent 10 μm.

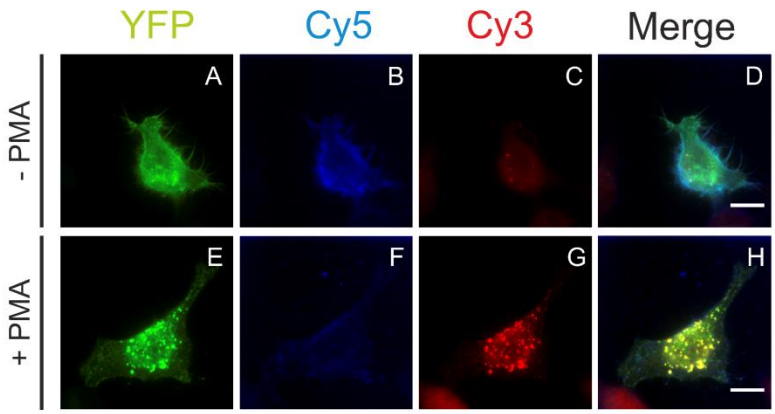

Figure S1

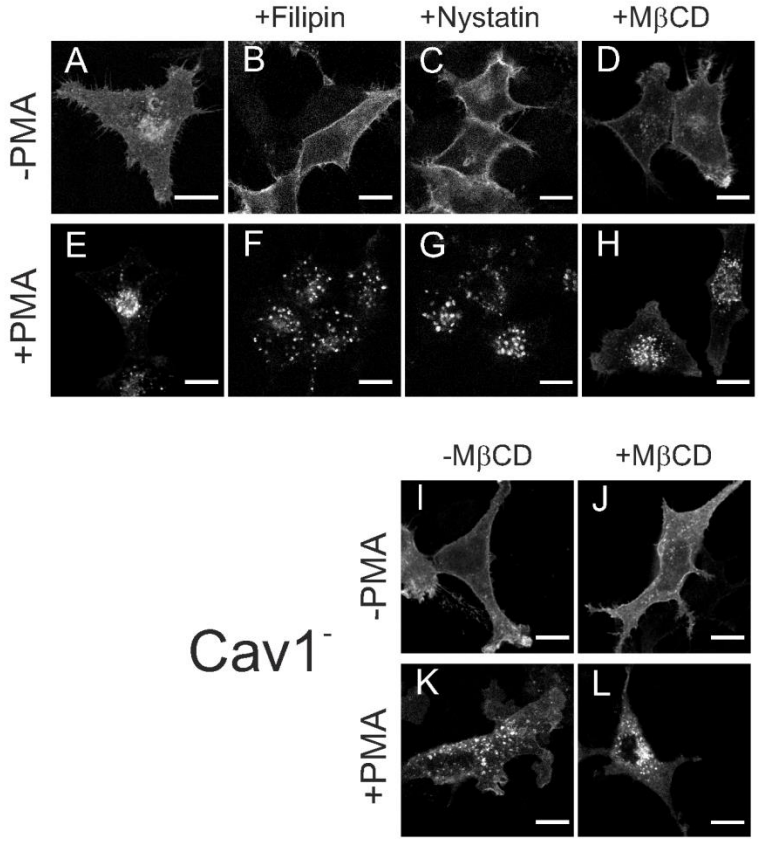

Figure S2

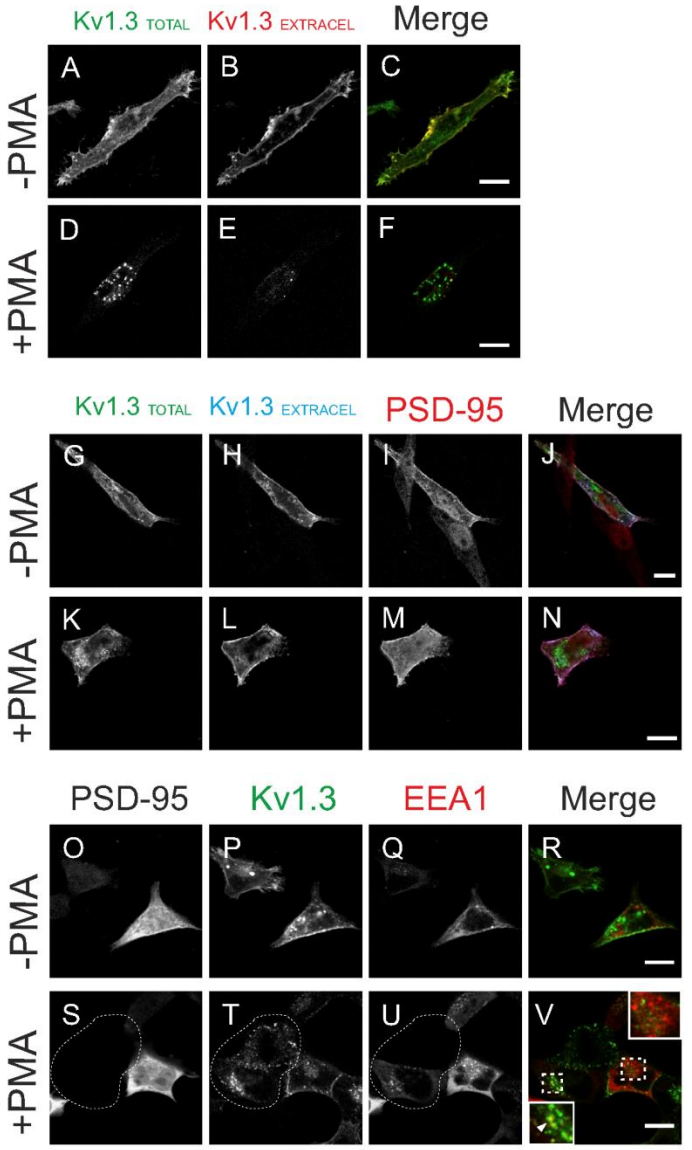
Kv1.3 TOTAL
Kv1.3 EXTRACEL
Merge
-PMA
+PMA
A
B
C
D
E
F
Kv1.3 TOTAL
Kv1.3 EXTRACEL
PSD-95
Merge
G
H
I
J
K
L
M
N
PSD-95
Kv1.3
EEA1
Merge
O
P
Q
R
S
T
U
V

Figure S3

3.3. Part Three:

Molecular determinants involved in the turnover of Kv1.3.

Contributions:

1. Signaling pathways triggering Kv1.3 internalization.

2. Lysine-targeting specificity of Kv1.3 poliubiquitination.

3.3.1. Contribution 1:

Signaling pathways triggering Kv1.3 internalization

Katarzyna Styrczewska[1], Irene Estadella.[1], Antonio Felipe[1]

[1]Molecular Physiology Laboratory, Departament de Bioquímica i Biomedicina Molecular, Institut de Biomedicina (IBUB), Universitat de Barcelona, Avda. Diagonal 643, 08028 Barcelona, Spain

ABSTRACT

Regulation of protein degradation is an important component of many cellular pathways. PKC-dependent internalization of Kv1.3 is dependent of ubiquitination of the channel and mediated by the clathrin-dependent endocytosis triggering lisosomal degradation.

To further investigate the molecular mechanisms of the Kv1.3 internalization in response to adenosine, we have examined the effects of PKA antagonists. Our results, for the first time, provided evidence on the effect of PKA activation on the Kv1.3 trafficking.

Report of the PhD student participation

Signaling pathways triggering Kv1.3 internalization

Katarzyna Styrczewska performed the main body of experiments and the data analysis of this article.

Antonio Felipe

PhD thesis director

Introduction

Voltage-gated K channels (Kv) is large family of channels that are expressed in both excitable and non-excitable cells. In nerve and muscle they contribute to the control of resting membrane potential and action potential frequency and duration. In non-excitable tissues Kv are involved in many processes such as secretion to cell proliferation (Pardo, 2004; Wulff et al., 2009; Chandy et al., 2004). Kv1.3 is a voltage-gated potassium channel that is crucial for T cell development and activation. Kv1.3 is highly expressed in effector memory T cells, where constitutes the predominant K^+ conductance for these cells and provides, together with KCa3.1, the electrochemical driving force for Ca^{2+} influx necessary for both T-cell proliferation and cytokine secretion (Cahalan and Chandy, 2009; Feske, 2007). Thus, Kv1.3 is regarded as an attractive target for treatment of autoimmune diseases (Rangaraju et al., 2009). In this context, several Kv1.3 channel blockers, such as 5-methoxypsoralen and acacetin have been proven to suppress cytokine secretion of T cells and alleviated autoimmune diseases in animal or cell models (Fu et al., 2013; Zhao et al., 2014). The importance of this channel on human health and disease assures that this protein must be under strictly regulation. Here we investigated different roles of PKC and PKA on the modulation of Kv1.3 endocytosis.

Protein kinases regulate the activity of ion channels by modulating intracellular trafficking and the abundance of functional proteins at the cell surface (Bradbury and Bridges 1994). Recently we demonstrated that Kv1.3 endocytosis is triggered by PKC activation and in a clathrin-

dependent manner which finally leads the channel to lysosomal degradation. However, Kv1.3 can be phosphorylated by both PKC and PKA (Szabo et al., 1996; Szigligeti et al., 2006). In this context, in the present work we have examined the PKC and PKA-mediated Kv1.3 internalization.

Material and Methods

Cell culture and cell transfection

Experiments were performed using the mammalian cell line HEK-293. Cells were grown in DMEM (Dulbecco's modified Eagle's medium) containing 10% fetal bovine serum (FBS), L-glutamine (2 mM) and antibiotics: penicillin G (10,000 U / ml) and streptomycin (10 mg / ml). Cells were harvested and plated on plastic Petri dishes and cultured in a 37 °C humidified incubator with 5% CO2. Cells were grown to confluence. HEK-293 cells were transfected using PEI (Polyethylenimine). Polyethylenimine is a polymeric transfection agent, which belongs to a group of cationic polymers. PEI forms a complex with DNA, and as a cationic carrier, PEI neutralize the negatively charged plasmid, allowing contact with the cells. Transport into the cell may take the form of endocytosis, or fusion with the cell membrane. There is a risk of degradation of the material introduced in the lysosome, but it can be transported to the nucleus and transcription and expression of the introduced material.

For immunocytochemistry experiments cells were plated into 12-well dishes containing 12 mm glass coverslips pretreated with poly-L-

lysine and into 1 ml of media. To conduct immunoprecipitation experiments cells were plated into Petri dish with 10 ml of media. The following DNA amounts were used; i) immunoprecipitation: 4 μg/P100 dish; ii) immunocytochemistry: 0.5 μg/12-multi-wells. PEI and DNA were diluted in 150 mM NaCl. Both mixtures were incubated for 15 min, mixed and still for 30 min. Cells were incubated for 4 hour with the Pei/DNA mixture diluted in media. After 4 h media was changed. In both experiments cells were harvested 24 h after transfection.

Immunochemistry and Microscopy studies

For immunocytochemistry cells were grown in multi-wells on glass slides and transfected. After 24 hours, the cells were incubated for 30 minutes at 37 °C with 200 μM ADO or 1 μM PMA in DMEM for the specified times. DMSO (dilution 1:1,000) was used as a negative control. The cells were then washed 3 times with PBS without K^+ (0.9% NaCl, 0.01 M NaH_2PO_4 • H_2O) at 37 ° C. The absence of K^+ in solution facilitates the adhesion of these cells which by nature tend to be easily separated from the surface on which they grow. Next, cells were fixed with freshly prepared 4% paraformaldehyde for 10 min at room temperature. After 3 washes of 5 min each with PBS without K^+, the coverslips were mounted in Mowiol media.

The data presented in this work were obtained using a spectral confocal microscope Leica TCS SL (Leica Microsystems, Heidelberg GmbH, Mannheim, Germany). The conditions, under which pictures were taken with the microscope confocal, were as follows: the pinhole used was 1 AE (Airy Units), line average used was 4, scan speed: 400 Hz,

resolution: 1024 pixels x 1024 pixels, zoom x 4. The level of endocytosis was quantified analyzing the number of intracellular vesicle accumulation by using the automatic particle counting protocol of the Image J software and setting threshold around 75% to discard the membrane surface mask.

Protein extraction, Immunoprecipitation and Western Blotting

To obtain total protein lysates, cells were split on plates 100 mm cell diameter, grown to confluence and transfected. One day after transfection, cells were incubated for 30 min at 37 °C with 1 μM PMA (in DMSO) or 200 μM adenosine, or with DMSO as a negative control. The whole process is carried out on ice. After 3 washes with cold PBS, cells were left in protein extraction buffer for 20 min. The buffer contained the following components: 50 mM Tris-HCl pH 7.4, 150 mM NaCl, 1% Triton x-100, 1 mM EDTA, supplemented with with 0.0125g N-ethylmaleimide (NEM), 5 μM MG-132, 1 mM Na_3VO_4, and 10 mM NaF and 0.1% protease inhibitors (pepstatin, leupeptin, phenylmethylsulfonyl fluoride (PMSF) and aprotinin). Cells were spun for 10 min at 14,000 rpm at 4 °C. The supernatant was collected and stored at -20 °C.

Protein concentrations were measured using Bradford protein assay. For coimmunoprecipitation assays, protein samples (from 1 to 2 μg) were pre-incubated with 50 μl of protein A sepharose (before washed 3 times with IP lysis buffer) for 2 h at 4° C. After this time, samples were gently centrifuged for 30 s at 1,000 *g* to minimize possible A sepharose non-specific binding. Next, .onspecific binding free supernatant was

added into a chromatographic column (Micro Spin Chromatography columns, BioRad). Columns had been prepared previously, washed Protein A (50 µl into each column) was added, then specific antibody against the protein under immunoprecipitate (GFP Polyclonal Antibody, GenScript at a ratio of 4 ng antibody per mg total protein) and incubated for 2 h. Next, DMP (dimethyl pimelimidate, Pierce) was also added, to generate imidioester bonds between antibody and sepharose. The incubation was performed at 4° C O/N with constant agitation. After this time, the supernatant was collected. Columns were placed onto eppendorfs that already had 20 µl of TC5x 10% β-mercaptoethanol and protein-antibody complex-protein A were eluted by adding a solution of glycine (0.2 M, pH 2.5).

The samples were separated on percentage suitable acrylamide-bisacrylamide SDS-PAGE gels. Proteins were transferred to a PVDF membrane (Immobilon-P, Millipore). Blocking was done for 1 h at room temperature (RT) with a solution of PBS with 0.05% Tween and 5% skimmed milk powder. Blocked membranes were incubated with primary antibody diluted in PBS 0.05% Tween O/N at 4° C.

Two different antibodies have been used. An anti-Kv1.3, Mouse Monoclonal Antibody (NeuroMab) - to detect the presence of Kv1.3, and anti-Ubiquitin (P4D1) Mouse Monoclonal Antibody (Santa Cruz Biotechnology, Inc.) to detect the ubiquitinated channels. Finally, membranes were incubated for 1 hour at RT with the secondary antibody (Goat Anti-Mouse IgG, Bio-Rad). ECL reagent (Biological Industries) was used to detect protein signals. Between antibodies, 4 washes of 5 min

with 0.05%Tween in PBS were made. Results were obtained in X-ray films. Western blots were quantified using MacBiophotonics ImageJ software. ImageJ was used to compare the density (intensity) of western blot bands.

Protein kinase inhibitors

For examination of protein ubiquitination and endocytosis, transfected cells were cultured O/N in serum-starvation (DMEM +0.02% BSA) medium. All assays were carried out in this serum free DMEM. Agonist and/or inhibitor were added as described in the figure legends. Briefly, inhibitors were added 30-15 min before the agonist, and then cells were incubated together with inhibitors and the indicated agonist for following 30 min. The incubation was terminated by removing the media. Next, we performed protein extraction or immunochemistry.

Ubiquitination assay

Cells were washed twice in cold PBS and frozen at -80ºC for at least one night. Cells were lysed 20 min on ice with 2 mL of lysis buffer (50 mM HEPES, 150 mM NaCl, 1% Triton X-100, 10% Glicerol, pH 7.5) supplemented with 0.0125 g NEM, 0.2 mM MG132, 1 mM EGTA 1 mM EDTA, 20 mM NaF, 1% NaOV, 2 mM DTT, 1 μg/ml aprotinin, 1 μg/ml leupeptin, 1 μg/ml pepstatin and 1 mM phenylmethylsulfonyl fluoride as protease inhibitors. Cells were scraped and further centrifuged at 14,000 g for 15 min. Co-immunoprecipitation assay was performed as previously described.

Cell-surface biotinylation

Cell-surface biotinylation was carried out using EZ-Link Sulfo-NHS-SS-Biotin (sulfosuccinimidyl-2-[biotinamido]ethyl-1,3-dithiopropionate) reagent (Pierce) diluted in PBS 1mM $MgCl_2$ 1mM $CaCl_2$ at 0.5 mg/mL. Cells were gently incubated in a rocking platform for 30 min at 4ºC. During the incubation an ester group of the biotinylation reagent reacted with primary amines of lysine amino acidic residues exposed extracellularly. Next, the reaction was quenched with Glycine 50 mM diluted in the same PBS buffer. Three washes of 5 min at 4ºC each were performed to allow the neutralization of the uncrosslinked reagent. Following, cells were lysed with 1% Triton X-100, 10% glycerol, 5 mM HEPES pH 7.2 and 150 mMNaCl supplemented with 1 μg/ml aprotinin, 1 μg/ml leupeptin, 1 μg/ml pepstatin and 1 mM phenylmethylsulfonyl fluoride as protease inhibitors. Homogenates were centrifuged at 12,000 g for 15 min and total protein content was obtained from supernatant. To isolate biotin-labelled proteins, samples were incubated with NeutrAvidin Agarose beads (Pierce) during 2 h at 4ºC. After 3 washes biotinylated proteins were eluted from NeutrAvidin beads in reducing conditions, 1X Laemmli SDS loading buffer, and 10 min at 100 º C

Statistical analysis

Results are expressed as mean ± s.e.m. Ubiquitination and endocytosis level and inhibition response curves were analyzed by computer-assisted iteration using the GraphPad Prism (GraphPad software, San Diego, U.S.A.). Statistical significance was determined by

analysis of variance (ANOVA) followed by post-test and Student *t* test, and $P<0.05$ was considered as the limit of statistical significance.

Results

Adenosine triggered both PKC and PKA-dependent internalisation of Kv1.3.

We have previously described that adenosine can activate PKC-dependent endocytosis of Kv1.3 (Martinez-Marmol et al., 2017). PKC activation triggers down-regulation of Kv1.3 by inducing a clathrin-mediated endocytic event that targets the channel to lysosomal-degradative compartments. The presence of the PKC inhibitor bisindolylmaleimide (BIM) hampered the internalization of channels. However, we wondered whether this was the unique signaling pathway activated by adenosine on the Kv1.3 regulation.

In order to determine the adenosine-dependent mechanisms implicated in Kv1.3 internalization and ubiquitination experiments were performed in HEK cells transfected with Kv1.3 YFP. Cells were treated with 200 μM adenosine and inhibitors of PKC (BIM; 1 μM), PKA (H89; 10 μM), and ERK1/2 (U0126; 10 μM) during 30 min. Cells were pretreated with inhibitors for 15 min.

Ubiquitination assays (Fig.1) showed that BIM partially inhibited adenosine-induced ubiquitination. Thus, we observed a resistant 31±2 % (n=5) of channel ubiquitination upon adenosine-incubation. In addition,

ubiquitination was also partially (65±4%, n=5) inhibited by H89 (a PKA inhibitor). These results indicated that adenosine induced Kv1.3 ubiquitination by both PKC and PKA signaling pathways. Furthermore, a combination of both inhibitors did not show a cumulative effect (30 ±2%, n=5). On the other hand, the ERK1/2 blocker U0126 had no significant effect on Kv1.3 adenosine-induced ubiquitination (87±8%, n=5).

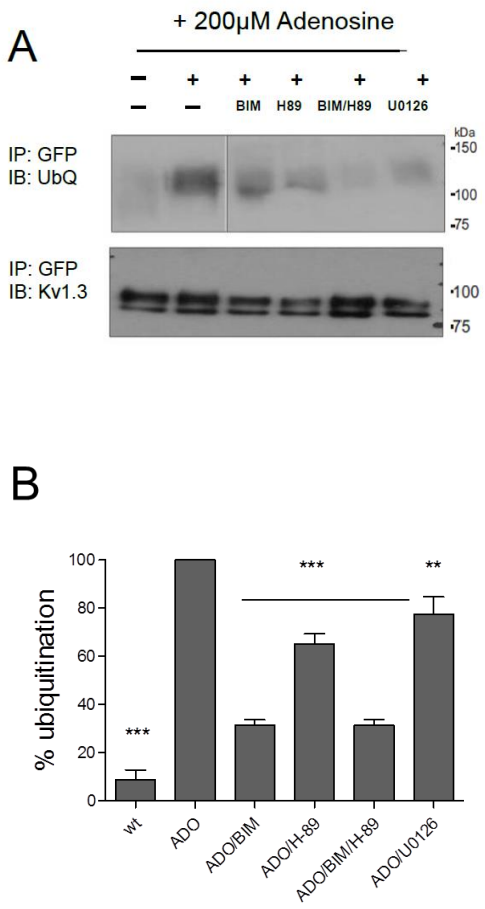

Figure 1. *Adenosine-dependent ubiquitination of Kv1.3.* Cells were pre-incubated with inhibitors for 15 min, prior the treatment of 200µM Adenosine during 30 min at 37 °C. BIM (PKC inhibitor, 1 µM), H-89 (PKA inhibitor, 10 µM), U0126 (ERK1/2 inhibitor, 10 µM). Ubiquitination values are mean ± SE of 4–5 independent experiments. Statistical analysis by One-Way ANOVA ($P < 0.001$) with a Tuckey post-test (*, $p < 0.05$; ***, $p < 0.001$).

Signaling pathways involved in the adenosine-mediated Kv1.3 endocytosis

By using confocal microscopy we examined the endocytosis of Kv1.3 upon incubation with 200 μM adenosine. Initially, we performed the relevant and essential controls required for the interpretation of data, measuring the effects of these inhibitors on the basal level internalization (Fig 2 A, left panel). Investigating adenosine-induced internalization we observed that the inhibition by the selective antagonists was partial.

Effects of BIM, H89, BIM+H89 and U0126 on Kv1.3 internalization are illustrated in Fig. 2. BIM reduced endocytosis up to 40 %. A 50% partial inhibition was achieved with H89. Similar to ubiquitination, no additive effects were achieved with BIM+H89. This data suggested that adenosine-induced internalization involved a cross-talk of both PKC/PKA pathways. The results of U0126 treatment indicated that again ERK1/2 was not involved in adenosine-induced endocytosis of Kv1.3.

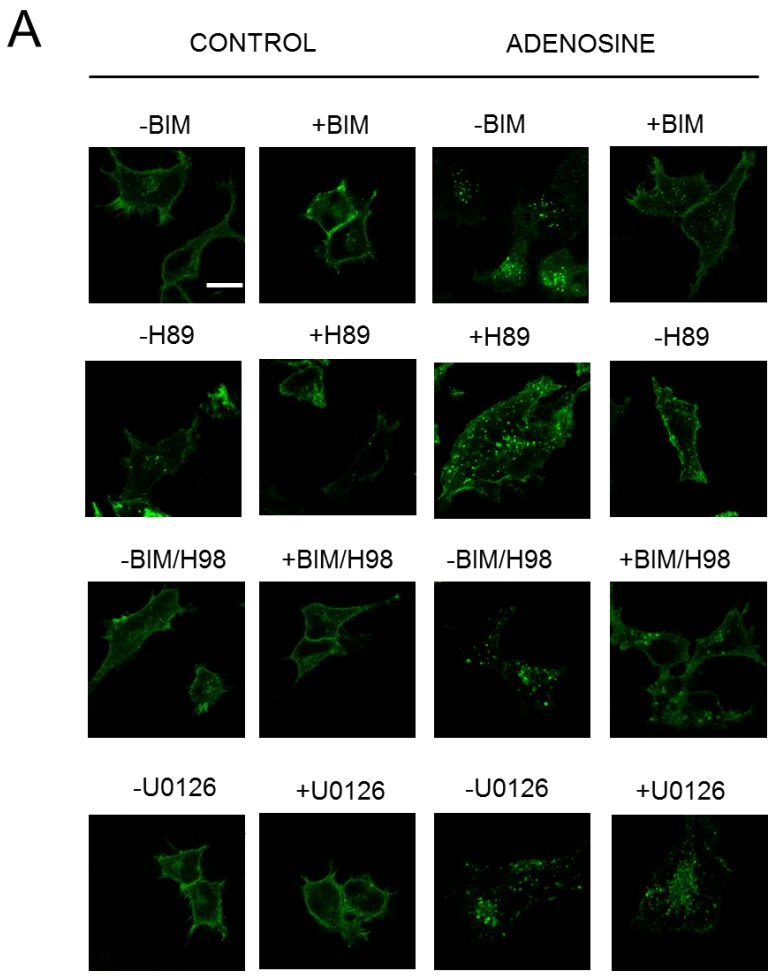
A
CONTROL
ADENOSINE
-BIM
+BIM
-BIM
+BIM
-H89
+H89
+H89
-H89
-BIM/H98
+BIM/H98
-BIM/H98
+BIM/H98
-U0126
+U0126
-U0126
+U0126

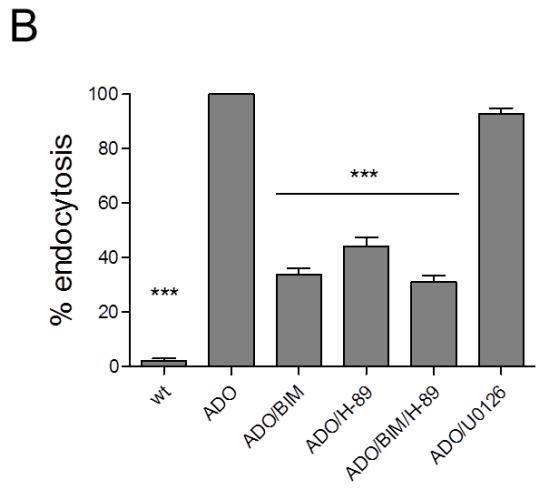

Figure 2. *Adenosine-dependent endocytosis of Kv1.3***.** HEK-293 cells were cultured with 200μM Adenosine for 30 min at 37 °C in the presence or the absence of BIM (PKC inhibitor, 1 μM), H-89 (PKA inhibitor, 10 μM) and U0126 (ERK1/2 inhibitor, 10 μM). (A) Representative confocal images. (B) Quantification of Kv1.3 intracellular vesicles from representative images. Values are mean + SE of n = 20–25 cells. Bars represent 10 μm. Statistical analysis by One-Way ANOVA ($P < 0.001$) with a Tuckey post-test (*, $p < 0.05$; ***, $p < 0.001$).

8-bromo-cAMP-induced Kv1.3 internalization

In a previous contribution we deciphered the PKC-dependent ubiquitin-mediated Kv1.3 internalization. In view of the role of PKA and PKC in the Kv1.3 ubiquitin-dependent internalization upon adenosine treatment, we decided to decipher the PKA impact in internalisation of the channel (Fig. 3). Evidence indicated that both kinases seemed to be involved in the Adenosine-dependent endocytosis of the channel.

However, we did not know the exact contribution of PKA in the process. To do so, we used 8-bromo-cAMP because this compound is specific agonist for the PKA signaling pathway.

HEK-932 cells were transfected with Kv1.3YFP and after 24h were treated with 0,5 mM 8-bromo-cAMP for 30 min. Figure 3A shows that direct PKA stimulation triggered indeed channel endocytosis. A timely study of the process showed that the Kv1.3 internalization began already after 15 min reaching the maximum at 30 min (Fig 3 B).

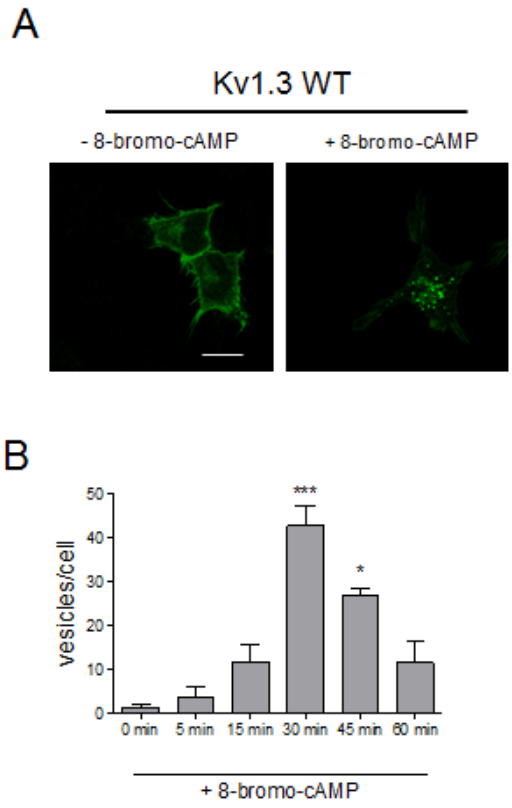

Figure 3.(**Previous page**) 8-*bromo-cAMP- dependent endocytosis of Kv1.3***.** Cells were cultured for 30 min at 37 °C in the presence of 0.5mM 8-bromo-cAMP or DMSO. (A) Representative images of 8-bromo-cAMP treatment. (B) Time course of Kv1.3 internalisation. 8-bromo-cAMP triggered a transient significant increase of endocytic vesicles. Values are mean + SE of n = 20–25 cells. Bars represent 10 µm. Statistical analysis by One-Way ANOVA ($P < 0.001$) with a Tuckey post-test (*, $p < 0.05$; ***, $p < 0.001$).

PKA impact in Kv1.3 ubiquitination

To determine whether, similar to PKC-activated endocytosis, this internalization was ubiquitin-dependent, we performed ubiquitination assays upon 8-bromo-cAMP stimulation. Fig. 4 shows the level of ubiquitination of Kv1.3. Fig 4A contain lysate extracted from cells treated with vehicle (negative control), PMA (positive control for ubiquitination of Kv1.3 in HEK cells) or 8-bromo-cAMP in the absence and presence of PKA inhibitor H89 (10 μM).

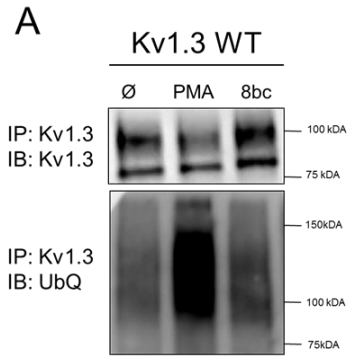

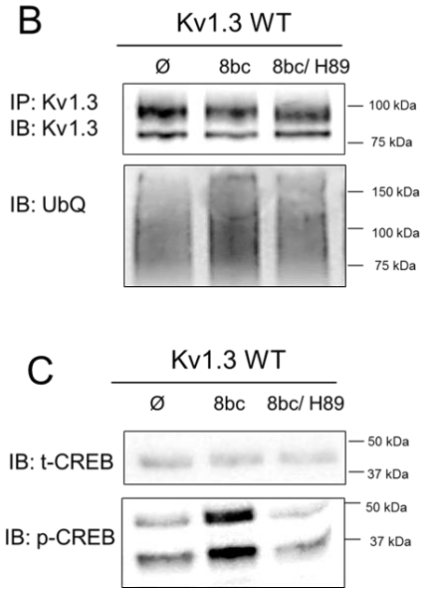

Figure 4. *8-bromo-cAMP-dependent ubiquitination of Kv1.3.* (A) Cells transfected with Kv1.3 were incubated in the absence (Φ) or the presence of 1μM PMA and 0.5mM 8-bromo-cAMP for 30 min at 37°C. Lysates were immunoprecipitated (IP) against GFP (Kv1.3 YFP). Membranes were probed (IB) with anti-ubiquitin antibody. (B) Transfected cells were pre-incubated or not for 15 min with H89 prior the treatment with 8-bromo-cAMP. (C) CREB and p-CREB abundance upon 8-bromo-cAMP stimulation in the the presence or absence of H89.

Surprisingly, under 8-bromo-cAMP treatment we observed a restricted level of ubiquitination, similar to that obtained with the control. The use of PKA inhibitor (Fig. 4B) did not alter the level of ubiquitination. This could indicate that PKA-mediated activation by 8-bromo-cAMP would not affect the ubiquitination of Kv1.3. Because upon 8-bromo-cAMP treatment it is mandatory to demonstrate that cells were

activated, we analysed the CREB phosphorylation. In our conditions, 8-bromo-cAMP clearly induced CREB phosphorylation, which indicated that PKA was indeed activated. Although H89 halted this activation, the ubiquitination levels of Kv1.3 were not affected. These data indicate that endocytosis via direct stimulation of PKA pathway might be a ubiquitin-independent phenomenon.

Effects of forskolin on Kv1.3 endocytosis

Considering the hypothesis of PKA ubiquitin-independent endocytosis of Kv1.3, we determined whether the lack of ubiquitination of Kv1.3 affected the channel internalization upon 8-bromo-cAMP incubation. For this purpose we used 10 μM forskolin, which is an alternative PKA agonist. As demonstrated in Fig.5A, forskolin, similarly to 8-bromo-cAMP, induced Kv1.3 internalization. Again, we did not observe alteration in ubiquitination upon forskolin treatment (Fig 5B).

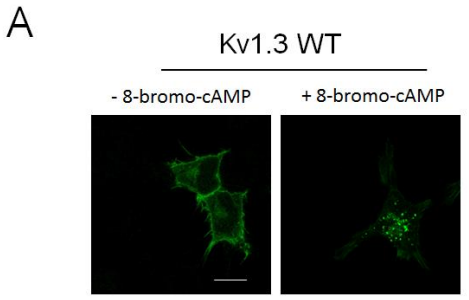

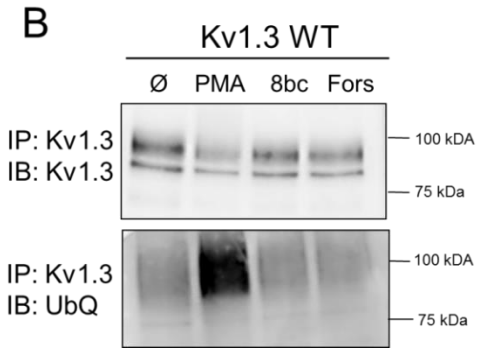

Figure 5. *Effects of forskolin on the Kv1.3 endocytosis and ubiquitination.* (A) Confocal images of HEK cells transfected with Kv1.3wt in the presence or the absence of 10 μM forskolin. Confocal images are representative from > 25 cells. Bars represent 10 μm. (B) HEK-293 cells were transfected with Kv1.3wt and persistent 30 min incubation with 1 μM PMA, 0.5 mM 8-bromo-cAMP and 10 μM forskolin was performed. Representative western blots are shown. Total lysates immunoprecipitated against GFP (IP: Kv1.3) were immunoblotted using anti-GFP (IB: Kv1.3) or anti-ubiquitin (IB: UbQ) antibodies.

Discussion

In this study, we showed that both PKC and PKA altered Kv1.3 channel abundance on the cell membrane. As we reported previously, Ado triggered PKC-dependent internalization. We herein reported that adenosine activated both PKC and PKA-mediated events on the Kv1.3 downregulation. We explored cellular aspects of PKA signaling that might contribute to Kv1.3 internalization using direct PKA agonist like 8-bromo-cAMP and forskolin.

Our findings indicated that PKA adenosine activation triggered Kv1.3 endocytosis redundantly to PKC. In addition, PKA downregulated Kv1.3 apparently in an ubiquitin-independent manner. We observed clear

channel internalization, with a minor level of ubiquitination, which was not altered upon PKA activation or inhibition. This allowed us to hypothesize that PKA activates a ubiquitin-independent endocytosis of Kv1.3.

PKC-mediated regulation of clathrin-dependent internalization of Kv1.3 is complex and involves ubiquitin-mediated endocytosis. Our data provide an important mechanistic insight into the ability of PKA to contribute to the downregulation of Kv1.3 in ubiquitin-independent manner. However, we do not know which mechanism is involved in this endocytosis pathway. The best-studied pathway is clathrin-dependent endocytosis (CDE), where clathrin is a major component of the endocytic vesicle coat (Ishii et al., 2012). But there are multiple clathrin-independent endocytosis (CIE) pathways that can depend on cholesterol-rich membrane domains (Boucrot et al., 2012). An example of dual action of both pathways is EGF receptor (EGFR) endocytosis under EGF stimuli, which follow different endocytic routes both ubiquitin-dependent and independent (Sigismund et al., 2005). We propose herein that Kv1.3 endocytosis is regulated by two autonomous mechanisms.

Overall, these studies demonstrated that adenosine triggers Kv1.3 ubiquitin-dependent endocytosis via PKC activation, and an unconventional redundant newly described PKA-mediated ubiquitin-independent internalization.

References

- Boucrot E, Howes MT, Kirchhausen T, Parton RG. (2011). Redistribution of caveolae during mitosis. *J Cell Sci* 124: 1965–1972.

- Bradbury NA, Bridges RJ.(1994). Role of membrane trafficking in plasma membrane solute transport. *Am J Physiol*. 267:C1–C24.

- Cahalan, M. D. & Chandy, K. G. 2009. The functional network of ion channels in T lymphocytes. *Immunol Rev* 231, 59–87.

- Chandy, K. G., Wulff, H., Beeton, C., Pennington, M., Gutman, G. A., and Cahalan, M. D. (2004). K+ channels as targets for specific immunomodulation. *Trends Pharmacol. Sci*. 25, 280–289.

- Feske, S. (2007). Calcium signalling in lymphocyte activation and disease. *Nat Rev Immunol* 7, 690–702.

- Fu, X. X., Du LL, Zhao N, Dong Q, Liao YH, Du YM. (2013). 18beta-Glycyrrhetinic acid potently inhibits Kv1.3 potassium channels and T cell activation in human Jurkat T cells. *J. Ethnopharmacol*. 148, 647–654.

- Martinez-Marmol, R., Comes, N., Styrczewska, K., Perez-Verdaguer, M., Vincente, R., PujadasS, L., Soriano, E., Sorkin, A. & Felipe, A. (2016). Unconventional EGF-induced ERK1/2-mediated Kv1.3 endocytosis. *Cell Mol Life Sci*, 73, 1515-28.

- Pardo, L. A. (2004). Voltage-gated potassium channels in cell proliferation. *Physiology* 19, 285–292.

- Rangaraju, S., Chi, V., Pennington, M. W. & Chandy, K. G. (2009). Kv1.3 potassium channels as a therapeutic target in multiple sclerosis. *Expert Opin Ther Targets* 13, 909–92.

- Szabo I, Gulbins E, Apfel H, Zhang X, Barth P, Busch AE, Schlottmann K, Pongs O, Lang F. (1996). Tyrosine phosphorylation-dependent suppression of a voltage-gated K channel in T lymphocytes upon Fas stimulation. *J Biol Chem* 271: 20465–20469.

- Szigligeti P, Neumeier L, Duke E, Chougnet C, Takimoto K, Lee SM, Filipovich AH, Conforti L. (2006). Signalling during hypoxia in human T lymphocytes– critical role of the src protein tyrosine kinase p56Lck in the O2 sensitivity of Kv1.3 channels. *J Physiol* 573: 357–370.

- Wulff, H., Castle, N. A., and Pardo, L. A. (2009). Voltage-gated potassium channels as therapeutic targets. *Nat. Rev. Drug. Discov*. 8, 982–1001.

- Zhao, N., Dong Q, Fu XX, Du LL, Cheng X, Du YM, Liao YH. (201)4. Acacetin blocks kv1.3 channels and inhibits human T cell activation. *Cell Physiol Biochem* 34, 1359–1372.

3.3.1. Contribution 2:

Lysine-targeting specificity in Kv1.3 poliubiquitination.

Styrczewska K[1], Vallejo-Gracia A[1], Pérez-Verdaguer M[1], Felipe A[1]

[1]Molecular Physiology Laboratory, Departament de Bioquímica i Biomedicina Molecular, Institut de Biomedicina (IBUB), Universitat de Barcelona, Avda. Diagonal 643, 08028 Barcelona, Spain

ABSTRACT

The voltage-dependent potassium channel Kv1.3 is expressed mostly in the nervous and immune systems, where participates in the sensory discrimination and leukocyte physiological responses. An altered function as well as an exacerbated expression or surface mistargeting is related with autoimmunitary diseases. Regulation of this transmembrane protein is therefore essential. The turnover of Kv1.3 is highly dynamic and, upon insults, the balance between the number of channels located at the membrane and the internalization is crucial for an appropriate signaling. Therefore, endocytosis is an essential mechanism for the regulation of Kv1.3 abundance on the cell surface. Ubiquitination has emerged as a crucial mechanism for membrane protein turnover. In this study we investigated ubiquitination-mediated endocytosis of Kv1.3.

To that end several Kv1.3 lysine mutants were created, in which we examined ubiquitination, endocytosis and membrane targeting. We observed ubiquitination and ubiquitin-mediated endocytosis using PMA and adenosine. Our results indicate that more than one lysine are involved in the ubiquitination of the channel. Furthermore, we have mapped the most relevant for the channel internalization and degradation. Our results indicate that Kv1.3 undergoes poliubiquitination in residues which participate in the endocytosis and the turnover of the channel.

Report of the PhD student participation

Lysine-targeting specificity in Kv1.3 poliubiquitination.

Katarzyna Styrczewska performed all the experiments and the data analysis of this work.

Antonio Felipe

PhD thesis director

Introduction

Kv1.3 is a member of the *Shaker* Kv1 family. These channels are homotetramers, so the ion pore is made of four α subunits arranged symmetrically around the conduction pathway. Each α subunit consists of six transmembrane segments called S1 through S6. Voltage-sensor domains consist of four transmembrane segments S1-S4, while S5-S6 contributes to assemble the porus. The P-loop, which contains the selectivity filter, is located between S5 and S6, (Littleton et al., 2000). Kv1.3 is present in many tissues, including nervous system, kidney (Cahalan et al., 2001), lymphocytes (Attali et al., 1992), skeletal muscle, osteoclasts (Desir et al., 2003). It is involved in repolarization after an action potential in excitable cells. In non-excitable cells it takes part in a variety of cellular functions including apoptosis, cell volume regulation and T cell proliferation (Jacob et al., 2000, Arkett et al., 1994), Kv1.3 exerts also a crucial role in cell activation. The importance of Kv1.3 in cell physiology makes this channel a target for different regulatory mechanisms. Some of these mechanisms are: post-translational modifications (glycosylation, phosphorylation, and ubiquitination), protein-protein interactions, protein-lipid interactions, heteroteramerization, etc. Ubiquitin-mediated endocytosis is a powerful mechanism to control the abundance of Kv1.3 at the cell membrane (Martinez-Marmol et al. 2017). Ubiquitination is a key regulatory mechanism of cell functions. This covalent modification involves the formation of an isopeptide bond between the C-terminal glycine residue of ubiquitin and a lysine residue on the target protein. Ubiquitin is a 76

amino acid protein that contains seven lysine residues (K6, K11, K27, K29, K33, K48, and K63). Substrate-conjugated ubiquitin itself can be further ubiquitinated through one of its seven lysines to form a polyubiquitin chain (Pickart and Fushman 2004). Ubiquitin signal might leads to either proteolytic or nonproteolytic functions, which are largely determined by the type of linkage through which the ubiquitin chain is attached (Hicke et al 2005). Ubiquitination reactions involve action of three enzymes: ubiquitin-activating enzymes (E1), ubiquitin-conjugating enzymes (E2), and ubiquitin ligases (E3). Two major E3 subfamilies are identified as homologous to E6AP C terminus (HECT) domain E3 and RING domain E3. Many E3 enzymes are capable of targeting themselves for ubiquitination (Hershko and Ciechanover, 1998**)**. Moreover, E3 ligase controls the specificity of the ubiquitination system. As we demonstrate in our previous work, Kv1.3 ubiquitination is regulated by Nedd4-2 (neuronal precursor cell-expressed developmentally downregulated protein) ligase. Nedd4-2 binds to the protein via WW domain and the proline-rich (PY) motifs of the substrate protein (Lu et al. 1999). Kv1.3 does not contain a PY motif. Therefore, Nedd4-2 is able to reduce number of channels at the membrane via another non-canonical motif or adaptor protein. The ligase of Nedd4-2 with Kv1.3 is a first major interaction before ubiquitin is transferred to specific lysines of Kv1.3. In this work, by using mutagenesis, the identification of the lysines involved in the ubiquitination of the channel was performed.

Material and methods

Cell culture and cell transfection

Experiments were performed using mammalian cell line HEK-293. Cells were grown in DMEM (Dulbecco's modified Eagle's medium) containing 10% fetal bovine serum (FBS), L-glutamine (2 mM) and antibiotics: penicillin G (10,000 U / ml) and streptomycin (10 mg / ml). For immunocytochemistry experiments cells were plated into 12-well dishes containing 12 mm glass coverslips pretreated with poly-L-lysine and into 1 ml of media. To conduct immunoprecipitation experiments cells were plated into Petri dish with 10 ml of media. The following DNA amounts were used; i) immunoprecipitation: 4 μg/P100 dish; ii) immunocytochemistry: 0.5 μg/12-multi-wells. PEI and DNA were diluted in 150 mM NaCl;. Both mixtures were incubated for 15 minutes, mixed and still for 30 minutes. Cells were incubated for 4 hour with the Pei/DNA mixture diluted in media. After 4 hours media was changed. In both experiments cells were harvested 24 hour after transfection. Cells were preincubated at 37 °C for 30 min with various inhibitors before stimulation. HEK-293 cells were incubated with 200 μM Adenosine (ADO) or 1μM phorbol-12-myristate-13-acetate (PMA) in DMEM for the specified time in the presence or absence of specific inhibitors. Cell pellets were frozen at −80°C.

DNA constructs and Site Directed Mutagenesis

To follow the endocytosis and the Kv1.3 traffic, we used a Kv1.3YFP-tagged channel at the N-term. To investigate the Kv1.3 endocytosis, we

mutated the lysines to arginines. For multiple mutations, QuikChange ™ mutagenesis Site-Directed Mutagenesis Kit was used (Stratagene). For each of the mutations specific oligonucleotide sequences were designed using the Clone Manager Suite v7.1 program (Scientific & Educational Software). Oligonucleotides were designed to allow the conversion of the intracellular lysines, which could be ubiquitinated, for arginine. As arginine, similarly to lysine, has a positively charged ε-amino group, these mutations have not changed the channel properties.

Each mutant was analyzed by sequencing. Samples were processed by the ABI3730 analyzer (Applied Biosystems) in the CCiT facilities at the University of Barcelona. The results were analyzed using the Clone Manager Suite v7.1 program (Scientific & Educational Software).

Immunochemistry and Microscopy studies

For immunocytochemistry cells were grown in multi-wells on glass slides and transfected. After 24 h, the cells were incubated for 30 min at 37 °C with 200 μM ADO or 1 μM PMA in DMEM for the specified times. DMSO (dilution 1:1,000) was used as a negative control. The cells were then washed 3 times with PBS without K^+ (0.9% NaCl in 0.01 M $NaH_2PO_4 \bullet H_2O$) at 37 ° C. The absence of K^+ in solution facilitates the adhesion of these cells which by nature tend to be easily separated from the surface on which they grow. Then cells were fixed with freshly prepared 4% paraformaldehyde for 10 min at room temperature. After 3 washes of 5 min each with PBS without K^+, the coverslips were mounted in Mowiol media.

The data presented in this work were obtained using a spectral confocal microscope Leica TCS SL (Leica Microsystems, Heidelberg GmbH, Mannheim, Germany). The conditions, under which pictures were taken with a microscope confocal, were as follows: the pinhole used was 1 AE (Airy Units), line average used was 4, scan speed: 400 Hz, resolution: 1024 x 1024 pixels zoom x 4. The level of endocytosis was quantified analyzing the number of intracellular vesicle accumulation by using the automatic particle counting protocol of the Image J software and setting threshold around 75% to discard the membrane surface mask.

Protein extraction, Immunoprecipitation and Western Blotting

To obtain a total protein lysate, cells were split on plates 100 mm cell diameter, grown to confluence and transfected. One day after transfection cells were incubated for 30 min at 37 °C with PMA (1 μM dissolved in DMSO) or adenosine (200 μM) to activate internalization or with DMSO as a negative control. Subsequently the whole process is carried out on ice. After 3 washes with cold PBS, the cells were left in protein extraction buffer for 20 min. The buffer contains the following components: 50 mM Tris-HCl pH 7.4, 150 mM NaCl, 1% Triton X-100, 1 mM EDTA , supplemented with N-ethylmaleimide (NEM), 5 μM MG-132, 1 mM Na_3VO_4, and 10 mM NaF and protease inhibitors (0.1%): pepstatin, leupeptin, phenylmethylsulfonyl fluoride (PMSF) and aprotinin. Cells were spun for 10 min at 14,000 rpm at 4 °C. The supernatant was collected and stored at -20 °C.

Protein concentrations were measured using Bradford protein assay. The first step consists of a pre-incubation of protein (from 1 to 2 μg) with 50 μl of protein A sepharose (before washed 3 times with IP lysis buffer) for 2 h at 4° C. After this time, samples were gently centrifuged for 30 s at 1,000 *g* speed to minimize possible A sepharose non-specific binding. The next step of the protocol is to add nonspecific binding free supernatant into a chromatographic column (Micro Spin Chromatography columns, BioRad). Columns have been prepared in advance, washed Protein A (50 μl into each column) was added, then specific antibody against the protein under immunoprecipitate (GFP Polyclonal Antibody, GenScript at a ratio of 4 ng antibody per mg total protein) and incubated for 2 h. Then DMP (dimethyl pimelimidate, Pierce) was also added, to generate imidioester bonds between the antybody and sepharose. The incubation was performed at 4° C O/N with constant agitation. After this time the supernatant was collected. Then the columns were placed in new eppendorfs that already have 20 μl of TC5x 10% β-mercaptoethanol and protein-antibody complex-protein A were eluted by adding a solution of glycine (0.2 M, pH 2.5).

The samples were separated on SDS-PAGE gels percentage suitable acrylamide-bisacrylamide. Proteins were transferred to a PVDF membrane (Immobilon-P, Millipore). Blocking was done for 1 h at room temperature (RT) with a solution of PBS with 0.05% Tween and 5% skimmed milk powder. Blocked membranes were incubated with primary antibody diluted in PBS 0.05% Tween overnight (ON) at 4° C.

Two different antibodies have been used: Anti-Kv1.3, Mouse Monoclonal Antibody (NeuroMab) - to detect the presence of Kv1.3, and Ubiquitin (P4D1) Mouse Monoclonal Antibody (Santa Cruz Biotechnology, Inc.) to detect whether the ubiquitinated channels. Finally membranes were incubated for 1 h at RT with the secondary antibody (Goat Anti-Mouse IgG, Bio-Rad). ECL reagent (Biological Industries) was used to detect protein signals. Between antibodies 4 washes of 5 min with 0.05%Tween in PBS were made. The results were obtained in photographic films. Western Blots were quantified using MacBiophotonics ImageJ software. ImageJ was used to compare the density (intensity) of western blot bands. In order to perform analysis, x-ray films were first scanned. This densitometry examination, allows making relative comparisons and average values for the relative abundance of proteins between various samples.

Ubiquitination assay

Cells were washed twice in cold PBS and frozen at -80ºC for at least one night. On ice, cells were lysed 20 min on ice with 2 mL of lysis buffer (50 mM HEPES, 150 mM NaCl, 1% Triton X-100, 10% Glicerol, pH 7.5) supplemented with 12.5 mg NEM, 0.2 mM MG132, 1 mM EGTA 1 mM EDTA, 20 mM NaF, 1% NaOV, 2m M DTT, 1μg/ml aprotinin, 1μg/ml leupeptin, 1μg/ml pepstatin and 1mM phenylmethylsulfonyl fluoride as protease inhibitors. After scrapping the cells, they were centrifuge at 14,000 g for 15min. Co-immunoprecipitation assay was performed as previously described.

Cell-surface biotinylation

Cell-surface biotinylation was carried out using EZ-Link Sulfo-NHS-SS-Biotin (sulfosuccinimidyl-2-[biotinamido]ethyl-1,3-dithiopropionate) reagent (Pierce) diluted in PBS 1 mM MgCl2 1 mM CaCl2 at 0.5 mg/mL. Cells were gently incubated in a rocking platform for 30 min at 4ºC. During the incubation an ester group of the biotinylation reagent reacts with primary amines of lysine amino acidic residues exposed extracellularly. Next, the reaction was quenched with Glycine 50 mM diluted in the same PBS buffer. 3 washes of 5 min at 4ºC were performed to allow the neutralization of the uncrosslinked reagent. Following, cells were lysed with 1% Triton X-100, 10% glycerol, 5 mM HEPES pH 7.2 and 150 mM NaCl supplemented with 1 µg/ml aprotinin, 1 µg/ml leupeptin, 1 µg/ml pepstatin and 1 mM phenylmethylsulfonyl fluoride as protease inhibitors. Homogenates were centrifuged at 12,000 g for 15 min and total protein content was obtained from supernatant. To isolate the labelled proteins, total protein content was incubated with NeutrAvidin Agarose beads (Pierce) during 2 h at 4ºC. After 3 washes biotinylated proteins were eluted from NeutrAvidin beads in reducing conditions, 1X Laemmli SDS loading buffer, and 10 min at 100 º C

Statistical analysis

Data are shown as the mean ± SEM. Statistical analysis was performed by Student's t-test or One-way ANOVA with a Tukey post-hoc test for single or multiple group comparisons respectively (GraphPad PrismTM).

Results

Polyubiquitination of Kv1.3

As we have previously described PMA and adenosine can activate PKC-dependent endocytosis of Kv1.3 (Martinez-Marmol et al., 2017). PKC activation triggers down-regulation of Kv1.3 by inducing a clathrin-mediated endocytic event that targets the channel to lysosomal-degradative compartments. However, we wanted to decipher which Kv1.3 lysines are crucial for ubiquitin conjugation. For this purpose all intracellular lysines in different combination were mutated to arginines (Table 1).

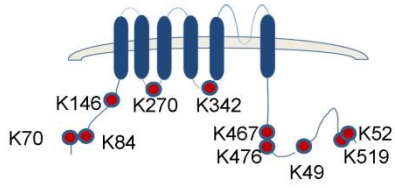

	70	84	146	270	342	467	476	498	519-520
Kless	70R	84R	146R	270R	342R	467R	476R	498R	519-520R
Mut. 1	70R	K	146R	270R	342R	467R	K	498R	519-520R
Mut. 2	K	K	146R	K	K	K	K	498R	KK
Mut. 3	K	K	K	K	K	K	K	498R	KK
Mut. 4	70R	84R	146R	270R	342R	467R	K	498R	519-520R
Mut. 5	K	K	146R	270R	342R	467R	K	498R	KK
Mut. 6	70R	84R	146R	K	342R	K	476R	498R	519-520R
Mut. 7	70R	84R	K	270R	342R	K	476R	498R	519-520R
Mut. 8	70R	84R	K	K	K	K	476R	K	519-520R
Mut. 9	70R	84R	K	K	K	K	476R	498R	519-520R
Mut. 10	70R	84R	K	270R	342R	467R	476R	K	519-520R
Mut. 11	K	84R	146R	K	K	K	K	K	KK
Mut. 12	K	K	146R	K	K	K	K	K	KK
Kv1.3 Wt	K	K	K	K	K	K	K	K	KK

Table 1. Kv1.3 mutants with different intracellular lysines mutated to arginines.

Cells were transfected with mutated DNAs, incubated with PMA (1μM) for 30 min at 37°C and protein lysates were collected. Equal amounts of proteins were immunoprecipitated and verified by Western blotting. Next, membranes were probed with antibody against ubiquitin (P4D1) and against Kv1.3 (NeuroMab). Results are shown in Figure 2.

Interestingly, Western blot analysis with an anti-Ubiquitin antibody reveals only ubiquitin and thus, we observed a polyubiquitination signal. The conjugation reaction yields a large number of ubiquitination products that generally appear as a smear or ladder of bands. This analysis verifies that the Kv1.3, in the smear, is ubiquitinated and that ubiquitin joined to the channel as a polyubiquitin chain.

All Kv1.3 constructs were immunoprecipitated and ubiquitinated (Fig 2B). However some differences in ubiquitination intensity may be observed. Once normalized by the Kv1.3wt signal, ubiquitination differences were observed upon specific lysines. For example, unlike the Kv1.3WT, in the Kless mutant which has no lysines, the ubiquitination was absent. So, by using the ubiquitin band intensity we may evaluate the importance of certain lysines involved in the Kv1.3 ubiquitination. To compare differences among Kv1.3 mutants, we performed a quantitative analysis of WB by using ImageJ (Fig 2C). We considered the ubiquitination level of Kv1.3 Wt as a reference (100% of ubiquitination).

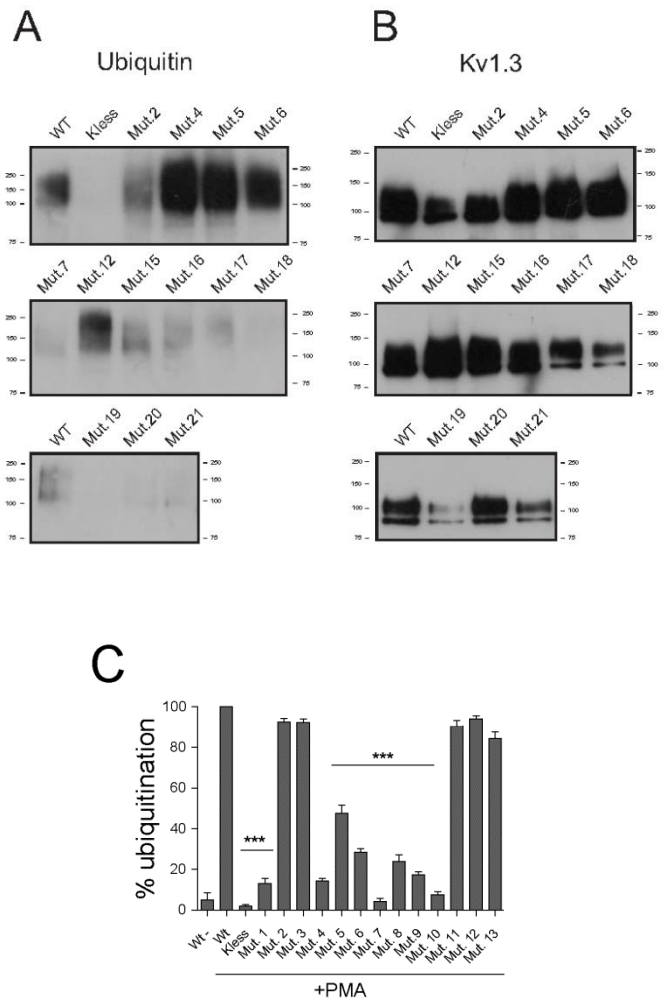

Figure 2. *Ubiquitination of Kv1.3 mutants.* (A)Cell lysates were immunoprecipitated with anti-GFP antibody and probed with anti-ubiquitin (IB: UBQ) and (B) anti-Kv1.3 (IB: Kv1.3). Only IP+ are shown. (C) Percentage of the PKC-mediated ubiquitination. Ubiquitination values are mean ± SE of 4–5 independent experiments. Statistical analysis by One-Way ANOVA ($P < 0.001$) with a Tuckey post-test (*, $p < 0.05$; ***, $p < 0.001$).

As shown in Fig. 2C Kv1.3 mutants: 2(K146/498R), 3(K498R), 11(K84R) and 12(K84/K164R) were ubiquitinated similar to the wt (93%, 89%, 95% and 85% respectively). This result suggested that these lysines were not involved in Kv1.3 ubiquitination. On the contrary, some lysines (mutants: 1, 4, 7 and 10) drastically decreased the ubiquitination level (8%, 11%, 8% and 15% respectively). Results suggested that there is more than one lysine being involved in the ubiquitin conjugation and that we observed polyubiquitination of more than one lysine residue.

Therefore, our results point to lysines which were presenting greater impact in ubiquitination. Thus, we observed that mutations at K70, K84 at the N-terminal and K519, K520 at the C-terminal, significantly altered ubiquitination of Kv1.3 under PMA treatment.

C-terminal lysines as targets for Kv1.3 ubiquitin-mediated internalization

Ubiquitin affects and regulates many cellular functions including signal transduction, cell cycle, apoptosis, immune response, DNA repair, transcription and chromatin remodeling and also endocytosis (Ciechanover et al. 2005). We showed that PMA induced ubiquitination in selected Kv1.3 lysine mutants. Therefore, we wonder whether observed ubiquitination drived the channel to the endocytic pathway.

Thus, as the detection of ubiquitin itself did not necessarily imply endocytosis, immunocytochemistry experiments were performed and

visualized by confocal microscopy. In this view, we analyzed PMA induced endocytosis of Kv1.3 mutants.

Under PMA incubation, endocytosis is enhanced decreasing the amount of channel at the cell surface and increasing its presence in intracellular vesicles due to PKC activation. In order to determine the presence of Kv1.3 in endocytic vesicles cells were transfected and treated with or without PMA and visualized by confocal microscopy.

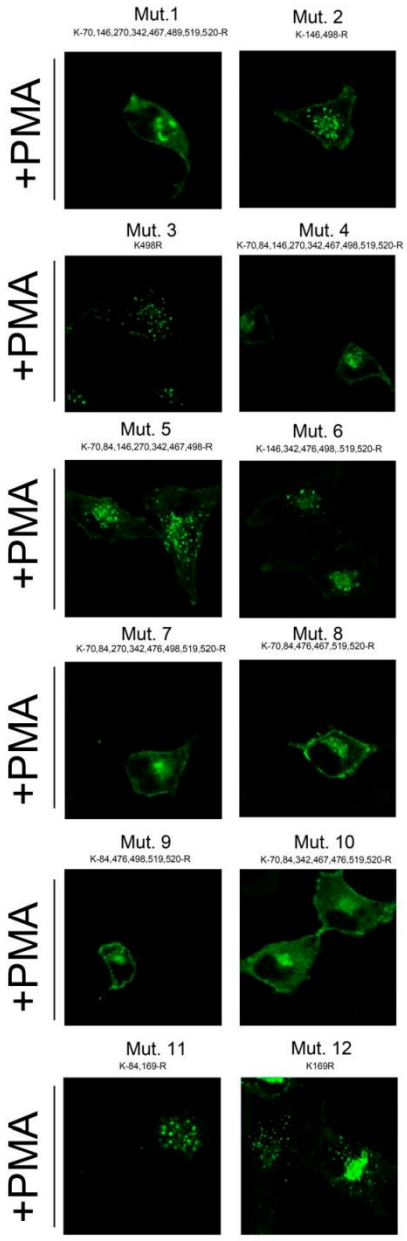

Figure 3. *Endocytosis of Kv1.3 lysine mutant.* Kv1.3 lysines were individually and collectively mutated to arginine. HEK-293 cells transfected with different Kv1.3 mutants were treated with 1 µM PMA for 30 min at 37 °C. Scale bar is 10µm

Analyzing the number of vesicles under PMA treatment we discovered that lysines on C-terminal were mainly involved in channel internalization. Especially de doublet previously found to be target for ubiquitination (K519/520).

Next, we studied the impact of individual lysines on ubiquitination and internalization. Single mutations were performed and examinated. As shown in Fig. 4 lysines on N-terminal (K70 and K84) exhibited an altered ubiquitination, specially when both lysines were mutated together (65%) but internalization assays demonstrated lower impact of these mutation in channel removal from the membrane (K70: 91%, K84: 85%, K70,84: 72% vs Kv1.3 wt). On the other hand selected C-terminal lysines (K519/520) exhibited profound impact in both phenomena. Nonetheless, mutant with all four N-terminal mutated residues, demonstrated a cumulative effect. This result suggested that lysine modification is restricted to residues in the C-terminal thereby acting as target sites to promote Kv1.3 poliubiquitin-dependent endocytosis.

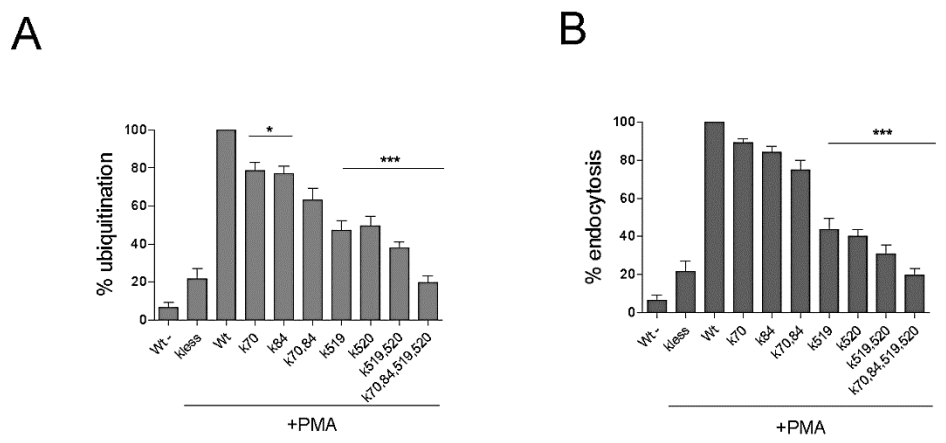

Figure 4. (A) *Percentage of ubiquitination.* Selected mutants were expressed and HEK cells treated with 1μM PMA for 30 min at 37ºC. Cell lysates were immunoprecipitated with Kv1.3 and probed against anti-UBQ and anti-Kv1.3 antibodies. (B) *Percentage of endocytosis.* Each mutant was referenced to the WT effect in the presence of PMA. Bars represent the mean ± s.e.m. (n=5). Statistical analysis by One-Way ANOVA ($P < 0.001$) with a Tuckey post-test (*, $p < 0.05$; ***, $p < 0.001$). (C) Crucial lysines involved in Kv1.3 internalization and ubiquitination.

Biotinylation of Kv1.3 mutants

The covalent modification of cell surface protein with biotin is another valuable technique for monitoring ion channels abundance at the plasma membrane. Biotinylation labels the surface channels. The subsequent fate of biotinylated proteins can then be determined through affinity purification followed by SDS-PAGE and Western blotting. During biotinylation experiments, the channels on millions of cells are assayed simultaneously, giving greater quantitative sensitivity than

immunofluoresence techniques, and so subtle differences in endocytosis and trafficking rates can be delineated. As we demonstrated in Fig. 5 mutation of lysines on the N-terminal did not alter channel endocytosis. Thus, upon PMA stimuli over 80% of the channels were removed from the surface similarly to that observed with Kv1.3wt. However, the mutation of C-terminal lysines K519/520 profoundly impaired channel endocytosis and less than 20% of the channels got internalized (Fig. 5).

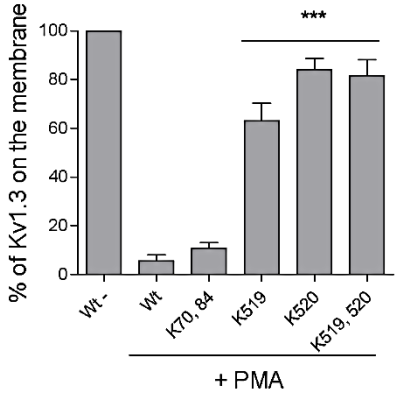

Figure 5. *Biotinylation of Kv1.3 Lys mutants*. Cells were transfected with selected mutants and treated with 1μM PMA for 30 min at 37ºC. Biotinylation assay was performed and the Kv1.3 presence was examined. Arginine substitution in residues K70, K84 did not altered channel removal (over 80% of the channel remain on the cell surface). Absence of C-terminal lysines (K519/520) decreased channel internalization (only 18% of the Kv1.3 undergoes endocytosis), data represents several independent experiments. Statistical analysis by One-Way ANOVA ($P < 0.001$) with a Tuckey post-test (*, $p < 0.05$; ***, $p < 0.001$).

Adenosine induced ubiquitination and endocytosis of selected lysines.

Adenosine (Ado) is an anti-inflammatory purine nucleoside that is released by cells in response to stress and hypoxia (Kobayashi et al., 2000). It has been described that Ado inhibits K^+ currents (Duffy et al., 2007). However, there is no indication of whether this down-regulation is due to a phosphorylation process and/or endocytosis phenomena. Thus, we incubated cells with 200µM Ado for 30 min at 37ºC. As depicted in Fig. 6, we observed similar results in ubiquitination and endocytosis similarly that these obtained with PMA incubation. Our results suggest that PMA and Ado, inducing ubiquitination and endocytosis, shared the same lysine targeting (Fig. 6).

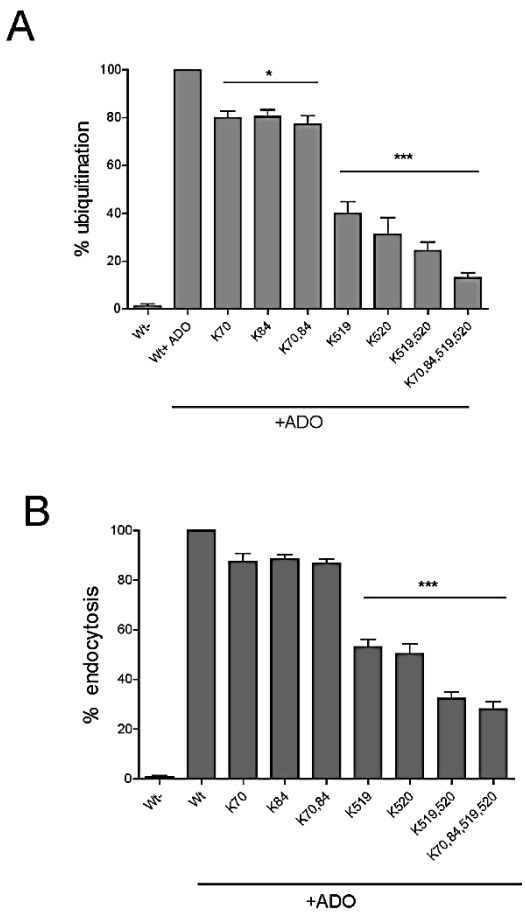

Figure 6. *Adenosine-mediated ubiquitination and endocytosis of Kv1.3*. HEK-293 cells, transfected with Kv1.3-YFP WT and mutants, were incubated with or without 200 µM Ado for 30 min at 37 °C. (A) Effects of Ado-dependent ubiquitination on selected Lysine mutants were investigated. To determine Ado-dependent ubiquitination, transfected cells were incubated with Ado and lysates were immunoprecipitated against GFP (Kv1.3) and probed with anti-ubiquitin antibodies. (B) Effects of Ado on channel endocytosis. Percentage of endocytosis. Each bar represents the mean ± s.e.m. of three independent experiments. Statistical analysis by One-Way ANOVA ($P < 0.001$) with a Tuckey post-test (*, $p < 0.05$; ***, $p < 0.001$).

Discussion

The voltage-dependent potassium channel Kv1.3 is widely expressed in many tissues, mostly in the nervous and immune systems, where is playing crucial role in many physiological events. Regulation of this transmembrane protein is therefore essential for a correct function of the living cell. The balance between synthesis and degradation is highly important and must be tightly regulated. Ubiquitination serves as a key mechanism which can control biological signaling in many cellular compartments. Moreover, ubiquitination controls subcellular localization and is involved in endocytic degradation.

Identifying a right target is a critical step in ubiquitination cascades. This process is precisely regulated by the E3 enzymes. As we mentioned before, Nedd4-2 is catalyzing ubiquitin conjugation of Kv1.3. A crucial part of the ubiquitin conjugation process is the identification of the lysine or amino group that is being modified. However, there are major differences of specificity for a particular lysine between different ubiquitination cascades.

Often, selection of target lysines is limited to general recognition of the target protein, without high selectivity for a specific lysine residue. Frequently, general target selectivity is sufficient for those modifications that do not require conjugation to one specific lysine, such has been described on targets such as p27, p21 or cyclins. Furthermore these nonselective lysine modifications include many polyubiquitination signals that lead to proteasomal degradation via K48- or K11-linked

polyubiquitin chains or K63-linked polyubiquitin chains related with lysosomal degradation (Kravtsova-Ivantsiv and Ciechanover, 2012, Galan et al., 1997).

Our study showed that both PMA and Ado triggered Kv1.3 endocytosis via ubiquitination. Upon both situations, ubiquitin targeted to the same group of lysines on the C-terminal and N-terminal. However, targeting mainly the lysines located in the C-terminal mainly resulted in channel endocytosis. We have previously described that PMA induced Kv1.3 endocytosis by ubiquitination targeting the channel to lysosomal degradation (Martinez-Marmol et al., 2017). Thus, C-terminal located lysines seem to be crucial for ubiquitin-mediated Kv1.3 degradation and turnover. We discovered that the supression of K519, K520 altered and inhibited in great level the ubiquitination and endocytosis. Contrarily, N-terminal ones can be considered as an ubiquitin target, but were not participating in channel internalization. Thus, we hypothesize that all five C-terminal lysines (K467, K476, K489, K519, K520) are targets site for ubiquitination involved in internalization of the channel. Form our date we cannot discard that Ubiquitination of one single lysine in this C-terminal domain can be probably sufficient to induce protein lysosomal degradation. However, further research must be done to confirm this fact. Nevertheless, differences in the rate of endocytosis were observed for different lysine mutants, indicating that the location of the ubiquitin chain can affect Kv1.3 turnover.

References

- Arkett S.A.J, Dixon J.N., Yang D.D., Sakai C., Minkin S., Sims M. (1994). Mammalian osteoclasts express a transient potassium

channel with properties of Kv1.3. *Receptors Channels*. 2: 281-293.

- Attali B., Romey G., Honore E., Schmid-Alliana A., Mattei M.G., Lesage F., Ricard P., Barhanin J.,Lazdunski M. (1992). Cloning, functional expression, and regulation of two K+ channels in human T lymphocytes. *J Biol Chem. 267*: 8650–8657.
- Cahalan M.D., Wulff H., Chandy K.G. (2001). Molecular properties and physiological roles of ion channels in the immune system. *J Clin Immunol*. 21.4: 235-52.
- Ciechanover A. (1998). The ubiquitin-proteasome pathway: on protein death and cell life. *EMBO J.* 15: 7151-60.
- Ciehanover A. (2005). Proteolysis: from the lysosome to ubiquitin und the proteasome. *Nat. Rev. Moll. Cell. Biol.* 6:79-87.
- Desir G. (1996). The structure, regulation and pathophysiology of potassium channels. *Curr Opin Nephrol Hypertens*. 4. 5: 402-5.
- Galan, J.M. and Haguenauer-Tsapis, R. (1997). Ubiquitin Lys63 is involved in ubiquitination of a yeast plasma membrane protein. *EMBO J*. 16, 5847–5854.
- Galan, J.M. and Haguenauer-Tsapis, R. (1997). Ubiquitin Lys63 is involved in ubiquitination of a yeast plasma membrane protein. *EMBO J*. 16, 5847–5854.
- Hershko A, Ciechanover A. (1998). The ubiquitin system. *Annu Rev Biochem* 67: 425–479.

- Hicke L, Dunn R. (200)3. Regulation of membrane protein transport by ubiquitin and ubiquitin-binding proteins. *Annu Rev Cell Dev Biol* 19: 141–172.
- Hicke L, Schubert HL, Hill CP. (2005). Ubiquitin-binding domains. *Nat Rev Mol Cell Biol* 6: 610–621
- Kravtsova-Ivantsiv,Y.,andCiechanover,A.. (2012). Non-canonicalubiquitin-based signalsforproteasomaldegradation. J. CellSci. 125, 539–548.
- Kravtsova-Ivantsiv Y.,and Ciechanover A. (2012). Non-canonicalubiquitin-based signalsforproteasomaldegradation. J. CellSci. 125, 539–548.
- Littleton J.T., Ganetzky B. (2000). Ion channels and synaptic organization: analysis of the Drosophila genome. *Neuron*. 26.1: 35-43.
- Lu PJ, Zhou XZ, Shen M, Lu KP. (1999). Function of WW domains as phosphoserine- or phosphothreonine-binding modules. *Science* 283:1325-8.
- Lu PJ, Zhou XZ, Shen M, Lu KP.(1999). Function of WW domains as phosphoserine- or phosphothreonine-binding modules. *Science* 1999; 283:1325-8.
- Pickart CM, Fushman D. (200)4. Polyubiquitin chains: polymeric protein signals. *Curr Opin Chem Biol* 8: 610–616
- Xu P, Duong DM, Seyfried NT, Cheng D, Xie Y, Robert J, Rush J, Hochstrasser M, Finley D, Peng J. (2009). Quantitative

proteomics reveals the function of unconventional ubiquitin chains in proteasomal degradation. *Cell*. 137(1):133–145.

4. General discussion

In an effort to elucidate the mechanisms involved in Kv1.3 turnover, we investigated the channel internalization under different stimuli in various cell lines. The intracellular trafficking of the ion channel involves complex processes. We studied endocytosis of Kv1.3 as a process controlling number of channels on the cell surface and the possible implication in cell destiny. Endocytosis is carried out by various mechanisms. Here we deciphered major endocytosis mechanisms triggered by EGF and Adenosine in HeLa and HEK 293 heterologous cell systems as well as in native cell lines (macrophages, dendritic or neuronal precursor). These studies pointed out the impact of endocytosis in turnover and homeostasis of Kv1.3 and possible physiological relevance of these finding.

In this dissertation we describe an EGF-induced downregulation of Kv1.3 via dual pathways: tyrosine phosphorylation and unconventional ERK1/2-dependent mechanisms. EGF treatments induce a decrease in Kv1.3 current as a result of tyrosine kinase receptor activation (Bowlby et al., 1997). These findings concur with our studies that show tyrosine kinase phosphorylation of Kv1.3. Moreover, we demonstrated that EGF-treatment caused Kv1.3 endocytosis. To decipher the endocytosis pathway, several markers of intracellular compartments were used and the co-localization with the channel under EGF treatment was analysed. Results showed that EGF triggered Kv1.3 endocytosis via CCP pathway and targeted the channel to lysosomal degradation.

Decrease of Kv1.3 plays an important role in immune system during activation and proliferation of leukocytes (Beeton and Chandy

2005). In addition, an increase of NPC (neural progenitor cells) proliferation was reported under EGF stimuli (Zhang et al. 2001). Our study supports the hypothesis that the enhancement of NPC proliferation is dependent on Kv1.3 inhibition

On this view, structural elements crucial for this phenomenon were studied. Unexpectedly, tyrosine kinase phosphorylation revealed not to be responsible for Kv1.3 internalization, which was suggesting another mechanism involved in this event. Therefore, the search for a new, not yet described EGF-dependent signal began. As result we found an unconventional threonine phosphorylation via ERK1/2 signaling pathway.

Downregulation of Kv1.3 in microglia results in attenuated microglial activation which prevents neurotoxicity (Fordyce et al., 2005). Kv1.3 and $K_{Ca3.1}$ inhibition could be useful to preferentially target detrimental pro-inflammatory microglia functions in ischemic stroke and other neurological disorders associated with neuroinflammation such as Alzheimer's and Parkinson's diseases (Rangaraju et. al., 2014, Tubert et al., 2016).

In summary, our experiments showed two different ways to control abundance of the Kv1.3 channel by EGF and revealed a great influence on the turnover of the channel. Our study have a high physiological relevance, pointing to EGF as a Kv1.3 inhibitor that might therefore reduce radiation-induced brain injury by targeting the key cells involved in the inflammatory process (microglia, lymphocytes, dendritic cells), while promoting neurogenesis.

Adenosine is an anti-inflammatory purine nucleoside that down-regulate Kv1.3. Adenosine signaling is mediated by four subtypes of G-protein–coupled receptors: A1, A2A, A2B, and A3. HEK-293 cells, which were used in this study, similarly to macrophages, endogenously express the A2B subtype of adenosine (ADO) receptors. In the second part of study we investigated ADO implication in Kv1.3 endocytosis.

Our results have shown that ADO hampers the LPS-dependent activation of macrophages and dendritic cells concomitantly with a down-regulation of Kv1.3. The results are broadly consistent with the idea of Kv1.3 as a novel target for immunomodulation of autoreactive effector memory T (TEM) cells that play a major role in the pathogenesis of autoimmune diseases. Other studies are showing that the treatments with several Kv1.3 antagonists are effective in ameliorating experimental allergic encephalomyelitis (EAE) (Beeton et al., 2001; Beeton et al., 2006). ADO-dependent endocytosis is directly related to the study of the therapeutic effects of Kv1.3 inhibition and may be a fine-tune cell mechanism controlling Kv1.3 activity.

Furthermore, we wanted to elucidate the mechanism of ADO-dependent Kv1.3 internalization. We observed that, similar to PMA, ADO is triggering ubiquitination-dependent endocytosis upon PKC activation. Figure 4, (Results: Part Two) in second part of this dissertation, demonstrates that PKC activation triggered clathrin-mediated endocytic mechanism. The findings presented in this work deciphered the degradation pathway which targets Kv1.3 to lysosomal degradation.

ADO triggered Kv1.3 ubiquitination and lysosomal degradation upon activation of PKC in heterologous system cells of HEK293 similarly to PMA. Using PMA we investigated molecular determinants involved in Kv1.3 ubiquitin-dependent endocytosis. Ubiquitination is a posttranslational modification which is mediated by covalent conjugation of ubiquitin to protein substrates and can be related to multiple events, one of them being membrane trafficking and endocytosis (Mukhopadhyay and Riezman, 2007). Ubiquitination serve as a mechanism regulating membrane abundance of many receptor and ion channel via internalization. The best studied ubiquitinated ion channel is ENaC (Abriel et al., 1999). Evidence reports that the ubiquitination of the receptor for nerve growth factor Trk resulted in decreased internalization and increased recycling. Ubiquitination required an activation of enzymatic cascade, where the last one, E3 ubiquitin-protein ligase is crucial. E3 enzymes provide the specificity to the cascade recognizing and promoting conjugation with the substrate. In this context we were investigating Kv1.3 ubiquitination and ubiquitin–dependent endocytosis trying to decipher molecular determinates controlled this processes. The data we present shows that E3 ubiquitin ligase Nedd4-2 associated with Kv1.3 and downregulated the activity of the channel. Nedd4-2 facilitates degradation and decrease in activity of ENaC channel (Kamynina and Staub, 2002). ENaC contain conserved Nedd4-2 binding motif PY (PPPXY) in cytosolic COOH termini (Staub et al., 1997). However, Kv1.3 does not present this motif which suggests an involvement of some adaptor protein or an unconventional binding side for Nedd4-2. Further studies are required to establish the exact position for E3 ligase

conjugation with Kv1.3. This could serve as a powerful tool to control the channel destination with direct impact in degradation and turnover.

Interestingly, we have observed that PSD-95, proteins from the MAGUK family, which recruits the channel into the immunological synapse (Szilagyi, et al., 2013), associated with Kv1.3 in HEK-293 cells and affect the channel membrane distribution. Even in the presence of PMA, the channel remained in lipid raft domains and was protected from degradation.

Kv1.3 activity can be modulated by PKC and PKA (Kuras et al., 2012; Vang, et al., 2001). Two PKA isoforms are expressed in human T cells: PKAI and PKAII. PKAI has been shown to inhibit T-cell activation via suppression of the tyrosine kinase Lck (Ruppelt et al., 2007). In the view of these studies, we were wondering whether ADO can activate both kinases. Therefore, given the important role of Adenosine as a physiological Kv1.3 modulator, next wwe wanted to characterize the possible signaling pathways involved in ADO-dependent Kv1.3 endocytosis. Unexpectedly, our data suggested that adenosine-induced internalization involved a cross-talk of both PKC/PKA pathways. However, it is not known in which manner, independently or synergistically, they control channel destination.

8-bromo-cAMP is an agonist which we used to activate directly PKA. PKA phosphorylation resulted in Kv1.3 endocytosis. These findings concur with other studies that show a PKA-dependent Kv1.3 current downregulation. This suggests that the decrease in the Kv.3 current could be due to channel internalization and thereby a reduction of the channel number on the cell surface. In contrast, PKA-mediated

phosphorylation of Nedd4-2 inhibits ENaC/Nedd4-2 interaction, which inhibits retrieval degradation of the channel (Zhou et al., 2007). On the contrary, PKA enhances some Kv7 channel currents (Bharath et al., 2016).

The PKA-dependent pathways induced Kv1.3 endocytosis, but our data is showing a low ubiquitination upon 8-bromo-cAMP and forskolin, another PKA agonist. Therefore, our data let us to suggest that PKA-induced endocytosis is an ubiquitin-independent event. Further studies are required to establish the role of PKA-induced channel degradation and the role of ubiquitin in this phenomenon.

In the last part of this dissertation we concentrated at molecular determinants involved in Kv1.3 ubiquitination. We report already that Kv1.3 ubiquitination required Nedd4-2 presence. Next following step in protein ubiquitination is attachment of ubiquitin to the substrate within lysine residues. This lysine-targeting specificity reveals as another mechanism in control of channel turnover. The choice of target lysines ranges broadly from completely nonspecific to highly selective. The best-studied site-selective ubiquitination reaction is that of the replication factor PCNA. PCNA is monoubiquitinated on a single lysine, K164, by the E2–E3 pair RAD6–RAD18, and this can be extended to K63-linked polyubiquitin (Moldovan et. al., 2007; Parker et al., 2009). On the other hand, lysine selection of Sic1 in yeast by an SCF complex is restricted to six lysine residues in the N-terminal domain that can serve as target site (Sadowski et al., 2010).

Mutation of multiple Kv1.3 lysine residues, help us to investigate lysine specify. Surprisingly, none single lysine shown to be sufficient to

revoke its ubiquitination. Our data suggest that there is more than one lysine being involved in ubiquitin conjugation. Nevertheless, some specificity was detected on C-termianl of the channel. Mutation on lysines of C-terminal, especially K519 and K520, impaired significantly channel ubiquitination and endocytosis under ADO stimuli. The complexity of lysine specificity required further studies. For example, mass espectrometry studies to elucidate the Lys involved would be of interest. Although the mechanism of Kv1.3 ubiquitination remains elusive, the impact in channel regulation is clear and reveals itself as an important process controlling Kv1.3 turnover, thereby fine tuning the physiological response.

5. Conclusions

1. EGF triggered Kv1.3 downregulation via tyrosine kinase phosphorylation and unconventional ERK1/2-dependent phosphorylation. ERK1/2 threonine phosphorylation is crucial for EGF-mediated CME endocytosis.

2. PMA and Adenosine induced Kv1.3 polyubiquitination via PKC activation and led channel to lysosomal degradation. This ubiquitination was dependent of Nedd4-2.

3. Adenosine triggered ubiquitination and endocytosis of Kv1.3. Both processes are sensitive to BIM (PKC inhibitor) and H-89 (PKA inhibitor) treatments, suggesting both PKC and PKA – dependent pathways.

4. Direct PKA activation internalized Kv1.3 with no apparent ubiquitination. This would suggest that PKA, contrary to PKC, induced an ubiquitin-independent endocytosis of Kv1.3.

5. Complementary and redundant lysines participate in the ubiquitin-dependent PKC and PKA regulation of Kv1.3. While C-terminal Lysines (K519, K520) were mainly implicated in the channel internalization, those on the N-terminal (K70, K84) resulted in lower ubiquitination with no changes in endocytosis.

6. References

References

- Abriel H, Loffing J, Rebhun JF, Pratt JH, Schild L, Rotin D, and Staub O. (1999). Defective regulation of the epithelial Na+ channel by Nedd4-2 in Liddile's syndrome. J Clin Invest 103: 667-673.
- Abriel H., Zaklyazminskaya E.V. (2013). "Cardiac channelopathies: genetic and molecular mechanisms." Gene. 15. 517: 1-11.
- Alvi F., Idkowiak-Baldys J., Baldys A., Raymond J., Hannun Y. (2007). Regulation of membrane trafficking and endocytosis by protein kinase C: emerging role of the pericentrion, a novel protein kinase C-dependent subset of recycling endosomes. Cell Mol Life Sci. 64.3: 263-70.
- Arkett S.A.J, Dixon J.N., Yang D.D., Sakai C., Minkin S., Sims M. (1994). Mammalian osteoclasts express a transient potassium channel with properties of Kv1.3. Receptors Channels. 2: 281-293.
- Arkett, S. A., Dixon, J., Yang, J. N., Sakai, D. D., Minkin, C. and Sims, S. M. (1994). Mammalian osteoclasts express a transient potassium channel with properties of Kv1.3. Receptors Channels 2(4): 281-293.
- Arvelo , Waite, Rajagopal, Beyna, Chen , Lee, and Chao. (2006). Cell survival through Trk neurotrophim receptor is differentially regulated by ubiquitination. Neuron 50, 549-59.
- Attali B., Romey G., Honore E., Schmid-Alliana A., Mattei M.G., Lesage F., Ricard P., Barhanin J.,Lazdunski M. 1992. Cloning, functional expression, and regulation of two K+ channels in human T lymphocytes. J Biol Chem. 267: 8650–8657.
- Bernard, C., Anderson, A., Becker, A., Poolos, N. P., Beck, H. and Johnston, D. (2004). Acquired dendritic channelopathy in temporal lobe epilepsy. Science 305,532–535.
- Bharath K. Mani, Christina Robakowski, Lyubov I. Brueggemann, Leanne L. Cribbs, Abhishek Tripathi, Matthias Majetschak, and Kenneth L. Byron. (2016). Kv7.5 Potassium Channel Subunits Are the Primary Targets for PKA-Dependent Enhancement of Vascular Smooth Muscle Kv7 Currents. Mol Pharmacol. 89(3): 323–334.

- Bhowmick P., Pancsa R., Guharoy M., Tompa P. (2013). Functional diversity and structural disorder in the human ubiquitination pathway. PloS One. 29. 8(5).
- Bielanska, J., Hernandez-Losa, J., Moline, T., Somoza, R., Cajal, S. R., Condom, E., . . . Felipe, A. (2012). Increased voltage-dependent K(+) channel Kv1.3 and Kv1.5 expression correlates with leiomyosarcoma aggressiveness. Oncol Lett 4(2): 227-230.
- Blume-Jensen P, Hunter T. (2001). Oncogenic kinase signalling. Nature, 411:355–365.
- Boehmer, C., Laufer, J., Jeyaraj, S., Klaus, F., Lindner, R., Lang, F. and Palmada, M. (2008). Modulation of the voltage-gated potassium channel Kv1.5 by the SGK1 protein kinase involves inhibition of channel ubiquitination. Cell Physiol Biochem 22(5-6): 591-600.
- Bonifacino JS, Marks MS, Ohno H, Kirchhausen T. (1996). Mechanisms of signal-mediated protein sorting in the endocytic and secretory pathways. Proc Assoc Am Physicians 108:285–295.
- Bonifacino JS, Rojas R. (2006). Retrograde transport from endosomes to the trans-Golgi network. Nat Rev Mol Cell Biol 7: 568–579.
- Bonifacino JS, Traub LM. (2003). Signals for sorting of transmembrane proteins to endosomes and lysosomes. Annu Rev Biochem 72:395–447.
- Braakman, I. and Bulleid, N. J. (2011). Protein folding and modification in the mammalian endoplasmic reticulum. Annu Rev Biochem 80: 71-99.
- Brown FD, Rozelle AL, Yin HL, Balla T, Donaldson JG. (2001). Phosphatidylinositol 4,5-bisphosphate and ARF6-regulated membrane traffic. J Cell Biol 154:1007–1017.
- Cahalan M.D., Wulff H., Chandy K.G. (2001). Molecular properties and physiological roles of ion channels in the immune system. J Clin Immunol. 21.4: 235-52.
- Cai, Y. C. and Douglass, J. (1993). In vivo and in vitro phosphorylation of the T lymphocyte type n (Kv1.3) potassium channel. J Biol Chem 268(31): 23720-23727.
- Cai, Y. C., Osborne, P. B., North, R. A., Dooley, D. C. and Douglass, J. (1992). Characterization and functional expression of

genomic DNA encoding the human lymphocyte type n potassium channel. DNA Cell Biol 11(2): 163-172.

- Canto I, Trejo J. (2013). Palmitoylation of protease-activated receptor- 1 regulates adaptor protein complex-2 and -3 interaction with tyrosine-based motifs and endocytic sorting. J Biol Chem 288: 15900–15912.
- Chen B, Dores MR, Grimsey N, Canto I, Barker BL, Trejo J. (2011). Adaptor protein complex-2 (AP-2) and epsin-1 mediate proteaseactivated receptor-1 internalization via phosphorylation- and ubiquitination-dependent sorting signals. J Biol Chem 286:40760–40770.
- Chi, V., Pennington, M. W., Norton, R. S., Tarcha, E. J., Londono, L. M., Sims-Fahey, B., . . . Chandy, K. G. (2012). Development of a sea anemone toxin as an immunomodulator for therapy of autoimmune diseases. Toxicon 59(4): 529-546.
- Chibalin A.V., Ogimoto G., Pedemonte C.H., Pressley T.A., Katz A.I., Féraille E., Berggren P.O., Bertorello A.M. (1999). Dopamine-induced endocytosis of Na+,K+-ATPase is initiated by phosphoryl.tion of Ser-18 in the rat alpha subunit and Is responsible for the decreased activity in epithelial cells. J Biol Chem. 22. 274(4): 1920-1927.
- Chung I, Akita R, Vandlen R, Toomre D, Schlessinger J, Mellman I. (2010). Spatial control of EGF receptor activation by reversible dimerization on living cells. Nature 464:783–787.
- Ciechanover A. (1998). The ubiquitin-proteasome pathway: on protein death and cell life. EMBO J. 15: 7151-60.
- Ciehanover A. (2005). Proteolysis: from the lysosome to ubiquitin und the proteasome. Nat. Rev. Moll. Cell. Biol. 6:79-87.
- Desir G. (1996). The structure, regulation and pathophysiology of potassium channels. Curr Opin Nephrol Hypertens. 4. 5: 402-5.
- Doherty GJ, McMahon HT. (2009). Mechanisms of endocytosis. Annu Rev Biochem 78:857–902.
- Dourado, M. M. and Dryer, S. E. (1994). Regulation of A-currents by cell-cell interactions and neurotrophic factors in developing chick parasympathetic neurones. J. Physiol. 474,367–377.
- Doyle D.A., Cabral J.M. Pfuetzner R., Kuo A. Gulbis J., Cohen J., Chait B., MacKinnon R. (1998). The Structure of the Potassium

Channel: Molecular Basis of K+ Conduction and Selectivity. Science. 280. 5360 pp: 69-77.

- Fadool, D. A., Holmes, T. C., Berman, K., Dagan, D. and Levitan, I. B. (1997). Tyrosine phosphorylation modulates current amplitude and kinetics of a neuronal voltage-gated potassium channel. J Neurophysiol 78(3): 1563-1573.
- Fadool, D. A., Tucker, K., Perkins, R., Fasciani, G., Thompson, R. N., Parsons, A. D., . . . Kaczmarek, L. K. (2004). "Kv1.3 channel gene-targeted deletion produces Super-Smeller Mice" with altered glomeruli, interacting scaffolding proteins, and biophysics. Neuron 41(3): 389-404
- Flick K., Ouni I., Wohlschlegel J.A., Capati C., McDonald W.H., Yates J.R., Kaiser P. (2004). Proteolysis-independent regulation of the transcription factor Met4 by a single Lys 48-linked ubiquitin chain. Nat Cell Biol. 6. 7:634-41.
- Garcia-Calvo, M., Leonard, R. J., Novick, J., Stevens, S. P., Schmalhofer, W., Kaczorowski, G. J. and Garcia, M. L. (1993). Purification, characterization, and biosynthesis of margatoxin, a component of Centruroides margaritatus venom that selectively inhibits voltage-dependent potassium channels. J BiolChem 268(25): 18866-18874.
- Geetha, Jing, and Wooten. (2005). Lysine 63 polyubiquitination of the nerve growth factor receptor Trka directs internalization and signaling. Mol. Cell 20, 301-312.
- Goh LK, Huang F, Kim W, Gygi S, Sorkin A. (2010). Multiple mechanisms collectively regulate clathrin-mediated endocytosis of the epidermal growth factor receptor. J Cell Biol. 189:871–883.
- Gulbins, E., Sassi, N., Grassme, H., Zoratti, M. and Szabo, I. (2010). Role of Kv1.3 mitochondrial potassium channel in apoptotic signalling in lymphocytes. Biochim Biophys Acta 1797(6-7): 1251-1259.
- Gutman, G. A., Chandy, K. G., Adelman, J. P., Aiyar, J., Bayliss, D. A., Clapham, D. E., . . . Wymore, R. S. (2003). International Union of Pharmacology. XLI. Compendium of voltage-gated ion channels: potassium channels. Pharmacol Rev 55(4): 583-586.
- Hesketh GG, Van Eyk JE, Tomaselli GF. (2009). Mechanisms of gap junction traffic in health and disease. J Cardiovasc Pharmacol 54:263–272.

- Hille B. (2001). Ion channels of excitable membranes. Sinauer, Sunderland,Mass. xviii, 814 pp.
- Hunter T. (2000). Signaling–2000 and beyond. Cell, 100:113–127.
- Ishii K., Norota I., Obara Y. (2012). Endocytic regulation of voltage-dependent potassium channels in the heart. J Pharmacol Sci. 120. 4:264-273.
- Jacob A.I.R., Hurley L.O., Goodwin G.W., Cooper S., Benoff S. (2000). Molecular characterization of a voltagegated potassium channel expressed in rat testis. Mol Hum Reprod. 6:303-313.
- Kamynina E and Staub O. (2002). Concerted action of ENaC,Nedd4-2, and Sgk1 in transepithelial Na transport. Am J Physiol Renal Physiol 283: F377–F387.
- Kellenberger S., Schild L. (2002). Epithelial sodium channel/degenerin family of ion channels: a variety of functions for a shared structure. Physiol Rev. 82.3:735-67.
- Kobayashi H, Fukuda M. (2013). ARF6, Rab11 and transferrin receptor define distinct populations of recycling endosomes. Commun Integr Biol 6:e25036.
- Koni, P. A., Khanna, R., Chang, M. C., Tang, M. D., Kaczmarek, L. K., Schlichter, L. C. and Flavella, R. A. (2003). Compensatory anion currents in Kv1.3 channel-deficient thymocytes. J Biol Chem 278(41): 39443-39451.
- Kupershmidt, S., Yang, T., Chanthaphaychith, S., Wang, Z., Towbin, J. A. and Roden, D. M. (2002). Defective human Ether-a-go-go-related gene trafficking linked to an endoplasmic reticulum retention signal in the C terminus. J Biol Chem 277(30): 27442-27448.
- Kuras Z., Kucher V., Gordon S.M., Neumeier L., Chimote A.A., Filipovich A.H., Conforti L. (2012). Modulation of Kv1.3 channels by protein kinase A I in T lymphocytes is mediated by the disc large 1-tyrosine kinase Lck complex. Am J Physiol Cell Physiol. 15. 302:C1504-12.
- Lakadamyali M, Rust MJ, Zhuang X. (2006). Ligands for clathrinmediated endocytosis are differentially sorted into distinct populations of early endosomes. Cell 124:997–1009.
- Li, D., Takimoto, K. and Levitan, E. S. (2000). Surface expression of Kv1 channels is governed by a C-terminal motif. J Biol Chem 275(16): 11597-11602.

- Littleton J.T., Ganetzky B. (2000). Ion channels and synaptic organization: analysis of the Drosophila genome. Neuron. 26.1: 35-43.
- MacKinnon, R. (1991). Determination of the subunit stoichiometry of a voltage-activated potassium channel. Nature 350(6315): 232-235.
- MacKinnon, R. (2003). Potassium channels. FEBS Lett 555(1): 62-65.
- MacKinnon, R., Reinhart, P. H. and White, M. M. (1988). Charybdotoxin block of Shaker K+ channels suggests that different types of K+ channels share common structural features. Neuron 1(10): 997-1001.
- Manning G, Whyte DB, Martinez R, Hunter T, Sudarsanam S. (2000). The protein kinase complement of the human genome. Science 298:1912–1934.
- Manning G, Whyte DB, Martinez R, Hunter T, Sudarsanam S. (2002). The protein kinase complement of the human genome. Science 298:1912–1934.
- Martínez-Pinna, J., McCloskey, C., Fernandez-Martinez, V., Wright, J., Forsythe, I., Kaczmarek, L., Morales A., and Mahaut-Smith, M. (2012). Novel regulatoin of Kv1.3 channel inactivation by intracellular calcium. Proceedings of Acta Physiologica 206(Supplement 693).
- McCormack, T., McCormack, K., Nadal, M. S., Vieira, E., Ozaita, A. and Rudy, B. (1999). The effects of Shaker beta-subunits on the human lymphocyte K+ channel Kv1.3. J Biol Chem 274(29): 20123-20126.
- McMahon HT, Boucrot E (2011) Molecular mechanism and physiological functions of clathrin-mediated endocytosis. Nat Rev Mol Cell Biol 12:517–533.
- Mimnaugh E., Neckers L. (2005). Measuring Ubiquitin Conjugation in Cells. Methods Mol Biol. 301. 2: 23-41.
- Misonou, H., Mohapatra, D. P., Park, E. W., Leung, V., Zhen, D., Misonou, K., . . . Trimmer, J. S. (2004). Regulation of ion channel localization and phosphorylation by neuronal activity. Nat Neurosci 7(7): 711- 718.
- Moldovan, G.L., Pfander, B. & Jentsch, S. (2007). PCNA, the maestro of the replication fork. Cell 129, 665–679.

- motif. Plant J 56(6): 997-1006.
- Mukhopadhyay and Riezman, (2007). Proteasome-independent function of ubiquitin in endocytosis and signaling. Scieence 315, 201-205.
- Mullen, K. M., Rozycka, M., Rus, H., Hu, L., Cudrici, C., Zafranskaia, E., . . . Calabresi, P. A. (2006). Potassium channels Kv1.3 and Kv1.5 are expressed on blood-derived dendritic cells in the central nervous system. Ann Neurol 60(1): 118-127.
- Mullen, K. M., Rozycka, M., Rus, H., Hu, L., Cudrici, C., Zafranskaia, E., . . . Calabresi, P. A. (2006). Potassium channels Kv1.3 and Kv1.5 are expressed on blood-derived dendritic cells in the central nervous system. Ann Neurol 60(1): 118-127.
- Newton A. C. (1997). Regulation of protein kinase C. Curr Opin Cell Biol. 9: 161-167.
- Nicolaou, S. A., Neumeier, L., Takimoto, K., Lee, S. M., Duncan, H. J., Kant, S. K., . . . Conforti, L. (2010). Differential calcium signaling and Kv1.3 trafficking to the immunological synapse in systemic lupus erythematosus. Cell Calcium 47(1): 19-28.
- Nicolaou, S. A., Szigligeti, P., Neumeier, L., Lee, S. M., Duncan, H. J., Kant, S. K., . . . Conforti, L. (2007). Altered dynamics of Kv1.3 channel compartmentalization in the immunological synapse in systemic lupus erythematosus. J Immunol 179(1): 346-356.
- Nitabach, M. N., Llamas, D. A., Thompson, I. J., Collins, K. A. and Holmes, T. C. (2002). Phosphorylationdependent and phosphorylation-independent modes of modulation of shaker family voltage-gated potassium channels by SRC family protein tyrosine kinases. J Neurosci 22(18): 7913-7922.
- Noma, K., Kimura, K., Minatohara, K., Nakashima, H., Nagao, Y., Mizoguchi, A. and Fujiyoshi, Y. (2009). Triple N-glycosylation in the long S5-P loop regulates the activation and trafficking of the Kv12.2 potassium channel. J Biol Chem 284(48): 33139-33150.
- Panyi, G., Vamosi, G., Bacso, Z., Bagdany, M., Bodnar, A., Varga, Z., . . . Damjanovich, S. (2004). Kv1.3 potassium channels are localized in the immunological synapse formed between cytotoxic and target cells. Proc Natl Acad Sci U S A 101(5): 1285-1290.

- Parker, J.L. & Ulrich, H.D. (2009). Mechanistic analysis of PCNA poly-ubiquitylation by the ubiquitin protein ligases Rad18 and Rad5. EMBO J. 28, 3657–3666.
- Peng J., Schwartz1 D., Elias J., Thoreen C., Cheng D., Marsischky G, Roelofs J., Finley D.,Gygi S. (2003). A proteomics approach to understanding protein ubiquitination. Natur Biotechnol. 21. 8: 921-926.
- Pennington, M. W., Mahnir, V. M., Krafte, D. S., Zaydenberg, I., Byrnes, M. E., Khaytin, I., . . . Kem, W. R. (1996). Identification of three separate binding sites on SHK toxin, a potent inhibitor of voltagedependent potassium channels in human T-lymphocytes and rat brain. Biochem Biophys Res Commun 219(3): 696-701.
- Peter, M., Jr., Varga, Z., Hajdu, P., Gaspar, R., Jr., Damjanovich, S., Horjales, E., . . . Panyi, G. (2001). Effects of toxins Pi2 and Pi3 on human T lymphocyte Kv1.3 channels: the role of Glu7 and Lys24. J Membr Biol 179(1): 13-25.
- Pickart C.M., Eddins M.J. (2004). Ubiquitin: structures, functions, mechanisms. Biochim Biophys Acta. 29. 1695(1-3):55-72.
- Platta HW, Stenmark H. (2011). Endocytosis and signaling. Curr Opin Cell Biol 23:393–403.
- Pongs, O., Leicher, T., Berger, M., Roeper, J., Bahring, R., Wray, D., . . . Storm, J. F. (1999). Functional and molecular aspects of voltage-gated K+ channel beta subunits. Ann N Y Acad Sci 868: 344-355.
- Pottosin, II, Valencia-Cruz, G., Bonales-Alatorre, E., Shabala, S. N. and Dobrovinskaya, O. R. (2007). Methyl-beta-cyclodextrin reversibly alters the gating of lipid rafts-associated Kv1.3 channels in Jurkat T lymphocytes. Pflugers Arch 454(2): 235-244.
- Pourrier, M., Schram, G. and Nattel, S. (2003). Properties, expression and potential roles of cardiac K+ channel accessory subunits: MinK, MiRPs, KChIP, and KChAP. J Membr Biol 194(3): 141-152.
- Prigent M, Dubois T, Raposo G, Derrien V, Tenza D, Rosse C, Camonis J, Chavrier P. (2003). ARF6 controls post-endocytic recycling through its downstream exocyst complex effector. J Cell Biol 163:1111–1121.
- Qiu M. H., Zhang R. and Sun F. Y. (2003). Enhancement of ischemiainduced tyrosine phosphorylation of Kv1.2 by vascular

endothelial growth factor via activation of phosphatidylinositol 3-kinase. J. Neurochem. 87, 1509–1517.

- Radhakrishna H, Donaldson JG. (1997). ADP-ribosylation factor 6 regulates a novel plasma membrane recycling pathway. J Cell Biol 139:49–61.
- Reider A., Wendland B. (2011). Endocytic adaptors--social networking at the plasma membrane. J Cell Sci. 15. 124(Pt 10):1613-22.
- Ron D., Kazanietz M. (1999). New insights into the regulation of protein kinase C and novel phorbol ester receptors. FASEB Jour. 13. 13: 1658-1676.
- Rotin D., Kanelis V., Schild L. (2001). Trafficking and cell surface stability of ENaC. Am J Physiol Renal Physiol. 281:F391-399.
- Rotin D., Kumar S. (2009). Phisiological functions of the HECT family ubiquitin ligase. 2009. Nat Rev Mol Cell Biol. 10:398-409.
- Ruppelt A, Mosenden R, Gronholm M, Aandahl EM, Tobin D, Carlson CR, Abrahamsen H, Herberg FW, Carpen O, Tasken K. (2007). Inhibition of T cell activation by cyclic adenosine 5′-monophosphate requires lipid raft targeting of protein kinase a type I by the a-kinase anchoring protein Ezrin. J Immunol 179: 5159– 5168.
- Sadowski, M., Suryadinata, R., Lai, X., Heierhorst, J. & Sarcevic, B. (2010). lecular basis for lysine specificity in the yeast ubiquitin-conjugating enzyme Cdc34. Mol. Cell. Biol. 30, 2316–2329.
- Salinas, M., Duprat, F., Heurteaux, C., Hugnot, J. P. and Lazdunski, M. (1997). New modulatory alpha subunits for mammalian Shab K+ channels. J Biol Chem 272(39): 24371-24379.
- Schenck A, Goto-Silva L, Collinet C, Rhinn M, Giner A, Habermann B, Brand M, Zerial M. (2008). The endosomal protein Appl1 mediates Akt substrate specificity and cell survival in vertebrate development. Cell. 133:486–497.
- Shi, G., Nakahira, K., Hammond, S., Rhodes, K. J., Schechter, L. E. and Trimmer, J. S. (1996). Beta subunits promote K+ channel surface expression through effects early in biosynthesis. Neuron 16(4): 843-852.

- Sieben, C., Mikosch, M., Brandizzi, F. and Homann, U. (2008). Interaction of the K(+)-channel KAT1 with the coat protein complex II coat component Sec24 depends on a di-acidic endoplasmic reticulum export
- Sigismund S, Argenzio E, Tosoni D, Cavallaro E, Polo S, Di FiorePP. (2008). Clathrin-mediated internalization is essential for sustained EGFR signaling but dispensable for degradation. Dev Cell 15:209–219.
- Sigismund S, Woelk T, Puri C, Maspero E, Tacchetti C, Transidico P, Di Fiore PP, Polo S. (2005). Clathrin-independent endocytosis of ubiquitinated cargos. Proc Natl Acad Sci U S A. 102:2760–2765.
- Sokolova, O., Accardi, A., Gutierrez, D., Lau, A., Rigney, M., Grigorieff, N., (2003). Conformational changes in the C terminus of Shaker K+ channel bound to the rat Kvbeta2-subunit. Proc. Natl. Acad. Sci. USA 100, 12607–12612.
- Staub O, Gautschi I, Ishikawa T, Breitschopf K, Ciechanover A, Schild L, and Rotin D.(1997). Regulation of stability and function of the epithelial Na channel (ENaC) by ubiquitination. EMBO J 16: 6325–6336.
- Staub, O., Gautschi, I., Ishikawa, T., Breitschopf, K., Ciechanover, A., Schild, L. and Rotin, D. (1997). Regulation of stability and function of the epithelial Na+ channel (ENaC) by ubiquitination. EMBO J 16(21): 6325-6336.
- Steele, D. F., Eldstrom, J. and Fedida, D. (2007). Mechanisms of cardiac potassium channel trafficking. J Physiol 582(Pt 1): 17-26.
- Swanson, R., Marshall, J., Smith, J. S., Williams, J. B., Boyle, M. B., Folander, K., . . . et al. (1990). Cloning and expression of cDNA and genomic clones encoding three delayed rectifier potassium channels in rat brain. Neuron 4(6): 929-939.
- Szilagyi, O., Boratko, A., Panyi, G. & Hajdu, P. (2013). The role of PSD-95 in the rearrangement of Kv1.3 channels to the immunological synapse. Pflugers Arch 465, 1341–1353.
- Szilagyi, O., Boratko, A., Panyi, G. and Hajdu, P. (2013). The role of PSD-95 in the rearrangement of Kv1.3 channels to the immunological synapse. Pflugers Arch.

- Torgersen KM, Vang T, Abrahamsen H, Yaqub S, Taskén K. (2002). Molecular mechanisms for protein kinase A-mediated modulation of immune function. Cell Signal 14: 1– 9.
- Traub LM, Bonifacino JS. (2013). Cargo recognition in clathrinmediated endocytosis. Cold Spring Harb Perspect Biol 5:a016790.
- Tsai W., Morielli A. D. and Peralta E. G. (1997). The m1 muscarinic acetylcholine receptor transactivates the EGF receptor to modulate ion channel activity. EMBO J. 16, 4597–4605.
- Tubert C, Taravini IR, Flores-Barrera E, Sánchez GM, Prost MA, Avale ME, Tseng KY, Rela L, Murer MG. (2016). Decrease of a Current Mediated by Kv1.3 Channels Causes Striatal Cholinergic Interneuron Hyperexcitability in Experimental Parkinsonism. Cell Rep 16(10):2749-62.
- Vang T, Torgersen KM, Sundvold V, Saxena M, Levy FO, Skalhegg BS, Hansson V, Mustelin T, Tasken K. (2001). Activation of the COOH-terminal Src kinase (Csk) by cAMP-dependent protein kinase inhibits signaling through the T cell receptor. J Exp Med 193: 497– 507.
- Veh RW, Lichtinghagen R, Sewing S, Wunder F, Grumbach IM, Pongs O. (1995). Immunohistochemical localization of five members of the Kv1 channel subunits: contrasting subcellular locations and neuronspecific co-localizations in rat brain. Eur J Neurosci. 7(11):2189-2205.
- Vennekamp, J., Wulff, H., Beeton, C., Calabresi, P. A., Grissmer, S., Hansel, W. and Chandy, K. G. (2004). Kv1.3-blocking 5-phenylalkoxypsoralens: a new class of immunomodulators. Mol Pharmacol 65(6): 1364-1374.
- Vicente, R., Escalada, A., Villalonga, N., Texido, L., Roura-Ferrer, M., Martin-Satue, M., . . . Felipe, A. (2006). Association of Kv1.5 and Kv1.3 contributes to the major voltage-dependent K+ channel in macrophages. J Biol Chem 281(49): 37675-37685.
- Vicente, R., Villalonga, N., Calvo, M., Escalada, A., Solsona, C., Soler, C., . . . Felipe, A. (2008). Kv1.5 association modifies Kv1.3 traffic and membrane localization. J Biol Chem 283(13): 8756-8764.
- Villalonga, N., Escalada, A., Vicente, R., Sanchez-Tillo, E., Celada, A., Solsona, C. and Felipe, A. (2007). Kv1.3/Kv1.5

heteromeric channels compromise pharmacological responses in macrophages. Biochem Biophys Res Commun 352(4): 913-918.

- Villalonga, N., Escalada, A., Vicente, R., Sanchez-Tillo, E., Celada, A., Solsona, C. and Felipe, A. (2007). Kv1.3/Kv1.5 heteromeric channels compromise pharmacological responses in macrophages. Biochem Biophys Res Commun 352(4): 913-918.
- Wang T., Cheng Y., Dou Y., Goonesekara C., David J.P., Steele. D.F., Huang C., Fedida D. (2012). Trafficking of an endogenous potassium channel in adult ventricular myocytes. Am J Physiol Cell Physiol. 303.9: C963-76.
- Wilkinson K., Gan-Erdene T., Kolli N. (2005). Derivitization of the C-terminus of ubiquitin and ubiquitin-like proteins using intein chemistry: methods and uses. Methods Enzymol. 399:37-51.
- Yang, F., Feng, L., Zheng, F., Johnson, S. W., Du, J., Shen, L., Wu, C. P. and Lu, B. (2001). GDNF acutely modulates excitability and A-type K+ channels in midbrain dopaminergic neurons. Nat. Neurosci.4, 1071–1078.
- Ying Peng, Kui Lu, Zichen Li, Yaodong Zhao, YipingWang, Bin Hu, Pengfei Xu, Xiaolei Shi, Bin Zhou, Michael Pennington, K. George Chandy, and Yamei Tang. (2014). Blockade of Kv1.3 channels ameliorates radiation-induced brain injury. Neuro-Oncology 16(4), 528–539.
- Zerrin Kuras, Vladimir Kucher, Scott M. Gordon, Lisa Neumeier, Ameet A. Chimote, Alexandra H. Filipovich, and Laura Conforti. (2012). Modulation of KV1.3 channels by protein kinase A I in T lymphocytes is mediated by the disc large 1-tyrosine kinase Lck complex. Am J Physiol Cell Physiol 302: C1504–C1512.
- Zhang R. L., Zhang Z. G., Zhang L. and Chopp M. (2001). Proliferation and differentiation of progenitor cells in the cortex and the subventricular zone in the adult rat after focal cerebral ischemia. Neuroscience 105, 33–41.
- Zhou R, Patel SV, Snyder PM. (2007). Nedd4-2 catalyzes ubiquitination and degradation of cell surface ENaC. J Biol Chem.m282 (28):20207-12.
- Zhu, J., Gomez, B., Watanabe, I. and Thornhill, W. B. (2005). Amino acids in the pore region of Kv1 potassium channels dictate

cell-surface protein levels: a possible trafficking code in the Kv1 subfamily. Biochem J 388(Pt 1): 355-362.

- Zhu, J., Watanabe, I., Gomez, B. and Thornhill, W. B. (2003). "Trafficking of Kv1.4 potassium channels: interdependence of a pore region determinant and a cytoplasmic C-terminal VXXSL determinant in regulating cell-surface trafficking." Biochem J 375(Pt 3): 761-768.
- Zoncu R, Perera RM, Balkin DM, Pirruccello M, Toomre D, De Camilli P. (2009). A phosphoinositide switch controls the maturation and signaling properties of APPL endosomes. Cell. 136:1110–1121.
- Zuzarte, M., Rinne, S., Schlichthorl, G., Schubert, A., Daut, J. and Preisig-Muller, R. (2007). A di-acidic sequence motif enhances the surface expression of the potassium channel TASK-3. Traffic 8(8): 1093- 1100.